DISCRETE AND CONTINUOUS DYNAMICS MODELING OF A MASS MOVING ON A FLEXIBLE STRUCTURE

by

DEBORAH ANN HERMAN

B.S.A.E., Boston University
(1989)

SUBMITTED IN PARTIAL FULFILLMENT
OF THE REQUIREMENTS FOR THE
DEGREE OF MASTER OF SCIENCE
at the
MASSACHUSETTS INSTITUTE OF TECHNOLOGY
February, 1992

Signature of Author_____
Department of Aeronautics and Astronautics

Approved by_____
Dr. Achille Messac
Thesis Advisor, Draper Laboratory

Certified by_____
Professor John Dugundji
Thesis Advisor

Accepted by_____
Professor Harold Y. Wachman
Chairman, Departmental Graduate Committee

DISCRETE AND CONTINUOUS DYNAMICS MODELING OF A MASS MOVING ON A FLEXIBLE STRUCTURE

by

DEBORAH ANN HERMAN

Submitted to the
Department of Aeronautics and Astronautics
on January 17, 1992
in partial fulfillment of the requirements for the degree of
Master of Science
in
Aeronautics and Astronautics

ABSTRACT

The purpose of this thesis is to develop a general discrete methodology for modeling the dynamics of a mass that moves on the surface of a flexible structure. This model was motivated by the Space Station/Mobile Transporter system. A model reduction approach is developed to make the methodology applicable to large structural systems. To validate the discrete methodology, continuous formulations are also developed. Three different systems are examined: (1) Simply-Supported Beam, (2) Free-Free Beam, and (3) Free-Free beam with two points of contact between the mass and the flexible beam. In addition to validating the methodology, parametric studies were performed to examine how the system's physical properties affect its dynamics. Selected MATLAB programs are provided.

Thesis Advisor : Dr. Achille Messac
Title : Senior Staff Member, Draper Fellow Advisor, Dynamics Group, Charles Stark Draper Laboratory, Inc..

Thesis Advisor : Dr. John Dugundji
Title : Professor of Aeronautics and Astronautics, Massachusetts Institute of Technology

This Thesis is dedicated to the memory of my beloved father

Bernard Herman

ACKNOWLEDGEMENTS

First, I would like to thank the two people whose love and support made this document possible; my mother Marcia Herman, and my brother Scott Herman. Second, I would like to thank John Fullford for being there whenever I needed him.

I wish to thank my advisor, Dr. Achille Messac at the Charles Stark Draper, Laboratory, Inc., whose guidance helped me see the light at the end of the tunnel. Dr. Messac has enthusiastically taught me everything I know about dynamics. I would also like to thank Professor John Dugundji for his time, patience, and invaluable comments.

It is also appropriate to thank some special friends who have helped me throughout the years; Erin Daly, Dylan Kimmel, and Chrisitine Paras. Also thanks to Douglas Varela and Gary Edwards for making the trying times at MIT more bearable. A special thanks also goes to Dr. James Bethune for teaching me to have faith in myself.

Finally, I would like to thank Shari Kinzinger for helping me convert my thoughts into a readable document.

This thesis was prepared at The Charles Stark Draper Laboratory, Inc., under Contract 85988.

Publication of this thesis does not constitute approval by Draper or the sponsoring agency of the findings or conclusions contained herein. It is published for the exchange and stimulation of ideas.

I hereby assign my copyright of this thesis to The Charles Stark Draper Laboratory, Inc., Cambridge, Massachusetts.

Deborah Ann Herman

Permission is hereby granted by The Charles Stark Draper Laboratory, Inc., to the Massachusetts Institute of Technology to reproduce any or all of this thesis.

TABLE OF CONTENTS

LIST OF TABLES

LIST OF FIGURES

CHAPTER 1
INTRODUCTION

The concept of "Freedom" Space Station divulges a wide range of dynamics problems. The particular problem considered in this thesis will help examine how the mobile transporter motion affects the space station dynamics. In the current space station layout, the mobile transporter is connected to the main truss of the space station (see Figure 1). The mobile transporter moves along the length of the truss on a track carrying payload about the station. Since the sum of the mass of the mobile transporter and that of the payload it will carry is potentially comparable to the mass of the entire station, the inertial effects of the transporter should not be ignored.

The current analysis is motivated by the Space Station-Mobile Transporter (SS-MT) system. A simplified model of a mass moving over a flexible guideway is used to resemble the more complicated SS-MT system. This simplified system may be solved with a continuous formulation, but obtaining a continuous formulation that will simulate the complicated system containing the station, transporter, and shuttle is not feasible. Therefore, while a continuous analysis provides insight, a more general discrete formulation is needed to address the large-scale problem at hand.

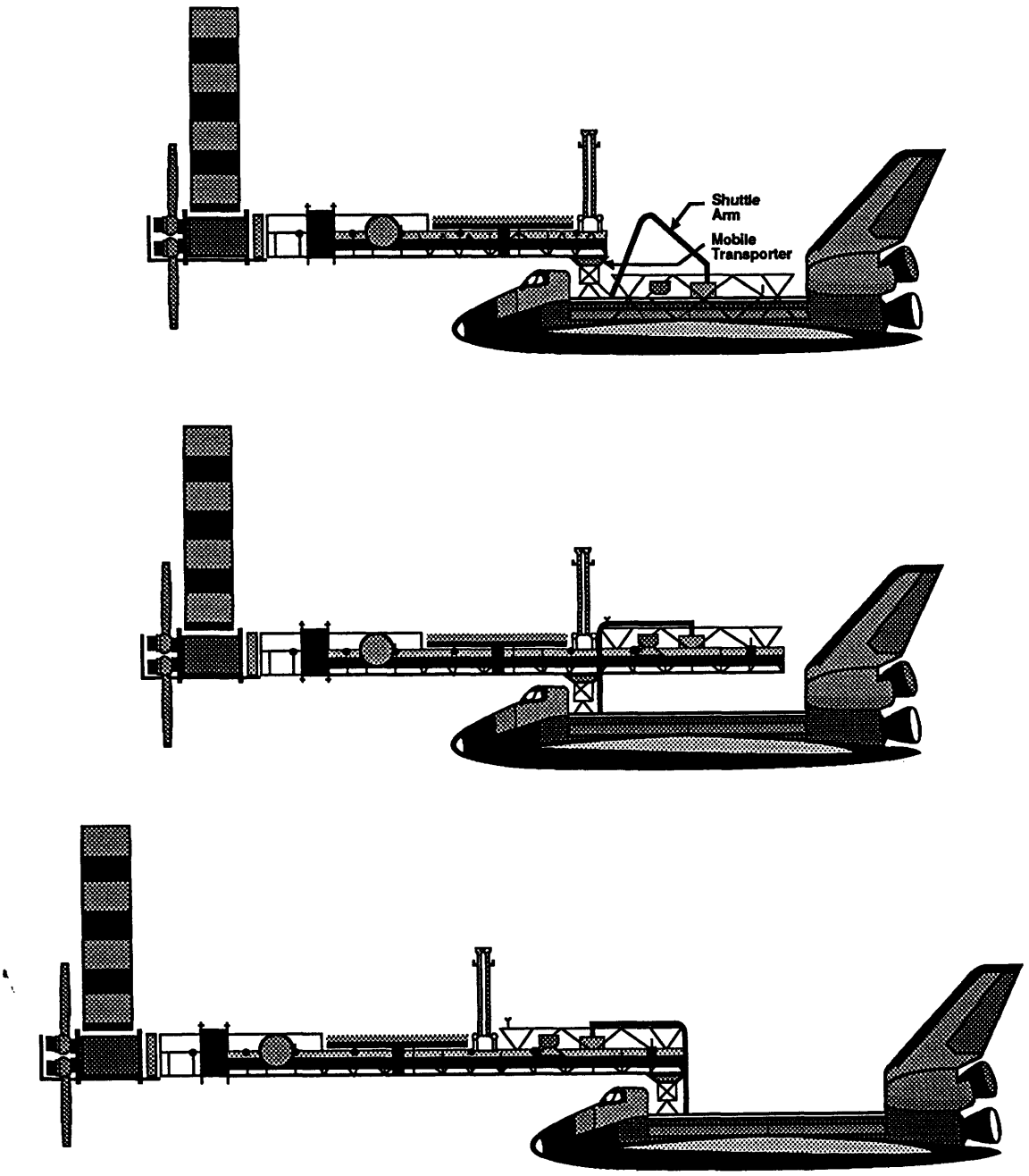

Figure 1. Space Station Assembly.

The objective is to develop a discrete algorithm that can be tested against a continuous formulation for the Flexible Structure/Moving Mass system. Once the validity of this discrete algorithm is proven, it may be extended to simulate the motion of the Space Station-Mobile Transporter system.

In both the continuous and the discrete analyses, the guideway is modeled as a flexible beam. The moving mass is considered to be a rigid body that moves along the beam's length. The inertial effects due to the motion of the mass are included in the derivation. For the discrete system, the flexible beam is divided into finite beam-elements. Using lumped-parameter and energy-consistent methods, respectively, the beam's mass and stiffness matrices are obtained. Then, an invertible operator is used to map the continuous spatial representation of the moving mass onto the discrete representation of the flexible structure.

A continuous and discrete formulation is used to examine the mass connected to the flexible guideway at only one point. This model does not correspond to the actual Space Station-Mobile Transporter system but it serves as an appropriate test article. A continuous formulation is developed to check the results of the discrete method, and numerical results are presented for a simply-supported and a free-free flexible beam. Once the validity of the

discrete methodology is established, parametric studies are performed for both the simply-supported and the free-free beams.

The final step in the analysis is to connect the moving mass to the flexible beam at two points. This model was chosen to represent the train/track aspect of the SS-MT system. Since a discrete methodology was validated, a continuous formulation of this new system is not necessary. To stay close to the SS-MT system, only the free-free beam case is examined here. Studies that examine how the spacing of the two contact points affects the dynamics of the entire system are presented.

There are four chapters and four Appendices following this introduction. Chapter 2 examines the relevant work that has been accomplished in this area. Most previous work concentrates on the motion of a truck travelling over a flexible bridge or on a train travelling over a track. The SS-MT dynamics are similar to the flexible bridge problem except for the rigid body motion that the inertially-free space station undergoes. Due to the increase in computer power in recent years, many dynamic simulation programs were developed. Chapter 2 also examines how well these existing dynamic codes can handle the specific problem at hand.

Chapter 3 describes the theoretical analysis: Section 3.1 focuses on the continuous formulation and Section 3.2 develops the

discrete formulation. The simply-supported and the free-free beam are examined here as special cases. Section 3.3 discusses the discrete, inertially free, multipoint-of-contact system. Each of the three sections in Chapter 3 starts with a mathematical model of the system. Then the equation of motion is developed using a Newtonian method. The equations are made nondimensional and placed into a reduced set of modal coordinates. The final equations are then cast in state-space form, which is well suited for numerical computation.

Chapter 4 displays the numerical results, and is divided into two sections. The first section, Section 4.1, outlines how the simulations are organized, and discusses the goals that the results are trying to obtain and the parameters used to develop the simulations. The second section, Section 4.2, displays and discusses each simulation that is run. In this section, the simply-supported case is examined first to compare the accuracy of the discrete and continuous formulations. Parametric studies are then performed in order to examine how a change in the system nondimensional parameters changes the system dynamics. Next, the free-free case is examined. Once again, the discrete and continuous formulations are compared to assess the accuracy of the discrete formulation. Parametric studies are again performed when the accuracy of the discrete case has been proved. Finally the two-point-of-contact case is displayed.

Chapter 5 offers conclusions and suggestions for further work; in particular, extending the discrete formulation presented here to model the Space Station-Mobile Transporter system. The concept of connecting the shuttle to the SS-MT system could also be considered, which would be a logical extension of the work presented in this thesis.

Appendix A offers a Lagrangian formulation of the continuous free-free beam, which is used to check the continuous formulation of the same system derived earlier using Newton's equation of motion. Appendix B describes the numerical integration process that was used to obtain the simulation results shown in Chapter 4. The Runge Kutta integration scheme is described. Appendix C provides numerical values of the matrices used in evaluating the free-free beam and expands the spatial derivatives of the shape functions used in the discrete formulations. Appendix D describes the Matlab programs that were written to simulate the Flexible Structure/Moving Mass system. Some selected MATLAB programs are displayed.

CHAPTER 2

PREVIOUS WORKS

Reaching as far back as the early nineteenth century, scientists and theorists have been intrigued by the dynamic interaction that occurs when a load travels over a flexible structure. In the past, common models of this interactive system have been that of a truck travelling over a bridge, a train travelling along a track, or a package moving on a conveyer belt. These systems are similar to the inertially free Flexible Structure/Moving Mass system that is used here to resemble the Space Station-Mobile Transporter (SS-MT) system.

Unlike the other systems mentioned, the Space Station-Mobile Transporter system is inertially free, and it is geometrically complex. It is necessary to obtain a discrete representation of the Flexible Structure/Moving Mass system that can be extended to the Space Station-Mobile Transporter system. A discrete representation is necessary in order to accommodate mass and stiffness matrices, rather than partial differential equations. References [1] and [2] were the first to address this important concept in a general way. This thesis is a detailed compilation of the analysis presented in those two papers, with the exception that Ref. [2] addresses the problem of a ***flexible structure*** moving on a ***flexible structure***.

This chapter introduces other work involving the dynamic interaction of the moving mass/flexible structure issue. Section 2.1 discusses some related previously released papers. Section 2.2 examines some existing multibody dynamics and finite-element codes in order to determine their ability to handle the proposed problem.

2.1 PREVIOUSLY PUBLISHED PAPERS

Three important features are needed to handle the Space Station-Mobile Transporter system and the dynamics of the Space Shuttle:

(1) A discrete representation.

(2) The ability to handle very large complex systems.

(3) Computational efficiency.

None of the previously published papers are well suited to meet all three of these requirements. Most of the previous work assumes that a continuous model of the flexible structure is available (Refs. [3]-[7]). References [3]-[6] assume that the beam is simply-supported. For example, Galerkin's method (Ref. [3]), Inverse Laplace transform (Ref. [5]), and Fourier series (Ref. [6]) are several of the analytical techniques discussed. The derived discrete methodology

outlined in Section 3.2 uses the continuous solution presented in Ref. [5] for its comparison.

Reference [7] presents a continuous formulation that may be applied to different boundary conditions. This continuous solution, however, is primarily beneficial when the inertial effects of the moving mass can be ignored, thus treating the travelling load as a moving force rather than as a moving mass. The repercussions of this assumption are disclosed in Chapter 4.

Two papers (Refs. [8] and [9]) present discrete methodologies capable of solving the moving mass/flexible structure problem. Reference [8] presents a methodology that is applicable for time-varying forces. Reference [9] presents a formulation that may be implemented into a general finite-element code, such as MSC NASTRAN. This method is valid for any boundary condition. Lagrange multipliers are used to obtain a linear time-invariant formulation, which can then be solved using NASTRAN. However, as explained in Ref. [2], this formulation is generally applicable when modal reduction is not necessary.

The papers discussed above (Refs. [3]-[9]) present methodologies that are well suited to study the motion of a heavy truck or train travelling over a flexible bridge. However, the methodology presented here is well suited for the complex inertially

free Space Station-Mobile Transporter system. It is a discrete representation that is independent on the boundary conditions of the beam. It is well suited for model reduction so can be altered to include the Space Shuttle's dynamics.

2.2 EXISTING CODES

In the past twenty years, the availability and power of computers has grown exponentially. Coinciding with the boom in computer hardware was an increase in computer software capabilities. Today there are hundreds of software packages available to handle very diverse tasks.

Among the codes that handle multibody dynamic interactions are: DISCOS (Ref. [10]), ADAMS (Ref. [11]), and DADS (Ref. [12]). These codes model the connection between two bodies as either a prismatic or a rotational joint. As was stated in Ref. [1], however, the motion of the Mobile Transporter is dependent on the flexible-body motion of the Space Station. Therefore, the SS-MT system cannot be modeled using these joints, without making far-reaching assumptions.

An alternative is to develop a formulation that could be implemented using an existing finite-element code, such as MSC NASTRAN (Ref. [13]) or ADINA (Ref. [14]). NASTRAN requires that

the equations be cast in a linear time-invariant form. Ref. [9] presents an effective approach to using NASTRAN for the moving mass problem in the case of low-order structures. ADINA's strength lies in other areas.

The discrete formulation presented in Section 3.2 is developed specifically with the application to large structural systems in mind.

CHAPTER 3

THEORETICAL ANALYSIS

Chapter 3 discusses the theoretical analysis: Section 3.1 presents the continuous formulation, Section 3.2 presents the discrete formulation with one point of contact, and Section 3.3 presents a discrete formulation for the multipoint-of-contact system.

Each section is set up in a similar manner. First, a mathematical model of the system is discussed. Using this model, equations of motion of the entire system are developed and placed into a nondimensional form in terms of the beam's modal coordinates. Then a state space matrix representation is formed so the formulation is suitable for numerical evaluation.

A general formulation valid for any boundary condition is presented in each section. Two systems are examined in detail: (1) the simply-supported beam and (2) the free-free beam.

3.1 CONTINUOUS FORMULATION

In the following sections, the continuous formulation of the SS-MT system is developed. The results from this formulation are compared to those obtained by the discrete analysis presented in Section 3.2.

Two different systems are examined here. The first system system model, shown in Figure 2, represents the inertially *fixed* space station with the transporter travelling along its length. This model represents many physical entities, the most popular example being a heavy truck travelling over a flexible bridge. The second system, shown in Figure 3, represents the inertially *free* space station with the transporter travelling along its length.

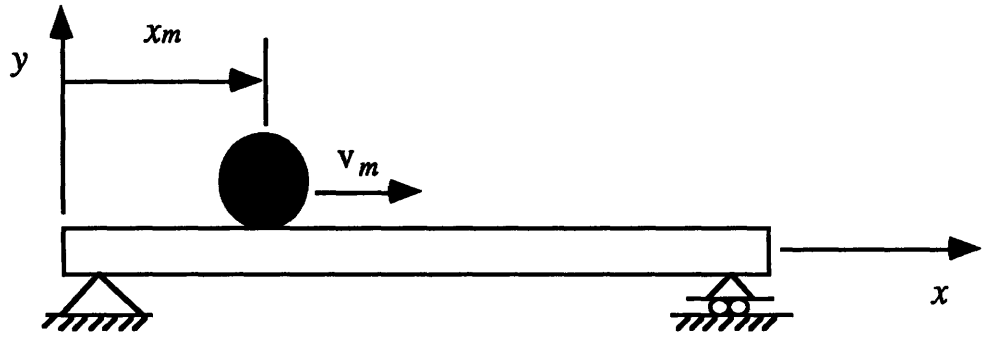

Figure 2. Simply-supported beam with a mass moving along its length.

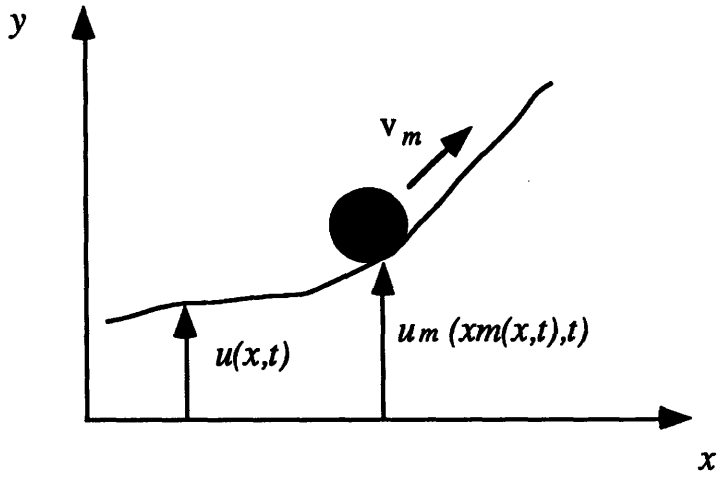

Figure 3. Free-free beam with a mass moving along its length.

The dynamics analysis presented is a general methodology applicable to both systems. In Sections 3.1.5 and 3.1.6, the equations are made specific to the inertially fixed and the inertially free systems, respectively.

3.1.1 Mathematical Model

There are several ways to formulate the equations of motion for the systems depicted in Figures 2 and 3. For an inertially fixed system, an exact continuous solution using an inverse Laplace transform may be used (Ref. [5]). For a more general system, an exact continuous solution is not available.

In this analysis, however, an assumed modes approach, which accurately gives the deformation while retaining only three modes, is used to solve the systems shown in the above figures. The assumed modes approach uses Galerkin's method to determine the beam deformation due to the motion of the mass. Galerkin's method assumes that the beam deflection can be approximated by a superposition of orthogonal mode shapes. The assumption here is that, using orthogonal modes, the error of the approximation vanishes as the number of modes retained is increased.

The inertial effects of the moving mass are included in this analysis. If these effects are ignored, the mobile transporter is

modeled as a moving force rather than as a moving mass. If the mass of the moving object is considered negligible compared to that of the flexible structure, the inertial effects can be ignored; however, if the mass of the object is comparable in size to the structure, these inertial effects should not be ignored.

Several cases of the two approaches for different moving object/flexible structure mass ratios were studied. The results are presented in Chapter 4. In the continuous and the discrete formulations, the flexible structure is modeled as a Bernouille-Euler beam.

3.1.2 Equations of Motion

The equations of motion for the flexible beam-moving mass system are derived in three steps:

(1) The partial differential equation describing the motion of the flexible structure is determined.

(2) The moving mass equation is obtained.

(3) A compatibility condition is invoked to obtain the equation of motion for the entire system. The compatibility condition is a direct consequence of Newton's third law. It states that for every force there is a reactive force equal in magnitude but opposite in direction. Thus, the force on the

beam due to the moving mass is equal to the force created by the acceleration of the mass but opposite in direction.

Flexible Structure Equation

The fourth-order partial differential equation describing the motion for a Bernoulli-Euler beam is (Ref. [15]):

$$\rho\,\ddot{u}(x,t) + EI\frac{\partial^4 u(x,t)}{\partial x^4} = F_{ext}(x,t) \tag{3.1}$$

The displacement field, $u(x,t)$, describes the motion of the mean chord of the deformed beam with respect to an inertial reference frame. This field contains any rigid body translation and rotation as well as flexible motion of the beam. Since the structure is modeled as a Bernouille-Euler beam, the mean chord of the beam is assumed to undergo pure translation as a result of the deformation. F_{ext} is the vector sum of the external forces applied to the beam. The material properties of the beam are considered to be homogeneous.

Moving Mass Equation

The equation describing the motion of the moving mass is considered. This equation is derived using Newton's second law of mechanics, which states that the force exerted on the mass is proportional to the absolute acceleration of the mass.

$$m_m \left(\frac{\partial^2 u_m (x_m (x,t),t)}{\partial t^2} \right)_{abs} = F_m (x_m (x,t),t) \tag{3.2}$$

where $F_m(x_m(x,t),t)$ is the force exerted on the moving mass.

The absolute acceleration of the beam is the acceleration of the moving mass displacement field, $u_m(x_m(x,t),t)$, with respect to an inertial reference frame. When differentiating the moving mass's displacement field, it is important to imagine a reference frame embedded in the moving mass. Since the mass is moving, the reference frame is also moving with respect to the inertial frame and adds its own terms to the acceleration of the mass. In this analysis, the mass is moving at a constant velocity v_m. Therefore, the absolute acceleration of the moving mass is

$$\left(\frac{\partial^2 u_m}{\partial t^2} \right)_{abs} = \ddot{u}_m + 2 v_m \frac{\partial^2 u_m}{\partial t \, \partial x_m} + v_m^2 \frac{\partial^2 u_m}{\partial x_m^2} \tag{3.3}$$

where the functional dependence of the variables are omitted for brevity.

As it stands, Eq. (3.3) is written as a function of the moving mass displacement field, u_m. To easily formulate the system equation, it would be helpful to express this equation in terms of the beam's displacement u. Since the mass is fixed to the beam, it cannot

slip and, at any time, the beam and the moving mass have the same displacement in terms of F_m. This relationship can be expressed mathematically by using the dirac delta function, which is a continuous function that depicts the value of a function at discrete times. Using this, the displacement of the mass is rewritten as a function of the displacement of the beam:

$$u_m = u_m \, \delta(x - x_m) \tag{3.4}$$

Since the dirac delta function is not a function of time, the spatial derivatives in Eq. (3.3) are rewritten as

$$\frac{\partial^2 u_m}{\partial x_m^2} = \frac{\partial^2 u}{\partial x^2} \delta(x - x_m) \tag{3.5}$$

$$\frac{\partial^2 u_m}{\partial x_m \partial t} = \frac{\partial^2 u}{\partial x \ \partial t} \delta(x - x_m) \tag{3.6}$$

Equations (3.5) and (3.6) are substituted into the absolute acceleration expression for the moving mass. The force equation for the moving mass then can be written in a form more compatible to the flexible beam equation:

$$m_m \left[\ddot{u} + 2 \, v_m \frac{\partial^2 u}{\partial t \, \partial x} + v_m^2 \frac{\partial^2 u}{\partial x^2} \right] \delta(x - x_m) = F_m \tag{3.7}$$

Compatibility Equation

Newton's third law of dynamics states that for every force there is a reactive force equal in magnitude but opposite in direction. Using this law, the compatibility equation between the moving mass and the flexible beam is determined. The force exerted on the beam due to the moving mass is equal in magnitude but opposite in direction to the force defined by Eq. (3.7). The total force exerted on the beam is the sum of the force due to the moving mass plus any other external forces acting on the beam:

$$F_{ext} = f_{ext} - F_m \tag{3.8}$$

where f_{ext} is any arbitrary external force. The external force applied to the beam varies depending on which environment is being simulated. The actual value of f_{ext} for the two systems studied is shown in Sections 3.1.5 and 3.1.6. Using Eq. (3.7) the total force applied to the beam is

$$F_{ext} = f_{ext} - m_m \left[\ddot{u} + 2\, v_m \frac{\partial^2 u}{\partial t\, \partial x} + v_m^2 \frac{\partial^2 u}{\partial x^2} \right] \delta(x - x_m) \tag{3.9}$$

System Equation

The equation of motion for the entire system is obtained by using the force expression found in Eq. (3.9) and substituting it into

the beam equation (Eq. (3.1)). For clarity, any terms involving the displacement of the beam are shown on the left-hand side of the equation even though they appear due to the force exerted by the moving mass. A fourth-order partial differential equation describing the total displacement of the beam as a mass moves at a constant velocity along its length is

$$\rho \ddot{u} + EI \frac{\partial^4 u}{\partial x^4} + m_m \left[\ddot{u} + 2 v_m \frac{\partial^2 u}{\partial t \partial x} + v_m^2 \frac{\partial^2 u}{\partial x^2} \right] \delta (x - x_m) = f_{ext} \tag{3.10}$$

The displacement field can contain translations and rotations. The boundary condition of the beam does not change the form of this general equation.

Modal Solution

Equation 3.10 must be rewritten into a form more suitable for numerical computation. For certain systems, this equation can be solved directly using an inverse Laplace transform. A more general approach is described here. A linear superposition of orthogonal modes is used to represent the beam's vibration. The new modal representation contains a mode shape, ϕ_i, which is only dependent on space, and a modal coordinate, η_i, which is only a function of time.

$$u(x,t) = L \sum_{i=1}^{N} \phi_i(x) \eta_i(t) \tag{3.11}$$

where N is the number of modes. As the number of modes approaches infinity, the modal approximation approaches the exact displacement of the beam $u(x,t)$. The actual modes used depend on the system being analyzed. The mode shapes used for the simply-supported and free-free beam systems are shown in Sections 3.1.5 and 3.1.6, respectively.

It is not feasible to use an infinite amount of modes to model the displacement. Different variations of the assumed modes approach that drive the error of the approximation to zero for a small amount of modes have been developed. One of these methods is known as Galerkin's method, which uses the orthogonal property of the modes to drive the error to zero.

Equation (3.11) is used to substitute the modal coordinate $\eta_i(t)$ for the natural coordinate $u(x,t)$; this substitution is used in Eq. (3.10). This new equation can be integrated since the mode shapes ϕ_i are not a function of time. Before the integration takes place, the new equation is premultiplied by the transpose of the mode shapes $\phi_j(t)$. Since the modes are orthogonal, this step reduces the error of the approximation. The resulting integral equation is

$$\int_0^L \phi_j \left(\sum_{i=1}^{N} EI\, \phi_i^{IV}\, \eta_i + \rho\, \phi_i\, \ddot{\eta}_i \right) dx + \qquad j = 1, 2, \cdots N$$

$$m_m\, \phi_j \sum_{i=1}^{N} \left(\phi_i\, \ddot{\eta}_i + 2\, v_m\, \phi_i'\, \dot{\eta}_i + v_m\, \phi_i''\, \eta_i \right)_{@\, x_m} = f_{\eta ext_j} \tag{3.12}$$

where

$$f_{\eta ext_j} = \frac{1}{L} \int_0^L \phi_j\, f_{ext}\, dx \tag{3.13}$$

The roman numeral superscript indicates a spatial derivative of the appropriate order. A special relationship involving the dirac delta function was used in obtaining the above equation

$$\int f(x)\, \delta(x - x_m)\, dx = f(x_m) \tag{3.14}$$

Nondimensional Integrals

The mode shapes are only a function of space; therefore, the integral in Eq. (3.12) can be determined either analytically or numerically. To condense the equation into a more readable form, two nondimensional integrals are defined (Eqs. (3.15), (3.16)). The values of $I1$ and $I2$ for the simply-supported beam are found in Section 3.1.5. The values of the free-free beam are listed in Appendix C.

$$I_1(i,j) = \frac{1}{L}\int_0^L \phi_i \, \phi_j \, dx \tag{3.15}$$

$$I_2(i,j) = L^3 \int_0^L \phi_i^{IV} \, \phi_j \, dx \tag{3.16}$$

Equation (3.12) is rewritten using the definitions in Eqs. (3.15) and (3.16).

$$\sum_{i=1}^{N} \left(\rho L \, I_1(i,j) \, \ddot{\eta}_i + \frac{EI}{L^3} I_2(i,j) \eta_i \right) + \qquad j = 1, 2, \cdots N$$

$$m_m \, \phi_j \sum_{i=1}^{N} \left(\phi_i \, \ddot{\eta}_i + 2 \, v_m \, \phi_i' \, \dot{\eta}_i + v_m \, \phi_i'' \, \eta_i \right)_{@ \, x_m} = f_{\eta ext_j} \tag{3.17}$$

Equation (3.17) represents n first-order differential equations describing the total modal displacement of the system. Next, Eq. (3.17) must be put into a nondimensional form.

3.1.3 Nondimensional Equations of Motion

A general procedure for placing the equations of motion into a nondimensional form is presented. First, the reference parameters for each variable in the equation must be defined. Then, each variable is divided by the appropriate reference parameter. The reference parameters for the mass, time, and length variables are:

$$Mass \rightarrow \rho L \tag{3.18}$$

$$Time \rightarrow \frac{L}{v_m} \tag{3.19}$$

$$Displacement \rightarrow L \tag{3.20}$$

The mass terms are made nondimensional by the beam's mass. The time reference parameter is the time required for the moving mass to travel the beam's length. The beam's length is used as the reference parameter for displacement.

For clarity, nondimensional parameters are defined below and appear after the terms are divided by their respective reference parameters.

$$\Omega_i = \omega_i t_r = \frac{\omega_i L}{v_m} \tag{3.21}$$

$$\mu_m = \frac{m_m}{\rho L} \tag{3.22}$$

$$\lambda = \frac{EI}{\rho L^4} t_r^2 = \frac{EI}{\rho \, v_m^2 \, L^2} \tag{3.23}$$

$$\tau = \frac{t}{t_r} = \frac{t \, v_m}{L} \tag{3.24}$$

$$\mu_{f_j} = \frac{f_{\eta ext_j}}{\rho L^2} t_r^2 = \frac{f_{\eta ext_j}}{\rho \, v_m^2} \tag{3.25}$$

where $t_r = \frac{L}{v_m}$ is the reference time defined above. The parameters represent the frequency, mass, stiffness, time, and external force of the system, respectively. In the following equations, an over-script o is used to represent a derivative with respect to the nondimensional time parameter τ, i.e.,

$$(\,)^o = \frac{\partial}{\partial \tau} = t_r \frac{\partial}{\partial t} = \frac{L}{v_m} \frac{\partial}{\partial t} \tag{3.26}$$

Using the nondimensional procedure outlined previously, Eq. (3.17) is made nondimensional:

$$\sum_{i=1}^{N} \left(I_1(i,j) \, \eta_i^{oo} + \lambda \, I_2(i,j) \, \eta_i \right) + \\ + \mu_m \phi_j \sum_{i=1}^{N} \left(\phi_i \, \eta_i^{oo} + 2 \, \phi_i' \, \eta_i^{o} + \phi_i'' \, \eta_i \right) @ \, x_m = \mu_{f_j} \qquad j = 1, 2, \ldots N \tag{3.27}$$

Equation (3.27) describes the displacement of the modal coordinate due to the motion of a moving mass and an externally applied force. Next, this equation must be rewritten in a form suitable for numerical simulation.

3.1.4 State Space Representation

The system depicted in Eq. (3.27) is described using a state-determined mathematical model. In this type of model, the system is described by a set of ordinary differential equations in terms of state variables (Ref. [16]). The future of all the variables associated with the system is predicted from the previous time history of the state variables. The only information needed about the system is the initial condition of the state variables and the equations defining the future time history of these variables.

To obtain a state space representation, an n^{th}-order differential equation must be transformed into n first-order differential equations. Equation (3.27) is already in the required form. Next, an arbitrary set of state variables are chosen. For this model, the modal displacements and their associated velocities are chosen as the state variables: the displacements are chosen since they are the desired output, and the velocities are chosen so the

matrices take on a familiar form. The two sets of state variables are combined into one state vector

$$x = \left\{ \eta_1 \quad \cdots \quad \eta_N \quad \overset{o}{\eta}_1 \quad \cdots \quad \overset{o}{\eta}_N \right\}^T \tag{3.28}$$

In a state-determined formulation, the time derivative of the state vector is a function of the state variables

$$\overset{o}{x} = F(x) \tag{3.29}$$

Equations (3.28) and (3.29) show that the acceleration at any point can be expressed as a function of the velocity and displacement at that point. Once the accelerations are known, the velocities and displacements are obtained by numerically integrating the system equation of motion forward in time.

Matrix Representation

For easy evaluation, Eq. (3.27) is placed into a matrix representation describing the states of the system. The equation is first rewritten so that it follows the standard matrix equation describing a dynamical system

$$M \overset{oo}{\eta} + C \overset{o}{\eta} + K \eta = F \tag{3.30}$$

where M, C, K, and F represent the mass, damping, stiffness, and force matrices, respectively. η is the vector containing the modal displacements

$$\eta = [\ \eta_1 \quad \cdots \quad \eta_N\ ] \tag{3.31}$$

The definition of the state vector is used to place Eq. (3.30) into the form of Eq. (3.29). The final result is an equation that can be integrated to obtain the modal displacements and the modal velocities:

$$\overset{o}{x} = \begin{bmatrix} 0 & E \\ -M^{-1}K & -M^{-1}C \end{bmatrix} x + \begin{bmatrix} 0 \\ M^{-1}F \end{bmatrix} \tag{3.32}$$

where E is the identity matrix.

Additional terms representing structural damping are added to the damping matrix. It is easier to represent structural damping in modal coordinates rather than natural coordinates; therefore, the additional terms are already in modal form. Any off-diagonal modal terms are assumed to be negligible so the only extra terms appear on the diagonal. From Ref. [15], modal damping takes the form

$$[C_o]_{i,i} = 2\,\zeta\sqrt{\lambda\ I_1\ (i,i)\ I_2\ (i,i)} \tag{3.33}$$

where Ω_i is the nondimensional frequency of the beam. The beam's frequency depends on its boundary condition. The natural frequencies for the two systems examined are shown in Sections 3.1.5 and 3.1.6.

The mass, stiffness, and damping matrices all contain a constant and a time-varying component. The form of the force matrix depends on the type of external force applied to the system. The constant matrix is diagonal and represents the dynamics of the flexible beam without any moving mass. The time-varying matrix is fully populated and comes directly from the inertial effects of the moving mass. The combination of both matrices forms the total mass, stiffness, and damping matrices that are fully populated and time-varying. The constant matrices have the subscript o and the time-varying matrices have the subscript var. The total matrices are the sum of the two:

$$M = M_o + M_{var} \tag{3.34}$$

$$C = C_o + C_{var} \tag{3.35}$$

$$K = K_o + K_{var} \tag{3.36}$$

First, the constant mass and stiffness matrices are determined. The constant modal damping matrix was defined by Eq. (3.33). Even

though the actual values of the integrals have not been shown, the mode shapes used are orthogonal, ensuring the corresponding matrices will be diagonal.

$$[M_o]_{i,i} = I_1(i,i) \tag{3.37}$$

$$[K_o]_{i,i} = \lambda I_2(i,i) \tag{3.38}$$

Next, the time-varying matrices are shown. Note that in the following matrices the mode shapes and their derivatives are evaluated at the position of the moving mass, x_m. Since x_m depends on time, the values of the matrices also vary with time.

$$[M_{var}]_{i,j} = \mu_m \phi_i \phi_j \tag{3.39}$$

$$[C_{var}]_{i,j} = 2 \mu_m \dot{\phi}_i \phi_j \tag{3.40}$$

$$[K_{var}]_{i,j} = \mu_m \ddot{\phi}_i \phi_j \tag{3.41}$$

As stated previously, the vector containing the external forces may or may not be time varying, depending on the actual value of the external force applied. In symbolic terms, the force vector is

$$F = \begin{bmatrix} \mu_{f1} \\ \vdots \\ \mu_{fN} \end{bmatrix} \tag{3.42}$$

The matrices shown in the Eqs. (3.37), (3.38), (3.39), (3.40), (3.41), and (3.42) are used in Eq. (3.32). The resulting expression is then numerically integrated to obtain the modal displacements and velocities at every point in time. Using Eq. (3.11) the modal displacements are transformed into the desired natural displacements.

To reiterate, the analysis presented so far has been for the general flexible beam/moving mass system. Two systems are examined in detail using numerical methods: the inertially fixed system, which is modeled using a simply-supported beam, and inertially free system, which is modeled using a free-free beam. Both systems are explained in greater detail in Sections 3.1.5 and 3.1.6, respectively.

3.1.5 Applications to a Simply-Supported Beam

The simply-supported system shown in Figure 2 represents many different physical systems. The most common physical system associated with this model is a truck traveling over a flexible bridge. The simply-supported beam model is used in this analysis to check the discrete methodology. One advantage of using this model is the availability of previously published results. Another advantage of simulating this system is the simplicity of the mode shapes. The

nondimensional integrals can be calculated by hand; therefore, the numerical code used to simulate the system is easily checked when the simply-supported modes are used.

The modes of a simply-supported beam are (Ref. [17])

$$\phi_i(x) = \sin \frac{i \pi x}{L} \tag{3.43}$$

These modes are orthogonal but not orthonormal. The corresponding nondimensional frequencies of the beam are

$$\Omega_i = \omega_i \frac{L}{v_m} = (i \pi)^2 \sqrt{\lambda} \tag{3.44}$$

which are used in Eq. (3.33) to determine the constant component of the nondimensional damping matrix.

Once the mode shapes are known, the values of the nondimensional frequencies are determined. For the mode shapes shown in Eq. (3.43), the integrals are determined analytically:

$$I_1(i,i) = \frac{1}{2} \tag{3.45}$$

$$I_2(i,i) = \frac{(i \pi)^4}{2} \tag{3.46}$$

The mode shapes shown in Eq. (3.43) are also used to develop the matrices given by Eqs. (3.33)-(3.41). Since the mode shapes for this system are simple sine waves, the matrices can easily be put into their symbolic form:

$$M = \begin{bmatrix} \frac{1}{2} + \mu_m \sin \pi\tau \sin \pi\tau & \cdots & \mu_m \sin \pi\tau \sin N\pi\tau \\ & & \vdots \\ sym & & \frac{1}{2} + \mu_m \sin N\pi t\tau \sin N\pi\tau \end{bmatrix} \tag{3.47}$$

$$C = 2\pi \begin{bmatrix} \zeta\pi\frac{\sqrt{\lambda}}{2} + \mu_m \sin\pi\tau \cos\pi\tau & \cdots & \mu_m N \sin\pi\tau \cos N\pi\tau \\ \vdots & \vdots & \vdots \\ \mu_m \sin N\pi\tau \cos\pi\tau & \cdots & \zeta N^2\pi\frac{\sqrt{\lambda}}{2} + \mu_m N \sin N\pi\tau \cos N\pi\tau \end{bmatrix} \tag{3.48}$$

$$K = \begin{bmatrix} \frac{1}{2}\pi^4\lambda - \pi^2 \sin N\pi\tau \sin \pi\tau & \cdots & -N^2\pi^2 \sin \pi\tau \sin N\pi\tau \\ \vdots & \vdots & \vdots \\ -\pi^2 \sin N\pi\tau \sin \pi\tau & \cdots & \frac{1}{2}(N\pi)^4\lambda - N^2\pi^2 \sin N\pi\tau \sin N\pi\tau \end{bmatrix} \tag{3.49}$$

It is easy to see the constant and time-varying components of these matrices. It is also apparent that only the total mass matrix and the constant components of the damping and stiffness matrices are symmetric. For more complex systems it is harder to write these matrices in their symbolic form.

The simply-supported beam is used to model an inertially fixed space station. To correctly model this environment, a gravitational field is imposed on the system. The external force applied to the beam is the gravitational force of the moving mass, $f_{ext} = -m_m\, g\, \delta(x - x_m)$. Since the mass is moving, this force varies with time. Using Eqs. (3.13) and (3.14), the force vector used for this simulation is

$$F = -\begin{bmatrix} \mu_g \sin \pi\tau \\ \vdots \\ \mu_g \sin N\pi\tau \end{bmatrix} \tag{3.50}$$

where μ_g is a nondimensional parameter for the gravitational force applied to the beam:.

$$\mu_g = \frac{m_m\, g}{\rho\, L^2}\, t_r^2 = \frac{m_m\, g}{\rho\, v_m^2} \tag{3.51}$$

The results of this simulation are presented in Chapter 4.

3.1.6 Applications to a Free-Free Beam

The free-free system, shown in Figure 3, may represent a crude model of the space station-mobile transporter system as it orbits around earth. The transporter is connected to the space station at one point. Therefore, this model depicts the transporter as a wheel travelling over the truss, rather than as a train travelling on a track. The train/track aspect of the mobile transporter is examined in Section 3.3.

The model used to describe the inertially free system is a free-free flexible beam with the rigid transporter travelling along its length. The modes of a free-free beam are (Ref. [17])

$$\phi_1 = 1$$

$$\phi_2 = \bar{x} - 1/2 \tag{3.52}$$

$$\phi_i = \cos \beta_i \bar{x} + \cosh \beta_i \bar{x} - \sigma_i (\sin \beta_i \bar{x} + \sinh \beta_i \bar{x}) \qquad 3 \le i \le N$$

where

$$\bar{x} = \frac{x}{L} \tag{3.53}$$

The first mode corresponds to rigid body translation. The second mode corresponds to rigid body rotation. The next N+2 modes are the flexible modes of the free-free beam. All the mode shapes are nondimensional, orthogonal, and orthonormal. The values for β_i and σ_i for the first three flexible modes are located in Appendix C.

The corresponding nondimensional frequencies of the free-free beam are

$$\Omega_i = \beta_i^2 \sqrt{\lambda} \tag{3.54}$$

which, for this system, are the frequencies used when forming the constant modal damping matrix.

For the free-free beam system, the nondimensional integrals are not determined analytically. Instead, I_1 and I_2 are determined by numerical integration. A fourth-order Runge Kutta integration scheme (detailed in Appendix B) is used, which is the same integration scheme used to integrate the equations of motion.

The constant matrices are formed using the nondimensional integrals and the nondimensional frequencies. The time-varying matrices are formed using the mode shapes given in Eq. (3.52) at the appropriate value of τ. There is nothing gained by writing out the specific matrices in their symbolic form for this system. The constant mass, stiffness, and damping matrices for the first three flexible modes are available in Appendix C.

Since this system is designed to model an inertially free system, there is no gravitational field present. An initial vibration or an external force is needed to excite the system. For this simulation, an initial vibration was used rather than an external force. When the SS-MT system is attached to the shuttle system it is possible for the first mode to be excited due to the attitude control system of the shuttle. To create an initial excitation the left and right tip deformations were set equal to .02L with the contributions from the first mode only. The moving mass was then released onto the beam as it was vibrating. The results are presented in Chapter 4.

3.2 DISCRETE FORMULATION

Section 3.2 develops the discrete formulation of the SS-MT system that was analyzed in Section 3.1. The results obtained from this derivation are compared to the results obtained by the continuous formulation derived in Section 3.1. As before, two different systems are examined. The first system model, shown in Figure 2, represents a moving mass traveling along an inertially fixed structure. The second system, shown in Figure 3, represents the mass moving over an inertially free structure such as the space station.

A general methodology is presented for analyzing any system. In Sections 3.2.5 and 3.2.6 the methodology is made specific for the two systems described above.

3.2.1 Mathematical Model

In this formulation, the continuous systems of the previous sections will be placed into a discrete representation. As stated previously, a Bernouille-Euler beam is used to model the flexible structure. Discrete mass and stiffness matrices are determined for the flexible beam. The deflection of the beam and all the external forces applied to the beam are made discrete by introducing an

invertible operator that distributes the effects of the moving mass over the appropriate discrete elements.

First, the discrete equation of motion for the flexible structure is developed by creating discrete mass and stiffness matrices using either finite-element or lumped-parameter methods. These matrices represent the physical properties of the flexible structure. The goal is to discretize the load exerted on the beam due to the moving mass so it can be used with the already existing property matrices. To achieve this, a vector is formed that distributes the continuous forces along the beam's discrete points. A vector is created using two different finite-element shape functions: linear and cubic, which are compared in Chapter 4. Using the equivalent forces, the discrete equation is formed. To coincide with the continuous formulation, the discrete equation is formed in terms of modal coordinates. This equation is then made nondimensional and placed into state space domain. The results for the simply-supported and the free-free beam are shown in Chapter 4.

3.1.2 Equations of Motion

The discrete matrices that represent the mass and stiffness of the beam are determined and are used to write the general matrix equation of motion for a beam. This equation is the same one shown in Eq. (3.30) but is rewritten here for convenience

$$M\ddot{q} + C\dot{q} + Kq = F \tag{3.55}$$

where M, C, K, and F represent the mass, damping, stiffness, and force matrices, respectively. When this equation was used in Section 3.1, the matrices used represented the physical properties of the modes used to describe the motion. In the above equation, the matrices represent the discrete properties of the different beam elements used to model the beam. Even though the two equations have the same form, they represent two different systems.

First, the discrete mass and stiffness matrices are formed. A discrete matrix for the damping is not developed in this subsection; however, a modal damping matrix is introduced in Section 3.2.4. The discrete stiffness matrix is developed using finite-element (or energy-consistent) techniques. Two different discrete mass matrices are formed. One matrix, developed from finite-element techniques, is used when it is important to keep the rotational inertias of the beam elements. The other mass matrix, formed using a lumped parameter model, is used when only the translational degrees of freedom of the beam elements are required.

Next, a vector is developed that weights the continuous force due to the mass over the discrete beam elements. This vector is also used to discretize the deflection due to the moving mass. By

combining the discrete property matrices and the discrete forces due to the moving mass, the discrete equation of motion for the system is formed.

Mass Matrix

The mass matrix for the beam is derived using both a lumped-parameter analysis and the energy-consistent finite-element method. When the linear shape function is used, the rotational degrees of freedom are statically condensed out of the mass and stiffness matrices; therefore, a lumped-parameter model is easily used. When the cubic shape function is used, each element's rotational degrees of freedom are needed; therefore, the mass matrix will be developed using the finite-element method.

Lumped-Parameter Model. The lumped-parameter method is appropriate only when the beam's material properties are homogeneous. In this particular analysis, this requirement is met; therefore, the model is valid. First, the beam is broken up into n finite elements. Then the mass of each element is distributed between the two neighboring nodes. In the case of the lumped-parameter model, the mass contribution at each node is half the mass of each element. The mass of each element is

$$m_e = \rho l_e \tag{3.56}$$

where l_e is the length of each element and is defined as

$$l_e = \frac{L}{n} \tag{3.57}$$

Since the material properties are continuous throughout the beam, the total mass at each node is the sum of the contributions from the two neighboring elements. The total mass at each node is

$$\begin{aligned} m_i &= \frac{1}{2} m_e + \frac{1}{2} m_e \\ &= m_e \end{aligned} \qquad 2 \le i \le n \tag{3.58}$$

Since the first and last nodes only feel the effects of one finite element, the mass contribution at those nodes is half the mass contribution at the inner nodes.

Each node has a corresponding translation and rotation. Since the rotational inertias of each beam element are so small, the rotational degree of freedom can be eliminated from the stiffness matrix by using static condensation.

When the linear shape function is used to distribute the force, only the translations at each node are important. Therefore, the mass matrix should only contain the translational degrees of freedom, which is accomplished fairly easily in a lumped-parameter mass matrix. The lumped mass matrix is diagonal with every other

row, starting with the first row, corresponding to the translational degrees. The other rows correspond to the rotational inertias of each node. Since this will not be included in the mass matrix, the rotational inertias have not been shown. The final translational mass matrix has n+1 degrees of freedom and is in the following form

$$M_t = \begin{bmatrix} \ddots & 0 & 0 \\ 0 & m_i & 0 \\ 0 & 0 & \ddots \end{bmatrix} \begin{matrix} \\ n+1 \\ \\ \\ n+1 \end{matrix} \tag{3.59}$$

This matrix is constant and discrete.

Finite-Element Model. The matrix shown in Eq. (3.59) is used with the linear shape function. However, when the cubic shape function is used it is necessary to have access to *both* the translational and rotational degrees of freedom. It is possible to simply add the rotational inertias of the elements into the lumped-parameter model shown above. Instead, however, an energy-consistent mass matrix is developed. The finite-element approach is used to show another way to obtain a discrete mass matrix and is also used for the stiffness matrix. Each element of the finite-element mass matrix is (Ref. [15])

$$m_{ij} = \int_0^L s_i \, s_j \, dx \tag{3.60}$$

where s_i is a finite-element trial function. To correctly model a beam element, Hermites cubics are chosen for the trial functions because they have a continuous spatial second derivative (Ref. [15]). A trial function is needed for the deflection and the slope at each end of the element. Therefore, four trial functions for each element are needed. The four cubics are shown below.

$$s_1 = 1 - 3\left(\frac{x}{l_e}\right)^2 + 2\left(\frac{x}{l_e}\right)^3 \tag{3.61}$$

$$s_2 = \frac{x}{l_e} - 2\left(\frac{x}{l_e}\right)^2 + \left(\frac{x}{l_e}\right)^3 \tag{3.62}$$

$$s_3 = 3\left(\frac{x}{l_e}\right)^2 - 2\left(\frac{x}{l_e}\right)^3 \tag{3.63}$$

$$s_4 = -\left(\frac{x}{l_e}\right)^2 + \left(\frac{x}{l_e}\right)^3 \tag{3.64}$$

To determine the mass matrix for one element, the above trial functions are substituted into Eq. (3.60). This expression is then integrated to obtain the elemental mass matrix. The mass matrix is partitoned into four different matrices

$$m = \frac{m_e l_e}{420}\begin{bmatrix} m_{11} & m_{12} \\ m_{21} & m_{22} \end{bmatrix} \tag{3.65}$$

where m_e and l_e are the mass and length of each element, respectively. The four matrices are

$$m_{11} = \begin{bmatrix} 156 & 22\,l_e \\ 22\,l_e & 4\,l_e^2 \end{bmatrix} \tag{3.66}$$

$$m_{12} = \begin{bmatrix} 54 & -13\,l_e \\ 13\,l_e & -3\,l_e^2 \end{bmatrix} \tag{3.67}$$

$$m_{21} = \begin{bmatrix} 54 & 13\,l_e \\ -13\,l_e & -3\,l_e^2 \end{bmatrix} \tag{3.68}$$

$$m_{22} = \begin{bmatrix} 156 & -22\,l_e \\ -22\,l_e & 4\,l_e^2 \end{bmatrix} \tag{3.69}$$

Next, the elemental mass matrices are combined to form the final global mass matrix. At this point all the degrees of freedom, translational and rotational, are present. Since the inner nodes connect two consecutive elements, the elemental mass matrices overlap. Therefore, the final global mass matrix is

$$m = \frac{m_e}{420n} \begin{bmatrix} m_{11} & m_{12} & 0 & 0 & 0 \\ m_{21} & m_{11} + m_{22} & m_{12} & 0 & 0 \\ 0 & \ddots & \ddots & \ddots & 0 \\ 0 & 0 & \ddots & m_{11} + m_{22} & m_{12} \\ 0 & 0 & 0 & m_{21} & m_{22} \end{bmatrix} \tag{3.70}$$

Stiffness Matrix

The stiffness matrix is developed using finite-element techniques. When the linear shape function is used, only the translations at each node are required. Therefore, the rotational degrees of freedom are statically condensed out. The global stiffness matrix is developed the same way as the energy-consistent mass matrix. Using the finite-element method, the elemental stiffness matrix is determined by (Ref. [15])

$$k_{ij} = \int_0^L \frac{\partial s_i}{\partial x} \frac{\partial s_j}{\partial x} \, dx \tag{3.71}$$

Once again the cubics shown in Eqs. (3.61)-(3.64) are substituted into Eq. (3.71). After integration, the elemental stiffness matrix is obtained and, like the mass matrix, is also partitoned into four different matrices:

$$k = \frac{(EI)_e}{l_e^3} \begin{bmatrix} k_{11} & k_{12} \\ k_{21} & k_{22} \end{bmatrix} \tag{3.72}$$

where $(EI)_e$ is the elemental bending stiffness. The four matrices are

$$k_{11} = \begin{bmatrix} 12 & 6l_e \\ 6l_e & 4l_e^2 \end{bmatrix} \tag{3.73}$$

$$k_{12} = \begin{bmatrix} -12 & 6l_e \\ -6l_e & 2l_e^2 \end{bmatrix} \tag{3.74}$$

$$k_{21} = \begin{bmatrix} -12 & -6l_e \\ 6l_e & 2l_e^2 \end{bmatrix} \tag{3.75}$$

$$k_{22} = \begin{bmatrix} 12 & -6l_e \\ -6l_e & 4l_e^2 \end{bmatrix} \tag{3.76}$$

Next, the element stiffness matrices are combined to form the global stiffness matrix. At this point all the degrees of freedom, translational and rotational, are present. Since the inner nodes connect two consecutive elements, the stiffness matrices overlap. Therefore, the final global stiffness matrix is

$$k = \frac{(EI)_e}{l_e^3} \begin{bmatrix} k_{11} & k_{12} & 0 & 0 & 0 \\ k_{21} & k_{11} + k_{22} & k_{12} & 0 & 0 \\ 0 & \ddots & \ddots & \ddots & 0 \\ 0 & 0 & \ddots & k_{11} + k_{22} & k_{12} \\ 0 & 0 & 0 & k_{21} & k_{22} \end{bmatrix} \tag{3.77}$$

When the linear shape function is used, Eq. (3.77) is altered to condense out the rotational degrees of freedom. This reduced stiffness matrix is used in conjunction with the mass matrix shown in Eq. (3.59). For the cubic shape function, the matrix, as it stands in Eq. (3.77), is used with the similar mass matrix shown in Eq. (3.70) that contains both the translational and rotational degrees of freedom.

The global stiffness matrix of Eq. (3.76) can again be partitoned into four separate matrices, k_{tt}, k_{tr}, k_{rt}, and k_{tt}. The subscripts indicate either translational or rotational degrees of freedom. The partitoned stiffness matrix is

$$k = \frac{(EI)_e}{l_e^3}\begin{bmatrix} k_{tt} & k_{tr} \\ k_{rt} & k_{rr} \end{bmatrix} \tag{3.78}$$

As stated previously, the rotational degrees of freedom are eliminated when using the linear shape function. The rotational degrees of freedom are statically condensed out. This is achieved by using the static matrix equation in Eq. (3.79):

$$\begin{bmatrix} k_{tt} & k_{tr} \\ k_{rt} & k_{rr} \end{bmatrix}\begin{Bmatrix} v \\ \theta \end{Bmatrix} = \begin{bmatrix} 0 \\ 0 \end{bmatrix} \tag{3.79}$$

where v is a generic translational coordinate and θ is a generic rotational coordinate. Solving for θ in terms of the translation, v, the reduced stiffness matrix becomes

$$K_t = k_{tt} - k_{tr}\, k_{rr}^T\, k_{rt} \tag{3.80}$$

Eq. (3.79) is a square matrix that is constant and has (n+1) degrees of freedom. When the rotational degrees are not eliminated, the stiffness and the matching mass matrix has (2n + 2) degrees of freedom.

Beam Equation

Using the mass and stiffness matrices defined above the beam equation of motion is determined as

$$\widetilde{M}\,\ddot{q} + \widetilde{K}\,q = \widetilde{F}_t \tag{3.81}$$

where $\widetilde{M}$ and $\widetilde{K}$ are generic discrete matrices representing the appropriate mass and stiffness matrices, depending on which case is being examined. The nodal displacements, contained in the q vector, represent the displacement at each node for the different elements. The nodal displacements, q, should not be confused with the modal displacements, η, discussed in Section 3.1.2. The total discrete force vector, $\widetilde{F}_t$, is a combination of any external forces applied to the beam and the inertial effects of the moving mass. This force vector is the discrete form of the vector F_t. It correctly weights the effects of the moving mass onto the nodes of the beam. It is made discrete by using the discretization vector defined below.

Discretization Vector

In order to weight the effects of the continuous force between two discrete nodes, an invertible operator, called the discretization vector because it places the continuous forces into a discrete form

suitable for Eq. (3.81), is developed. For any arbitrary time the discretization vector weights the effects of the moving mass. Since the mass is moving along the the beam, the vector must change with time to reflect this motion. Finite-element shape functions are used to distribute the forces. Two different shape functions are examined below. The first function, which is based on a linear interpolation, only looks at the translation at each node. The second function, which is of cubic order, takes into account the translation and rotation at both nodes. The difference between the two approaches is examined at length in Chapter 4.

The two shape functions are developed in the same manner. A weighting function is used to locate the position of the moving mass with respect to the two appropriate nodes. The weighting function is defined as

$$\xi = \frac{x_m - x_i}{x_{i+1} - x_i} \tag{3.82}$$

The weighting function, ξ, depends on the distance between two neighboring nodes, x_i and x_{i+1}. Note that x_i is defined as the nodal position that is either directly at or to the immediate left of the moving mass. As soon as the point mass passes the x_i node location it is considered to be at the x_{i+1} position. The other variable, x_m, has previously been defined as the location of the moving mass.

The weighting function ξ in Eq. (3.82) is the discrete version of the continuous dirac delta function. The continuous function places the mass at a specific point, whereas ξ weights the force between two neighboring nodes.

To simplify the numerical evaluation of ξ, x_i is written in a suitable style for numerical evaluation. Two relationships are needed to accomplish this. First, as stated previously, the mass is considered to move at a constant speed; therefore, the position of the mass at an arbitrary time is always known. Next, it is assumed that the finite elements are of equal length. Using these facts, the distance between the two elements can be expressed as a function of the total beam length. These two relationships are shown symbolically as

$$x_m = v_m t \tag{3.83}$$

$$x_{i+1} - x_i = \frac{L}{n} \tag{3.84}$$

Using the above two relationships, weighting function ξ is rewritten as

$$\xi = (v_m t - x_i)\frac{n}{L} \tag{3.85}$$

where x_i is numerically calculated from

$$x_i = int\left(\frac{n}{L} v_m t\right) \Delta x \tag{3.86}$$

The *int ( )* function truncates and retains only the integer portion of a real number argument. Note that if the i^{th} node was defined as the node immediately to the right of the mass, then the position of x_i would be rounded up rather than truncated down as shown in Eq. (3.86).

Equations (3.85) and (3.86) are used to numerically evaluate the weighting function ξ. The first operator is linear with respect to the weighting function ξ.

$$V_1 = (1 - \xi) V_i + \xi V_{i+1} \tag{3.87}$$

where the following vectors are defined as

$$V_i^T = \left\{0, 0, \cdots, 0, \overset{i^{th}}{1}, 0, 0, \cdots, 0\right\}^{(1 \times f)} \tag{3.88}$$

$$V_{i+1}^T = \left\{0, 0, \cdots, 0, \overset{(i+1)^{th}}{1}, 0, 0, \cdots, 0\right\}^{(1 \times f)} \tag{3.89}$$

where f is the degree of freedom for the particular system being analyzed. When the above vectors premultiply the vector of nodal displacements, velocities, or accelerations, they will locate the i^{th} and $(i+1)^{th}$ values, respectively. In this method there are only

translational degrees of freedom; therefore, only one value at each node is required. In the cubic shape function, however, it is necessary to capture two values at each node.

When ξ is equal to zero, all the effects of the moving mass are placed at the i^{th} node. When ξ is equal to one, all the effects are placed at the $i^{th}+1$ node. For ξ values between zero and one, the effects are appropriately weighted between the two nodes.

The form of the linear interpolation function is easily determined without much computation. However, when the translations and the rotations at each node must be considered, the function's form is not easily seen. Therefore, the cubic shape function is developed in a more theoretical manner.

Cubic Shape Function Definition

As in the linear case, the cubic shape function is depicted as a function of ξ but for the cubic function, the coefficients are defined in terms of ξ, ξ^2, and ξ^3. Also, in this case, there are two displacements at each node - translation and rotation. The values of each node can be thought of as the boundary conditions for the shape functions. When there are only two boundary conditions to be satisfied, a linear function will suffice. To satisfy four boundary conditions, however, a cubic function is required.

Since there are four values that need to be captured (two at each node), four V vectors are needed, V_i, V_{i+1}, V_{i+2}, and V_{i+3}. The first and third vectors capture the translation at the i^{th} and $(i+1)^{th}$ nodes, respectively. The second and fourth vectors capture the rotation at the same respective nodes. Using these four vectors, the cubic shape function is determined using the standard finite-element method for determining shape functions, outlined below.

In determining the cubic shape function, it is necessary to develop four trial functions that will multiply the four vectors described above (Ref. [18]):

$$V_3 = T_i V_i + T_{i+1} V_{i+1} + T_{i+2} V_{i+2} + T_{i+3} V_{i+3} \tag{3.90}$$

Each trial function has the cubic form

$$T_i = a_i\xi + b_i\xi + c_i\xi^2 + d_i\xi^3 \tag{3.91}$$

The constants for each trial function are obtained by employing the four appropriate boundary conditions for each function (displayed in Table 1).

Table 1. Boundary Conditions used in Determining Cubic Trial Functions.

Trial Function	$\xi = 0$	$\xi = 1$
T_i	$T_i = l_e \quad T_{\xi i} = 0$	$T_i = 0 \quad T_{\xi i} = 0$
T_{i+1}	$T_{i+1} = 0 \quad T_{\xi i+1} = l_e$	$T_{i+1} = 0 \quad T_{\xi i+1} = 0$
T_{i+2}	$T_{i+2} = 0 \quad T_{\xi i+2} = 0$	$T_{i+2} = l_e \quad T_{\xi i+2} = 0$
T_{i+3}	$T_{i+3} = 0 \quad T_{\xi i+3} = 0$	$T_{i+3} = 0 \quad T_{\xi i+3} = l_e$

In Table 1 the subscript ξ indicates a derivative with respect to ξ. A similar table for the linear shape function could have been developed. However, in the linear shape function example it is trivial to develop the two trial functions.

Using these conditions the four shape functions are determined. It is found that the appropriate trial functions are the Hermite's cubics described in Eqs. (3.61)-(3.64). Substituting these trial functions into Eq. (3.90) leads to the final cubic shaping vector

$$V_3 = \left(1 - 3\,\xi^2 + 2\,\xi^3\right) V_i + \left(\xi - 2\,\xi^2 + \xi^3\right) \frac{1}{n} V_{i+1} + \left(3\,\xi^2 - 2\,\xi^3\right) V_{i+2} + \left(-\,\xi^2 + \xi^3\right) \frac{1}{n} V_{i+3} \tag{3.92}$$

For the general discrete derivation of the final equations, a generic discretization vector V is employed. This V vector represents either $V1$ or $V3$, depending on which interpolation function is used.

Load Modeling

The force exerted on the beam is broken up into two components: the first encompasses any external force that is applied to the beam, and the second is the force exerted on the beam due to the inertial effects of the moving mass. The total force is the sum of both components.

$$F_t = F_{ext} + F_m \tag{3.93}$$

Force Due to the Inertial Effects of the Moving Mass. The force due to the inertial effects of the moving mass is equal to the force created by the acceleration of the moving mass but it is opposite in direction. As seen in Section 3.1, the force is proportional to the absolute acceleration of the moving mass. This acceleration, however, is now given in terms of the discrete displacement field of the moving mass, q_m.

$$\tilde{F}_m(x_m(x,t),t) = - m_m \left(\frac{\partial^2 q_m(x_m(x,t),t)}{\partial t^2} \right)_{abs} \tag{3.94}$$

where $\tilde{F}_m$ is the moving mass's discrete force vector. Equation (3.94) is the discrete counterpart of Eq. (3.2). In the following derivation, the functional dependence of the variables are omitted for brevity.

The absolute acceleration of the discrete displacement field q_m, must be determined. In order to do this, a relationship is needed between the beam's displacement field and the moving mass' displacement field. In essence, a discrete counterpart of Eq. (3.4) is needed, which is accomplished by using the discretization vectors defined above. For a general methodology, the generic shape function V is used. The relationship between q_m and q is defined as

$$q_m = V^T q \tag{3.95}$$

Using Eq. (3.95), the absolute acceleration of the moving mass is written in terms of the beam's displacement. When determining the absolute derivatives, it is important to specify the variables of which V and q are a function. For simplicity it is assumed that V is a function of ξ only and ξ is independently a function of time. The beam's displacement field q, is only a function of time. Using these conventions and the definition of an absolute acceleration determined in Section 3.1, Eq. (3.94) becomes

$$\tilde{F}_m = - m_m \left[V^T \ddot{q} + 2 V_\xi^T \dot{\xi} \dot{q} + \left(V_\xi^T \ddot{\xi} + V_{\xi\xi}^T \left(\dot{\xi}\right)^2 \right) q \right] \tag{3.96}$$

In this system, the mass is assumed to move at a constant velocity; therefore, $\ddot{\xi}$ is equal to zero. Using the definition of ξ shown in Eq. (3.85), its derivative with respect to time is

$$\dot{\xi} = \frac{\mathrm{v}_m \, n}{L} \tag{3.97}$$

Using Eq. (3.19), the above equation is rewritten as

$$\dot{\xi} = \frac{n}{\tau} \tag{3.98}$$

where τ was previously defined as the time required for the mass to move over the entire beam length. Written in this form, it becomes apparent that $\dot{\xi}$ represents a first-order discrete spatial derivative. For the duration of the general derivation, the spatial derivatives, V_{ξ}^{T} and $V_{\xi\xi}^{T}$, are kept in their symbolic form. The actual values of both quantities for the linear and the cubic shape functions can be found in Appendix C.

When using the linear shape function, the last term in Eq. (3.96) is zero. This term represents the force exerted on the beam when the mass moves over the beam's curvature. By examining the continuous case, it is apparent that this term adds a substantial force to the beam. Therefore, an impulse force is added to correctly model this force that results from the difference in slope of two neighboring elements (see Figure 4 and Section 3.2.5).

When the higher-order, cubic shape function is used, the last term in Eq. (3.95) is not zero and the force from the beam's curvature appears without having to add an impulse force.

The inertial force due to the moving mass is now in a discrete form. The next challenge is to distribute the total force applied to the beam between appropriate nodes. Using Eqs. (3.93), (3.95,) and (3.98), the total force applied to the beam is

$$\widetilde{F}_t = \widetilde{F}_{ext} - m_m \left[V^T \ddot{q} + 2 \frac{n}{\tau} V_\xi^T \dot{q} + \left(\frac{n}{\tau}\right)^2 V_{\xi\xi}^T q \right] \qquad (3.99)$$

External Force. The external force applied to the beam is different for the two systems that are examined. For this derivation the external force is kept in its symbolic form.

The total force is distributed between the appropriate nodes of the beam, which, in this analysis, is accomplished by using the same finite-element shape functions described in detail in the beginning of this section. Using these shape functions, the total discrete force is distributed to the appropriate nodes as

$$\widetilde{F}_t = V \widetilde{F}_t \qquad (3.100)$$

Using Eq. (3.99) this force becomes

$$\tilde{F}_t = V\,\tilde{F}_{ext} - m_m \left(V\ V^T\,\ddot{q} + 2\left(\frac{n}{t}\right)\ V\,V_\xi^T\,\dot{q} + \left(\frac{n}{t}\right)^2\ V\,V_{\xi\xi}^T\,q \right) \quad (3.101)$$

Equation (3.101) is the discrete form of the force shown in Eq. (3.9).

System Equation of Motion

The entire discrete equation of motion for the system is obtained by substituting Eq. (3.101) into Eq. (3.99) resulting in Eq. (3.102) below. As in the continuous case, the terms involving the beam's deflection q, are shown on the left-hand side of the equation, even though they appear due to the inertial effects of the moving mass.

$$\left(\tilde{M} + m_m\,V\,V^T\right)\ddot{q} + 2\,m_m\,\frac{n}{t}\,V\,V_\xi^T\,\dot{q} + \left(\tilde{K} + m_m\left(\frac{n}{t}\right)^2 V\ V_{\xi\xi}^T\right) q = -\,V\,F_{ext} \quad (3.102)$$

Equation (3.102) is already in matrix form, unlike its continuous counterpart shown in Eq. (3.10), and is dimensional and in terms of the physical discrete beam coordinate q. Since the boundary conditions of the beam have not yet been specified, the above equation is valid for either the simply-supported or the free-free beam.

3.2.3 Nondimensional Equations of Motion

Unlike the equations in Section 3.1, Eq. (3.102) first is made nondimensional and then is transformed into the beam's modal coordinates. For the discrete analysis, it is easier to perform modal reduction once the equation is in nondimensional form. Even though Eq. (3.102) is a matrix equation, the same general procedure is used to place the equation into a nondimensional form. A matrix is considered nondimensional if each of its elements are nondimensional. Therefore, each element is divided by the appropriate reference parameter, defined in Section 3.1

When a common variable appears throughout an entire matrix, it can be extracted and placed in front of the matrix. This technique is used to define nondimensional mass and stiffness matrices. Referring to Eqs. (3.65) and (3.72), the new nondimensional matrices are

$$\widetilde{\widetilde{M}} = \frac{1}{\rho L}\widetilde{M} \tag{3.103}$$

$$\widetilde{\widetilde{K}} = \frac{L^3}{EI}\widetilde{K} \tag{3.104}$$

In a similar manner, the vectors containing the nodal accelerations, velocities, and displacements are made nondimensional by dividing each of their elements by the appropriate reference

parameters. Again, some variables can be extracted and placed in front of the vectors. Since all the variables are in front of the matrices, they are treated as scalars. These are combined to form the familiar nondimensional parameters defined in Eqs. (3.21)-(3.24). Using the new matrices, vectors, and nondimensional parameters previously defined, Eq. (3.102) in nondimensional form becomes

$$\left(\tilde{\tilde{M}} + \mu_m\right) \ddot{\bar{q}} + 2\,\mu_m\, n\, V\, V_\xi^T\, \dot{\bar{q}} + \left(\tilde{\tilde{K}} + \mu_m\, n^2\, V\, V_{\xi\xi}^T\right) \bar{q} = -\,\bar{\mu_f}\, V \qquad (3.105)$$

where

$$\bar{\mu_f} = \frac{F_{ext}}{\rho\, L^3}\, t_r^2 = \frac{F_{ext}}{\rho\, v_m^2\, L} \qquad (3.106)$$

is a new nondimensional force parameter representing a generic nondimensional external force. Equation (3.105) next is transformed into modal coordinates, making it easier to place into state space domain.

Modal Solution

Equation (3.105) is now transformed from the discrete physical beam nodal coordinates, q, to the beam's modal coordinates. At this point, the actual boundary conditions of the beam become integral. The equation, as it stands, is valid for any boundary condition; however, depending on the modes used, the equation is made

specific for the boundary condition being examined. The exact equations for the simply-supported and the free-free systems are shown in Sections 3.2.5 and 3.2.6, respectively.

In Section 3.1, a modal transformation was explained for the continuous formulation. The form for the discrete formulation is the same. Instead of defining a continuous mode shape $\phi_i(x)$, a discrete modal matrix ϕ, is defined. The actual modal coordinate η_i, is the same whether it is defined by the continuous mode shape and the beam's continuous displacement field u, or by the discrete modal matrix and the beam's discrete displacement field q.

$$\overline{q} = \varphi \eta \tag{3.107}$$

A description of some characteristics of the modal matrix follows. The actual transformation from physical coordinates to modal coordinates is completed. The resulting equation is nondimensional, is in modal coordinates, and is easily placed into state space domain.

Modal Matrix

The transformation from generalized coordinates to modal coordinates for the continuous formulation was shown in Eq. (3.11). A similar transformation, shown in Eq. (3.107), is valid for

nondimensional vectors. The mode shapes used are in the form of a modal matrix and, like the mode shapes already used, this modal matrix does not have any dimensions. Unlike the scalar operation shown in Eq. (3.11), Eq. (3.107) represents a matrix equation. The modal matrix consists of the eigenvectors of the simplified system

$$\tilde{\tilde{M}}\,\ddot{\underline{q}} + \tilde{\tilde{K}}\,\underline{q} = 0 \tag{3.108}$$

Equation (3.108) describes the discrete motion of the flexible beam without the moving mass. The number of modes present corresponds to the number of the system's degrees of freedom.

Transformation of Eq. (3.105)

Using the substitution shown in Eq. (3.107), Eq. (3.103) is transformed into modal coordinates. A discrete version of Galerkin's method, outlined in Section 3.1, is used. The resulting equation is premultiplied by the transpose of the the modal matrix to reduce the modal reduction error. This process is the matrix equivalent of using the continuous mode orthogonality to drive the error of the approximation to zero. For clarity, a definition of certain relationships follows.

First, the modal matrix ϕ is orthogonal with respect to the mass matrix, and is also mass normalized. This state leads to the following two definitions:

$$\phi^T \tilde{\tilde{M}} \phi = E \tag{3.109}$$

$$\phi^T \tilde{\tilde{K}} \phi = \Lambda \tag{3.110}$$

E has previously been defined in the nomenclature. Λ is the nondimensional matrix of eigenvalues corresponding to the system shown in Eq. (3.108). The Λ matrix is different depending on the boundary condition being examined. The dimension of the modal matrix is equivalent to the system's degree of freedom. For example, a free-free beam that is divided into ten equal beam elements has twenty degrees of freedom. It is not numerically efficient to retain all of these modes; therefore, before doing any numerical evaluation, the modal matrix and the corresponding eigenvalue matrix are reduced to retain a small number of nodes. In the actual numerical analysis, three flexible modes are retained. The reduced matrices are identified by a subscript r.

Second, the following relationships are defined for the weighting vectors with the reduced modal matrix.

$$V_\eta^T \equiv V^T \phi_r \tag{3.111}$$

$$V_{\eta\xi}^{T} \equiv V_{\xi}^{T}\,\phi_r \tag{3.112}$$

$$V_{\eta\xi\xi}^{T} \equiv V_{\xi\xi}^{T}\,\phi_r \tag{3.113}$$

Third, the modal damping matrix is developed. Since the modal decomposition of the discrete system is equivalent to the modes used for the continuous system, the modal damping matrix is the same. The damping due to the motion of the beam is assumed to be diagonal where the elements are defined by Eq. (3.32). The modal damping matrix is rewritten below for convenience.

$$\bar{C}_{\eta} = 2\,\zeta\left(\lambda\,\Lambda_r\right)^{1/2} \tag{3.114}$$

The matrix of Eq. (3.114) is defined in terms of the reduced matrix containing the eigenvalues defined in Eq. (3.110).

Using the nondimensional modal coordinate η, and the relationships defined in Eqs. (3.109)-(3.114), the nondimensional equation in modal coordinates becomes

$$\left(E + \mu_m\,V_{\eta}\,V_{\eta}^{T}\right)\overset{oo}{\eta} + \left(2\;\zeta\left(\lambda\,\Lambda_r\right)^{1/2} + 2\,\mu_m\,n\,V_{\eta}\,V_{\eta\xi}^{T}\right)\overset{o}{\eta} + \left(\lambda\,\Lambda_r + \mu_m\,n^2\,V_{\eta}\,V_{\eta\xi\xi}^{T}\right)\eta = -\,\bar{\mu_f}\,V_{\eta} \tag{3.115}$$

Equation (3.115) is the discrete counterpart of Eq. (3.27). It is a nondimensional matrix equation rather than a continuous integral equation like that shown in Section 3.1. Though Eq. (3.114) is a matrix equation, it is not in the typical state space form easiest for numerical evaluation.

3.2.4 State Space Representation

Even with a matrix equation, the first step in forming a state space representation is choosing the state variables. Once the state vector is formed, Eq. (3.115) is transformed into the state space domain.

State Vector

Two states variables are defined for the continuous system: the modal displacements and the velocities. Since the discrete analysis is already in matrix form, the state vector is written as the combination of two vectors

$$\boldsymbol{x} = \left[\eta \;\; \overset{o}{\eta} \right]^T \tag{3.116}$$

There is a difference between the number of elements used to model the beam n, and the number of modes retained to model the displacement of the beam N. The modal vectors have N elements,

whereas the q vector contains n values. Usually only three flexible modes are retained, whereas there might be 100 beam elements used to capture the beam's physical displacement.

Matrix Representation

The mass, stiffness, damping, and force matrices that are used to describe the system's states are determined. Similar to the matrices obtained for the continuous formulation, the following matrices are a combination of a constant matrix and a time-varying matrix. The time-varying components are a function of the discretizations vector V.

$$M = E + \mu_m V_\eta V_\eta^T \tag{3.117}$$

$$C = 2\,\zeta(\lambda \Lambda_r)^{1/2} + 2\,\mu_m n\; V_\eta V_{\eta\xi}^T \tag{3.118}$$

$$K = \lambda \Lambda_r + \mu_m n^2 V_\eta V_{\eta\xi\xi}^T \tag{3.119}$$

It is interesting to see the similarities between the matrices shown here and the matrices shown in Eqs. (3.34)-(3.41) The matrices in Eqs. (3.117)-(3.119) are the discrete counterparts of the previously shown matrices. The constant components of Eqs. (3.117)-(3.119) are the standard mass, damping, and stiffness matrices obtained when developing a finite-element model of a

flexible beam. The time-varying components actually model the dynamics associated with the moving mass.

The matrix representing the total discrete modal force applied to the beam must be formed. The actual force applied depends on the physical system being modeled. For example, if the beam is considered to be simply-supported, then a gravitational field is included as part of the environment. However, when the free-free beam is examined, no gravitational field is included to correctly model the space environment. Sections 3.2.5 and 3.2.6 examine the discrete force matrix for each system in detail.

The mass, damping, stiffness, and force matrices are used in Eq. (3.32) to solve for the modal displacements and the modal velocities. Using Eq. (3.107), the nodal displacements and velocities are obtained.

This concludes the derivation of the general discrete formulation. Sections 3.2.5 and 3.2.6 examine two specific systems. Section 3.2.5 analyzes the inertially fixed system, which is modeled using a simply-supported beam. Section 3.2.6 examines the inertially free system, which is modeled as a free-free beam. The results for each model are presented in Chapter 4, which compares them to the results obtained from the continuous formulation of Section 3.1.

3.2.5 Applications to a Simply-Supported Beam

Unlike the continuous formulation examined in Section 3.1.6, the discrete formulation for the simply-supported beam is no easier to formulate than the free-free beam. The simply-supported beam is examined and presented first so that its discrete methodology can be validated against well-known results. The inertially fixed system is also used to determine which shape function, linear or cubic, accurately models the beam with the smallest number of finite elements.

Simply-Supported Beam using the Linear Shape Function

For a simply-supported beam modeled with n finite elements there are $2n$ degrees of freedom; there are $n - 1$ translational degrees of freedom and $n + 1$ rotational degrees of freedom. As stated earlier, the linear shape function only uses the beam's translational degrees of freedom; therefore, each element's rotational degrees of freedom can be ignored. The reduced mass and stiffness matrices are derived from the mass and stiffness matrices shown in Eqs. (3.59) and (3.77). Since the beam is simply-supported, the first and last nodes are constrained to zero translation, leading to a mass and stiffness matrix with $n - 1$ degrees of freedom.

Because the shape function is linear, its second spatial derivative is zero. However, as shown in Figure 4, there is a difference in slope between the two neighboring finite elements.

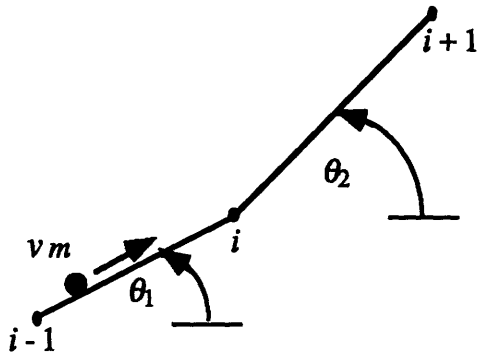

Figure 4. Difference in slope of two neighboring finite elements.

This difference in slope leads to an important component of the inertial force created due to the motion of the mass, which, for the linear shape function, is not present. To account for this inertial force, which is proportional to the beam's curvature, an artificial impulse force is added to the equation. In order to model this force, an impulse force is calculated as soon as the mass moves to the next element. Using the value of the resulting force, an equivalent constant force defined in Eq. (3.120) is applied over the entire element.

$$f_{ye} = \frac{f_y \, \Delta t}{\Delta t_e} \tag{3.120}$$

where Δt_e is the time required for the mass to travel over one element. The actual impulse force, $f_y \Delta T$, is defined as

$$f_y \, \Delta t = m_m \, v_m \frac{n}{L} B \, q \tag{3.121}$$

The vector B, defined in Eq. (3.122), is a central finite-difference operator that acts on the two V vectors, which determine the translations at each node.

$$B = \left\{ V_{i-1}^T - 2 \, V_i^T + V_{i+1}^T \right\} \tag{3.122}$$

Using Eqs. (3.120), (3.121), and (3.122), the final equivalent force vector due to the beam's curvature is

$$f_{ye} = m_m \left(\frac{n}{\tau}\right)^2 B \, q \tag{3.123}$$

This force is added to the force term shown in Eq. (3.96).

Comparing Eq. (3.123) with the term that appears in Eq. (3.99) it seems that the vector B is the linear equivalent of $V_{\xi\xi}^T$. However, B is actually the second-order finite-difference approximation to the second spatial derivative of the V vector.

Simply-Supported Beam using the Cubic Shape Function

When the cubic shape function is used, the component of the inertial force due to the beam's curvature results from the second derivative of the V vector. For the simply-supported beam depicted in Figure 2, the cubic shape function $V3$, has $2n$ elements. These $2n$ elements correspond to the $2n$ degrees of freedom of the simply-supported case when the rotational inertias are included.

Modal Matrix for the Simply-Supported Beam

The modal matrix is evaluated by finding the eigenstructure of the simplified system depicted in Eq. (3.108). The dynamics are dictated by the mass and stiffness matrices. For a simply-supported beam, the matrices are reduced to eliminate the constrained degrees of freedom. The beam's boundary conditions specify that the translations at each end are zero. To address this condition, the first and last rows and columns of the matrices are eliminated.

For the linear shape function, the mass and stiffness matrices contain only translations, which represents an $n - 1$ degree-of-freedom system. The reduced mass and stiffness matrices are variations of the matrices defined by Eqs. (3.59) and (3.77).

The cubic shape function requires that both the translation and the rotations are present. Therefore, the reduced matrices come from the matrices shown in Eqs. (3.70) and (3.77). Note that if the system is cantilevered, it is not possible to statically condense out the rotational degrees of freedom because they must be present in order to be eliminated to satisfy the boundary conditions.

When modeling the simply-supported environment it is essential to include a gravitational field, the only external force applied to the beam. The gravitational force is proportional to the moving mass. The discrete nondimensional form of this force is

$$V\widetilde{F}_{ext} = - \mu_g V \tag{3.124}$$

where μ_g is the nondimensional gravitational parameter defined by Eq. (3.50). This external force matrix is the same matrix F, used in Eq. (3.32).

3.2.6 Applications to a Free-Free Beam

There are three differences between the formulation of the free-free beam depicted in Figure 3 and the simply-supported beam evaluated in Section 3.2.5:

(1) The degree of freedom.

(2) The modes used.

(3) The external force.

It has been shown that the cubic shape function is more efficient than the linear interpolation function when using the simply-supported beam. Therefore, in analyzing the free-free beam, only the cubic shape function will be used. Consequently, the mass and stiffness matrices are variations of Eqs. (3.70) and (3.77). The boundary conditions of a free-free beam state that the shear and moment at each end must be zero. These conditions do not constrain any degree of freedom. Therefore, the free-free beam and, correspondingly, the mass and stiffness matrices have $2n+2$ degrees of freedom.

These mass and stiffness matrices are used in forming the system's mode shapes and eigenvalues. Before reduction, the modal matrix and the matrix of eigenvalues contains $2n+2$ elements. The first two modes correspond to rigid body rotation and translation and have zero frequency. The other $2n$ modes represent the beam's flexible motion.

The free-free beam is used to model an inertially free system. In the space environment there is no gravitational field. If there is no external force applied to the beam their would be no response

from the motion of the mass, unless an initial disturbance is used. The details of this vibration were outlined previously in Section 3.1.6.

3.3 DISCRETE FORMULATION FOR THE FREE-FREE BEAM WITH MULTIPOINT OF CONTACT

In the analysis thus far, the model has been a flexible beam with a rigid body attached at one contact point to the beam.. In both the continuous and discrete formulations, a free-free beam and a simply-supported beam were examined. The simply-supported beam model is used as a testing board for the discrete method outlined. The inertially free system is used to try and model the space environment of the Space Station-Mobile Transporter; however, it still only models the mass as a wheel moving over the beam rather than as the more realistic train moving along a track. The next system analyzed, a free-free beam with multipoint of contact, is used to consider the train/track aspect of the SS-MT system.

3.3.1 Mathematical Model

The mathematical model used here, as before, is essentially the inertially free flexible beam with a mass moving at a constant speed

along its length. For this analysis, however, the mass is attached at two points of contact (see Figure 5).

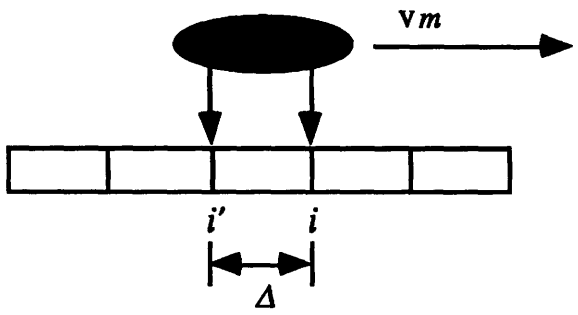

Figure 5. Mass attached at two-points of contact.

This final model attempts to represent the physical aspect of the mobile transporter as a train rather than simply a wheel as presented in Sections 3.1 and 3.2. The validity of the discrete methodology for this model is shown in Chapter 4, using the formulations developed in Sections 3.1 and 3.2.

For the train/track model, only a discrete formulation is considered. When the two points of contact become infinitely close, the equations developed in this section should converge to the discrete equations for the one-point-of-contact case. This is proven to be true in Chapter 4. Therefore, since this method converges to a method that is already proven to be valid, there is no need to compare the results obtained from the following formulation with those of a continuous formulation.

In Chapter 4, only an inertially free system is examined with two points of contact. In the following section a general derivation is developed. For the applications to the free-free beam see Section 3.2.6.

The only difference between the discrete system examined in Section 3.2 and the system analyzed here is the manner in which the inertial force due to the moving mass is applied to the beam. Because there are now two points of contact, there are correspondingly two continuous forces due to the mass acting on the beam. Both forces must be made discrete and must be incorporated into the beam's equation of motion.

As in Section 3.2, the analysis starts by discretizing the load applied to the beam. This new load is then incorporated into the beam's equation of motion to obtain the equation of motion for the entire system. This equation is made nondimensional and placed into state space form for numerical computation.

3.3.2 Equations of Motion

The equation of motion for the train/track system depicted in Figure 5 is obtained with a series of steps. First, the discrete equation representing the displacement of the flexible beam is determined. Next, the force due to the moving mass is examined.

Using compatibility, these equations are combined to form the system's equation of motion. Because this system is very similar to that depicted in Section 3.2, the following formulation is abridged to avoid repetition.

Beam Equation

The discrete equation of motion for a flexible beam, shown earlier in Eq. (3.81), is rewritten here for convenience.

$$\widetilde{M}\,\ddot{q} + \widetilde{K}\,q = \widetilde{F}_t \tag{3.125}$$

where, for an inertially free system, the mass and stiffness matrices are defined by Eqs. (3.70) and (3.77), respectively. $\widetilde{F}_t$ is the total discrete force vector and is a combination of the external forces applied to the beam and the inertial effects of the moving mass. $\widetilde{F}_t$ is the discrete form of F_t. As stated in Section 3.2.7, there are no external forces applied to the free-free beam. Therefore, without the loss of generality, the total force applied to the beam is only due to the inertial effects of the moving mass.

Load Modeling

The total load exerted on the beam due to the moving mass is the sum of the forces exerted by the two points of contact

$$F_t = f_{c1} + f_{c2} \tag{3.126}$$

The total load applied to the beam, due to the inertial effects of the moving mass, is the same as in the one-point-of-contact case. However, the load is now divided between the two points of contact. For simplicity, each point is assumed to carry half of the total load; therefore, the magnitude of the force at each contact point is half as great as the force exerted at the one contact point in Section 3.2. The force contribution from one of the contact points is

$$f_{c1} = -\frac{m_m}{2}\ddot{q}_{m1} \tag{3.127}$$

where q_{m1} is the discrete displacement of the first contact point. The load at the second point of contact is determined in a similar fashion. Substituting the actual values for the load contributions into Eq. (3.126), the load exerted on the beam due to the moving mass becomes

$$F_t = -\left(\frac{m_m}{2}\left(\frac{\partial^2 q_{m1}}{\partial t^2}\right)_{abs} + \frac{m_m}{2}\left(\frac{\partial^2 q_{m2}}{\partial t^2}\right)_{abs}\right) \tag{3.128}$$

Discretization Vectors

The force shown in Eq. (3.128) must be placed into a discrete form. In the derivation it is assumed that the distance between the

two contact points is a multiple of the elemental length of the finite beam elements:

$$\Delta = j\, l_e \tag{3.129}$$

where j is any integer between 0 and n. This assumption simply makes the bookkeeping a lot easier.

The cubic shape function outlined in Section 3.2.2 is used to distribute the forces. The location of the first point of contact, x_1, is determined. From this location, the position of the second point, x_2, is determined by knowing the speed of the moving mass and the spacing between the two points of contact.

Because the two locations are dependent on each other, it is only necessary to follow one of the points; x_1 has been chosen to locate the position of the mass. The force contribution from this point is discretized using the shape function shown in Eq. (3.92) and rewritten here:

$$\begin{aligned} V_3 = &\left(1 - 3\,\xi^2 + 2\,\xi^3\right) V_i + \left(\xi - 2\,\xi^2 + \xi^3\right) \frac{1}{n} V_{i+1} \\ &+ \left(3\,\xi^2 - 2\,\xi^3\right) V_{i+2} + \left(-\,\xi^2 + \xi^3\right) \frac{1}{n} V_{i+3} \end{aligned} \tag{3.130}$$

The load contribution due to the second point of contact is discretized using a shape function of the same form but with

different nodes that are determined by using the relationship between the two points of contact. If i represents the location of the first point $x1$, then i' represents the location of the second point $x2$. The relationship between i and i' is

$$i' = i - 2j \tag{3.131}$$

Next, the weighting vectors for the second point of contact are formed. The new vectors are denoted by a prime and are formed using i' rather than i.

$$V'^{T}_{i} = \{0, 0, \cdots, 0, \overset{i'\text{-}th}{1}, 0, 0, \cdots, 0\}^{f} \tag{3.132}$$

Using these new V' vectors, an equivalent cubic shape vector for the second point of contact is determined.

$$\begin{aligned} V'_3 = &\left(1 - 3\,\xi^2 + 2\,\xi^3\right) V'_i + \left(\xi - 2\,\xi^2 + \xi^3\right) \frac{1}{n} V'_{i+1} \\ &+ \left(3\,\xi^2 - 2\,\xi^3\right) V'_{i+2} + \left(-\,\xi^2 + \xi^3\right) \frac{1}{n} V'_{i+3} \end{aligned} \tag{3.133}$$

The equations in Section 3.2 were derived using a generic shape function V. The new shape function developed here, $V3'$, has the same basic format as V. Therefore, the discrete development that was shown in Section 3.2 is valid for the new vector $V3'$. The equations that will be developed, however, are different because the force applied to the beam now has two components rather than one.

In the following formulation, a generic V' is used to represent the new shaping function. Though a cubic shape function was developed (Eq. (3.133)) and is used in the numerical evaluation, the following methodology is valid for any order shape function.

Some relationships are defined between the displacements of the contact points, the shaping functions, and the beams displacement field.

$$q_{m1} = V^T q \tag{3.134}$$

$$q_{m2} = V'^T q \tag{3.135}$$

Using Eqs. (3.134) and (3.135), the absolute accelerations of the two points of contact are determined and substituted into Eq. (3.128). The resulting force is inserted into Eq. (3.100), resulting in the discrete force vector that is applied to the appropriate nodes of the flexible beam:

$$\begin{aligned}\tilde{F}_t = &- \frac{m_m}{2}\left(V\ V^T \ddot{q} + 2\left(\frac{n}{\tau}\right)\ V\ V_\xi^T \dot{q} + \left(\frac{n}{\tau}\right)^2 V\ V_{\xi\xi}^T q\right) \\ &- \frac{m_m}{2}\left(V'\ V'^T \ddot{q} + 2\left(\frac{n}{\tau}\right)\ V'\ V'^T_\xi \dot{q} + \left(\frac{n}{t}\right)^2 V'\ V'^T_{\xi\xi} q\right)\end{aligned} \tag{3.136}$$

where V'_ξ and $V'_{\xi\xi}$ represent the derivatives with respect to ξ of the new shape function. For the duration of this derivation, $V'\xi$ and $V'\xi\xi$

are shown in their symbolic form; their actual values are available in Appendix C. Now that the force due to the moving mass has been placed in a discrete form, it can be inserted into the discrete equation of the flexible beam.

System Equation of Motion

The discrete equation of motion for the system is obtained by combining Eqs. (3.136) and (3.125). As in the previous cases, the terms involving the beam deflection q, are shown on the left-hand side of the equation even though they appear due to the moving mass.

$$\left(\widetilde{M} + \frac{m_m}{2}\left(V\ V^T + V'\ V'^T\right)\right)\ddot{q} + 2\frac{m_m}{2}\frac{n}{\tau}\left(V\ V_\xi^T + V'\ V'^T_\xi\right)\dot{q} + \left(\widetilde{K} + \frac{m_m}{2}\left(\frac{n}{\tau}\right)^2\left(V\ V_{\xi\xi}^T + V'\ V'^T_{\xi\xi}\right)\right)q = 0 \tag{3.137}$$

Equation (3.137) represents a discrete equation of motion in physical coordinates. When the two points of contact are infinitely close to each other, Eq. (3.135) is equivalent to Eq. (3.105). This equation must be placed into a nondimensional form in terms of the beam's modal coordinates.

3.3.3 Nondimensional Equations of Motion

Noticing the similarities between Eqs. (3.105) and (3.137), it is trivial to place the latter equation into nondimensional modal form (see Sections 3.2.3). Therefore, to avoid repetition the derivation is not repeated here. The nondimensional form in modal coordinates of Eq. (3.135) is

$$\left(E+\frac{\mu_m}{2}\left(V_\eta\, V_\eta^T + V'_\eta\, V'^T_\eta\right)\right)\overset{oo}{\eta} +$$
$$\left(2\ \zeta\left(\lambda\Lambda_r\right)^{1/2} + 2\,\frac{\mu_m}{2}\,n\left(V_\eta\, V^T_{\eta\xi} + V'_\eta\, V'^T_{\eta\xi}\right)\right)\overset{o}{\eta}$$
$$+\left(\lambda\,\Lambda_r + \frac{\mu_m}{2}\,n^2\left(V_\eta\, V^T_{\eta\xi\xi} + V'_\eta\, V'^T_{\eta\xi\xi}\right)\right)\eta = 0 \qquad (3.138)$$

where the $V'\eta$ vectors are found using the relationships outlined in Eqs. (3.111)-(3.112) for the new shape function.

Equation (3.136) is the multipoint-of-contact counterpart of Eq. (3.115); it is in matrix form but not in state space domain. Equation (3.135) is placed into the state space form in preparation for numerical computation.

3.3.4 State Space Representation

The only differences between Eq. (3.136) and (3.115) are the additional terms to the time-varying mass, damping, and stiffness

matrices due to the second point of contact. The procedure for transforming Eq. (3.138) into state space domain is equivalent to that outlined in Section 3.2.4.

State Vector

The two states of the system are chosen as the modal displacements and velocities. The state vector is equivalent to the one presented in Eq. (3.116). Because a discrete analysis is already in matrix form, the state vector is rewritten in a slightly different manner than in the case of when the variables were scalars. This was first shown in Eq. (3.116) and is rewritten here:

$$x = \left[\eta \ \overset{o}{\eta} \right]^T \tag{3.139}$$

Matrix Representation

The matrices representing the system are a combination of a constant matrix and a matrix that varies with time. The constant matrices represent the dynamics of the flexible structure. Since the flexible structure modeled in this analysis is equivalent to that modeled in Section 3.2, the constant matrices are identical to those outlined previously. The matrices dependent on time model the dynamic interaction of the moving mass with the flexible structure. This interaction is the difference between the case in Section 3.2 and

this case. The total matrices used to formulate this system in the form shown in Eq. (3.32) are

$$M = E + \frac{m_m}{2} \left(V_\eta \, V_\eta^T + V'_\eta \, V'^T_\eta \right) \tag{3.138}$$

$$C = 2 \, \zeta \left(\lambda \, \Lambda_r \right)^{1/2} + 2 \, \frac{m_m}{2} \, n \, \left(V_\eta \, V^T_{\eta\xi} + V'_\eta \, V'^T_{\eta\xi} \right) \tag{3.139}$$

$$K = \lambda \, \Lambda_r + \frac{m_m}{2} \, n^2 \left(V_\eta \, V^T_{\eta\xi\xi} + V'_\eta \, V'^T_{\eta\xi\xi} \right) \tag{3.140}$$

The above matrix definitions are valid for any boundary conditions. For the numerical evaluation of this system, only the free-free beam is examined. For the alterations needed to specifically examine a free-free beam, see Section 3.2.6.

CHAPTER 4

RESULTS

Chapter 4 presents the results obtained using the analysis outlined in Chapter 3. Section 4.1 describes the layout of the results as well as the parameters used to create them. Section 4.2 displays and discusses the results.

4.1 RESULTS ORGANIZATION

Section 4.1 describes the organization of Section 4.2, which displays the results obtained from the different formulations of Chapter 3. Three different formulations were developed in Chapter 3:

(1) Continuous.

(2) Discrete - one point of contact.

(3) Discrete - multipoint of contact.

In addition to these three different formulations, two specific systems were examined:

(1) Simply-supported beam.

(2) Free-free beam.

To ease the complexity of the next section it is important to understand how the simulations are organized, what they are trying

to accomplish, and what parameters are used to create them. To aid in this understanding, Section 4.1 is divided into two subsections. Section 4.1.1 discusses the goals of Chapter 4 and the way they are obtained. Section 4.1.2 examines the nondimensional parameters used to set up the simulations. For a description and listing of the computer codes used to perform the simulations, see Appendix D.

4.1.1 Goals of Chapter 4

Chapter 4 has three main goals:

(1) Validate the discrete formulation for the one- and multipoint-of-contact cases with a simply-supported and a free-free beam.

(2) Determine which shape function, cubic or linear, best models the system's displacement.

(3) Perform several informative parametric studies. These studies show the effects of the nondimensional parameters, developed in Chapter 3, on the system's dynamics.

Section 4.2 contains fifteen pages of plots. Each page displays either two, four, or eight plots, depending on the specific study being run. Figures 6 through 11 represent the simply-supported system. Figures 6, 7, 8, 10, and 11 represent time history of the nondimensional midspan deflection. Figure 9 presents a profile of

the entire beam for different values of nondimensional time. The displacements shown in Figure 9 are also nondimensional. For the simply-supported beam all the displacements are made nondimenisonal by u_S, the static deflection of the beam.

Figures 12 through 20 display results for the free-free system. For each study performed there are two sets of plots. The first plots, Figures 12, 15, 17, and 19, display the time history of the nondimesional deflection at the beam's left tip. The second plots, Figures 13, 16, 18, and 20, display the time history of the nondimensional deflection at the beam's right tip. Figure 14 presents a profile of the entire beam's nondimensional deflection. First, the organization for the simply-supported beam is explained; then, the free-free system is discussed.

Simply-Supported Beam

The first study performed for the simply-supported beam determines the shape function that best models the beam's displacement while using the least amount of finite beam-elements. To accomplish this, a comparison using a different number of beam elements was made between a continuous formulation and both the linear and cubic shape functions. The results presented in Section 4.2.1 illustrate that the cubic shape function is better suited to model

the displacement; therefore, in the following discrete simulations only the cubic shape function is used.

The second study compares the discrete and continuous formulations for different values of the speed parameter α (see Eq. (4.5)). This study effectively validates the discrete formulation for the simply-supported beam. Consequently, the following simulations are performed for the discrete cubic formulation only.

The third study presents snapshots that show the profile of the entire beam for different time frames. The first set of snapshots models the beam as the mass is moving along the beam. The second set examines the beam in free vibration, after the mass has left the beam.

Finally, a parametric study is performed for the simply-supported system, which examines the result of including the inertial effects of the mass versus simply modeling it as a moving force. First, different runs are completed for a specific mass ratio with different speed parameters. Then, the speed parameter is specified and the value of the mass ratio is varied.

Section 4.2 contains the results outlined. They provide the information needed to reach the three goals set for the simply-supported system. The same basic tests outlined above, with the

same parameters, were completed for the free-free system. This compatibility facilitates the comparison of the two separate systems.

Free-Free Beam

The discrete methodology for the free-free, one-point-of-contact system is validated. To accomplish this, a comparison is made between the discrete formulation presented in Section 3.2 and the continuous formulation presented in Section 3.1, for various speed parameters. Based on the results of the simply-supported beam, only the cubic shape function is used. The speed parameters for the free-free beam (see Eq. (4.6)) are set to closely resemble those of the simulations performed for the simply-supported beam. Unlike the simply-supported plots, however, for the free-free beam all displacements are made nondimensional by the length of the beam.

Studies using the discrete formulation are also performed. First, snapshots of the beam are displayed for different time frames, as outlined for the simply-supported beam. The first set of curves models the beam with the mass travelling along its length; the second set of curves displays the beam in free vibration without the mass.

The next set of plots explore the results of ignoring the inertial effects of the mass. If the inertial effects are ignored in the simply-supported beam, the mass still creates a gravitational force on the beam. When there is no gravity, no gravitational force is applied. Therefore, the two formulations compared in this study are:

(1) With the moving mass.

(2) Without the moving mass.

The next study examines when it becomes important to include the inertial effects of the moving mass by varying the mass ratio for one speed parameter. Once again, the values of the parameters used are the same as those used for the simply-supported beam.

The final curves examines the multipoint-of-contact formulation. Different contact spacing simulations were compared, again using the same speed parameters that were used for the simply-supported beam. It is important to show that as the contact spacing approaches zero, the simulations approach the one-point-of-contact case. It is also interesting to see how the speed parameter alters the effects of the contact spacing.

The above-mentioned curves help to achieve the goals that the simply-supported system could not obtain. Using the results from both the simply-supported and the free-free systems, the best shape

function is determined, the discrete methodology is completely validated, and important parametric studies are performed.

In the following simulations, the continuous formulation that was outlined in Section 3.1 is used for the validation of the discrete formulation. As an added assurance, an exact formulation developed by Kurihara and Shimogo (Ref. [5]) for the simply-supported beam was compared to the discrete simulation. The results obtained completely agreed with those obtained using the formulation detailed in Section 3.2.

4.1.2 Parameter Discussion

Each system is described by a stiffness parameter and the mass ratio between the structure and the moving mass. For both the simply-supported and the free-free systems, the stiffness of the system is represented by the nondimensional parameter λ, and the mass ratio is represented by μ_m. The external load for the simply-supported system is characterized by μ_g. There is no external load applied to the free-free system. Before specifying the values of these parameters, it is important to define the speed parameter that was discussed in Section 4.1.1.

Speed Parameter

A convenient way to describe the flexible-structure/moving-mass system is to define a speed parameter α.

$$\alpha = \frac{T_p}{2\ t_r} = \frac{T_p\ v_m}{2\ L} \tag{4.1}$$

where T_p is the fundamental period of the system and $t_r = \frac{L}{v_m}$ was previously defined as the time required for the mass to travel the beam's length. To gain a more physical understanding of this parameter, a relationship between the fundamental period and the natural frequency of the beam is:

$$T_p = \frac{2\ \pi}{\omega_1} \tag{4.2}$$

which gives

$$\alpha = \frac{\pi\ v_m}{\omega_1\ L} \tag{4.3}$$

where ω_1 is the beam's fundamental natural frequency.

Because α depends on both the speed of the moving mass and the frequency of the system, there are two different ways to look at the meaning of α. A low α represents either a system in which the

mass travels at a very slow speed or a very stiff system. Conversely, a high α represents either a system where the mass travels at very high speeds or a flexible system. The actual physics of the system are the same regardless of how the speed parameteris interpreted. In this analysis, α is referred to as the speed parameter and consequently is used to describe the relative speed of the moving mass.

The nondimensional natural frequencies of the simply-supported and the free-free beams can be expressed in terms of the nondimensional stiffness parameter:

$$\Omega_{1_s} = \pi^2 \sqrt{\lambda} \tag{4.4}$$

$$\Omega_{1_f} = 22.4 \sqrt{\lambda} \tag{4.5}$$

where Ω_{1_s} and Ω_{1_f} represent the natural frequency of the simply-supported and the free-free beams, respectively.

Using Eqs. (4.3) and (4.4), a unique relationship is determined between the speed and stiffness parameters for the simply-supported and the free-free systems. The two speed parameters, α_s and α_f, one for each specific system, are defined as

$$\alpha_s = \frac{1}{\pi\sqrt{\lambda}} \tag{4.6}$$

$$\alpha_f = \frac{\pi}{22.4\sqrt{\lambda}} \tag{4.7}$$

Using Eqs. (4.6) and (4.7), the nondimensional stiffness parameter λ, is specified to achieve different speed parameters. Table 2 outlines the speed parameters used and the resulting value of λ for both beams. Either the speed parameter α, or the stiffness parameter λ, can be used to identify a specific case, because of the unique relationship between the two parameters.

Remaining Parameters for the Simulations

In addition to the speed parameter α (or stiffness parameter λ), there are three other parameters of interest to the simulation:

(1) The mass ratio, μ_m.

(2) The load parameter, μ_g.

(3) The contact point spacing, s.

The mass ratio parameter μ_m, is defined the same for both the simply-supported and the free-free systems. The load parameter μ_g, is used only for the simply-supported system, and is not really an independent parameter, as will be seen. The contact point spacing parameter s, is used only for the free-free system with multipoint of contact.

Table 2. Stiffness and Speed Parameters Used in Simulations.

Simply-Supported Beam		Free-Free Beam	
α_s	λ	α_f	λ
0.01	1013.72	0.1	1.967
0.2	2.53	0.2	0.492
0.3	1.12	0.3	0.219
0.4	0.633	0.4	0.123
0.6	0.281	0.6	0.055
0.8	0.158	0.8	0.031
1.0	0.101	1.0	0.019
1.2	0.070	1.2	0.014
1.4	0.051	1.4	0.010
1.6	0.039	1.6	0.007
2.0	0.025	2.0	0.005
3.0	0.011	3.0	0.002
4.0	0.006	4.0	0.001

As defined previously, μ_m represents the ratio of the moving mass to the flexible structure. This ratio is varied only in one set of simulations for each system (see Figures 11, 17, and 18). The purpose of varying μ_m is to determine the lowest mass ratio permissible to treat the mass as a moving force rather than as a moving mass. The value of the mass ratios vary from 0.01 to 2.0 and are indicated in the legends of the appropriate curves. For the remaining curves, the mass ratio is kept at a value of 0.5; therefore, the moving mass is half as massive as the flexible structure. To model the mass as a moving force, the mass ratio is set to 0.

In Section 3.1.5, a nondimensional load parameter, μ_g, was developed to characterize the load applied to the system due to the gravitational force of the moving mass. The definition of μ_g is rewritten from Eq. (3.51) as,

$$\mu_g = \frac{m_m\, g}{\rho\, v_m^2} \tag{3.51}$$

This load parameter in Eq. (3.30) would lead to nondimenisonal deflections u/L in the beam. For the simply-supported beam, it is more convenient to express the deflections in reference to the maximum static deflection of the beam u_S. For the load $m_m g$ acting at the midspan, the maximum static deflection occurs at the midspan and is given as

$$u_s = \frac{m_m\, g\, L^3}{48\, EI} \tag{4.8}$$

Hence, to provide the nondimensional deflections u/u_S rather than u/L would require one to pick the new load parameter μ_g in Eqs. (3.30) and (3.50) as

$$\mu_g \rightarrow \frac{\frac{u}{L}}{\frac{u_s}{L}} = \frac{\frac{m_m\, g}{\rho\, v_m^2}}{\frac{m_m\, g\, L^2}{48\, EI}} = 48\,\lambda \tag{4.9}$$

Using Eq. (4.9), the value of the load parameter μ_γ is directly specified for the appropriate value of λ or α specified in Table 2, or Eq. (4.6).

The final parameter to be explained is s, the contact spacing parameter:

$$s = \frac{j}{100} \tag{4.10}$$

where j is any integer. The parameter s represents the percentage of beam length by which the two points are separated. For example, if s is set equal to zero, only one point of contact is achieved. For s equal to 0.02, the two points are separated by a distance that is 2 percent of the beam length.

Four different values of s were compared for different speed parameters:

$s = 0.000$

$s = 0.005$

$s = 0.010$

$s = 0.020$

The parameters needed to describe the system have now been thoroughly explained. However, there are two more parameters that do not define the physical property of the system but do appear in Section 4.2. First, the simulations were run in terms of the nondimensional time parameter τ and were run up to a value of $\tau. = 2$ As a reminder, when τ is equal to one, the mass has travelled over the entire beam length. Second, the parameter n defines the number of finite beam elements used. In Figure 6, n is varied. For the remaining discrete simulations, 40 beam elements are used. Finally, in the simulations, three flexible modes were retained.

4.2 RESULTS DISCUSSION

Section 4.2 presents the results for both the simply-supported and the free-free systems. Each graph is discussed as it appears in the text.

The results that were outlined in Section 4.1 and their significance follow. Section 4.2 contains two subsections, Section 4.2.1 discusses the simply-supported system, and Section 4.2.2 expounds on the free-free system. The organization of each section was developed in the previous section.

4.2.1 Results for the Simply-Supported Beam

The plots are in terms of the nondimensional deflections u/u_S, and the nondimensional time parameter $\tau = v_m t/L$.

Figure 6

Figure 6 compares the discrete formulation with both a cubic and a linear shape function and with the continuous formulation. Each curve was simulated for α equal to 1.0.

These curves are used to determine the shape function that accurately models the displacement with the least number of elements. Figure 6 (a) shows that for as little as 10 finite beam elements, the cubic shape function is almost identical to the continuous formulation. Therefore, for the rest of the discrete simulations the cubic shape function is used. It is also important to note that for sixty finite elements, almost no difference is seen in the three curves portrayed.

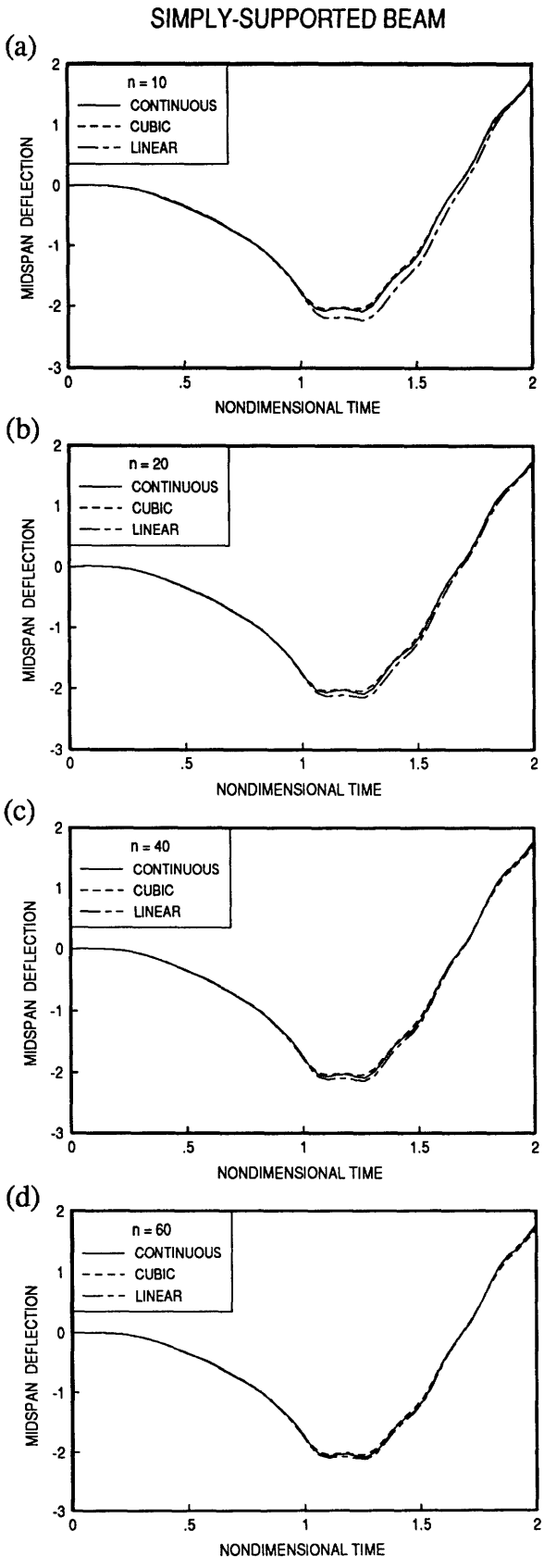

Figure 6. Discrete vs continuous for α = 1.0, μm = 0.5.

Figure 7

Figure 7 compares the discrete and continuous formulations for different speed parameters. These curves provide two useful pieces of information: they validate the discrete methodology for different speed parameters and they show the effect of varying the speed parameter.

For each plot in Figure 7, the discrete and continuous formulations are almost identical. Figure 7 proves the validity of the discrete methodology for the simply-supported system. The plots were run up to a value of $\tau = 2$ in order to check the formulation when the mass is on the beam, and the free vibration when the mass leaves the beam.

The speed parameters chosen to model the system range from a very slow-speed system of 0.01 to a high-speed system of 1.4. Figure 7(a), $\alpha = 0.01$, represents a system where the mass is travelling at a very slow speed. In this case, the beam sees the mass as a static force. The speed parameter is increased until $\alpha = 1.4$. By scanning the deflections as the speed parameter is increased, the effects of α on the system dynamics becomes obvious.

For values of α less than 1, the maximum effects of the moving mass occur while the mass is still on the beam. Even for slow speeds,

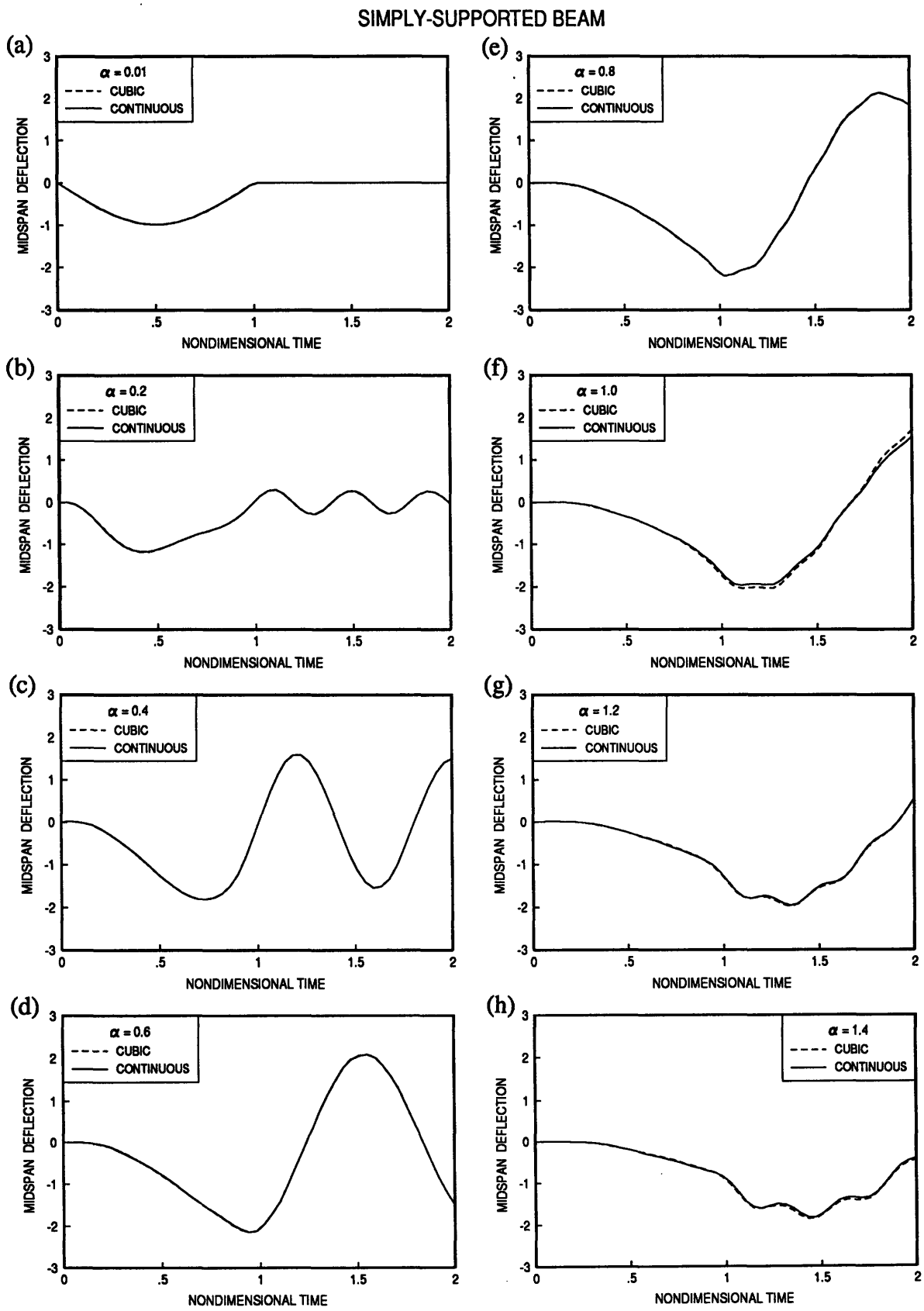

Figure 7. Discrete vs continuous for varying α, μm = 0.5

i.e., α = 0.2, the motion of the mass affects the system dynamics, as indicated by the vibration that occurs even after the mass has left the beam. The largest deflection is detected when α = 0.6 (Figure 6(d)). For higher values of α, the damping terms due to the inertial effects decrease the midspan deflection.

For speed parameters greater than one, the maximum effects of the moving mass occur after the mass has already left the beam.

Figure 8

Figure 8 displays the midspan deflection of the system for very large values of α. These α values represent the speeds that may be seen by a high-speed ground transport vehicle. As α is increased, the beam does not see the effect of the moving mass until values near τ. = 1.5 It is suspected that as the speed parameter gets extremely large, the mass will have very little effect on the beam. This trend can be seen in Figures 8(a) through 8(d), especially in Figures 8(c) and 8(d).

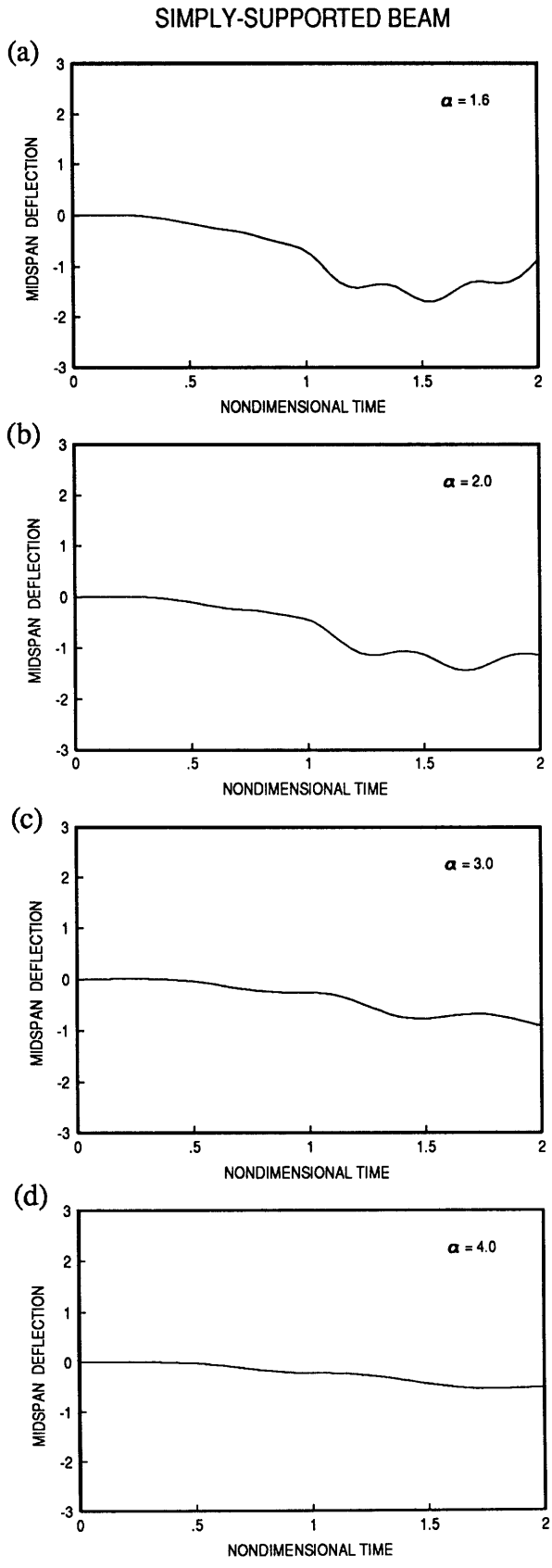

Figure 8. Very large values of α, μm = 0.5.

Figure 9

Figure 9 displays two sets of curves. Each curve represents a profile of the entire beam at different time frames. For a speed parameter of 0.6, Figure 9(a) displays how the beam's deflection changes as the mass travels along its length. The maximum deflection occurs near $\tau = 1$. Figure 9(b) simply shows the beam in free vibration after the mass has left the beam. As shown in Figure 8, for $\alpha = 0.6$, no higher frequencies are present in the beam's vibration.

Figure 10

Figure 10 represents the first set of curves in a parametric study that examines the effects of the mass ratio parameter. In Figure 10, the mass ratio is set equal to 0.5, four different speed parameters are used, and two different formulations are displayed. The solid line represents the formulation where the inertial effects of the mass are included. The dotted line shows the deflection when the mass is treated as a moving force.

For the static case, $\alpha = 0.01$ (Figure 10(a)), no difference is detected between the two formulations. For the other speed parameters in Figures 10 (b)-10 (d), however, a large difference in the two curves can be seen. The added inertial effects increase

(a)

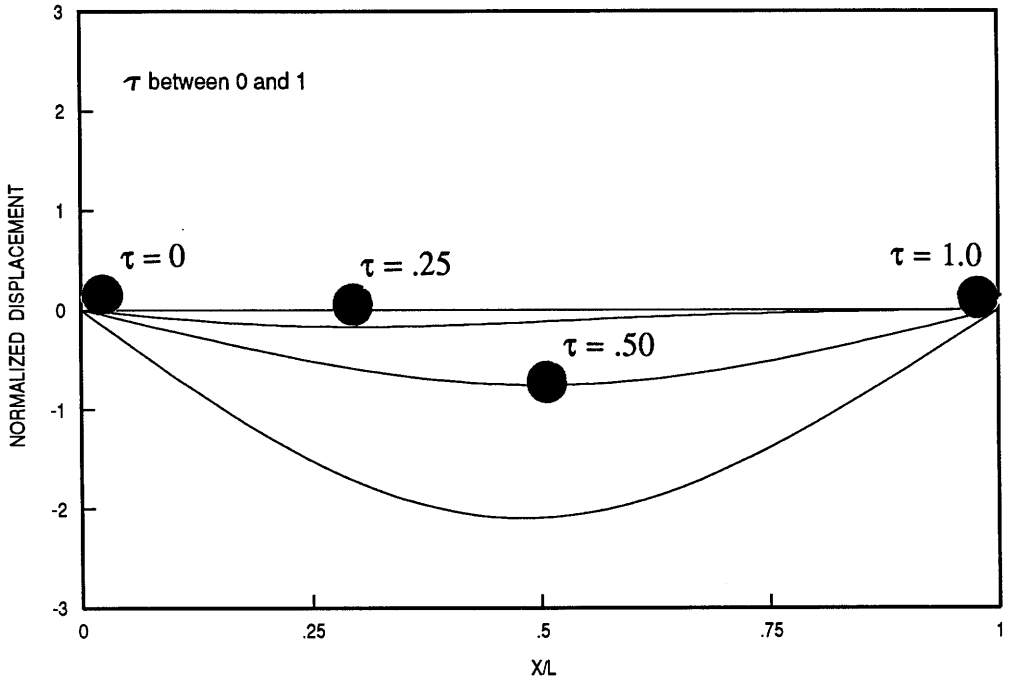

(b)

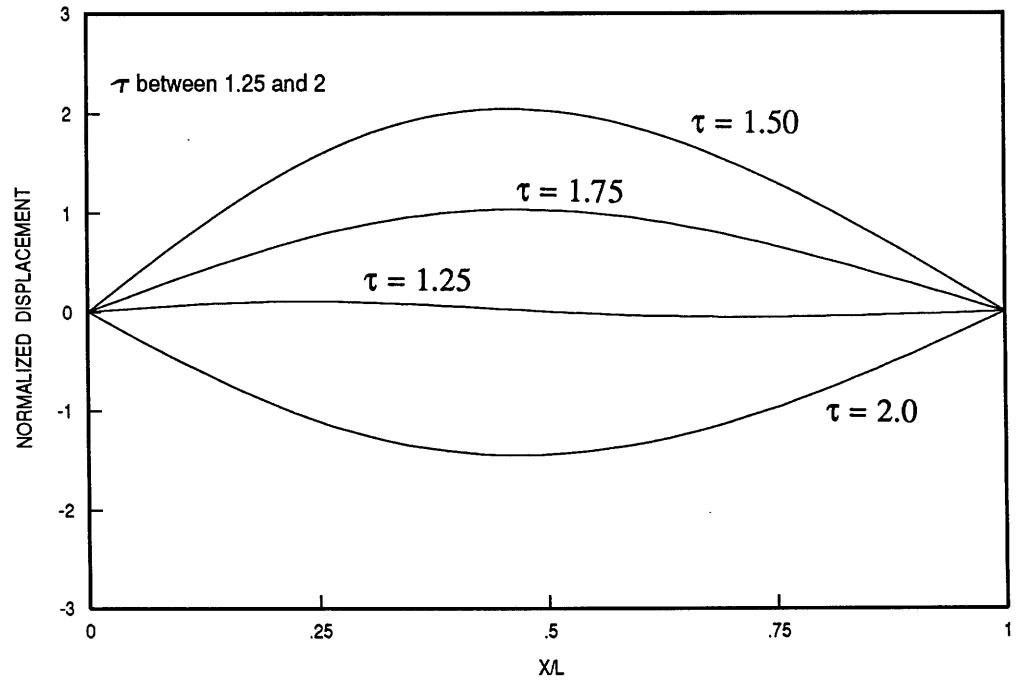

Figure 9. Snapshot of beam with $\alpha = 0.6$, $\mu m = 0.5$.

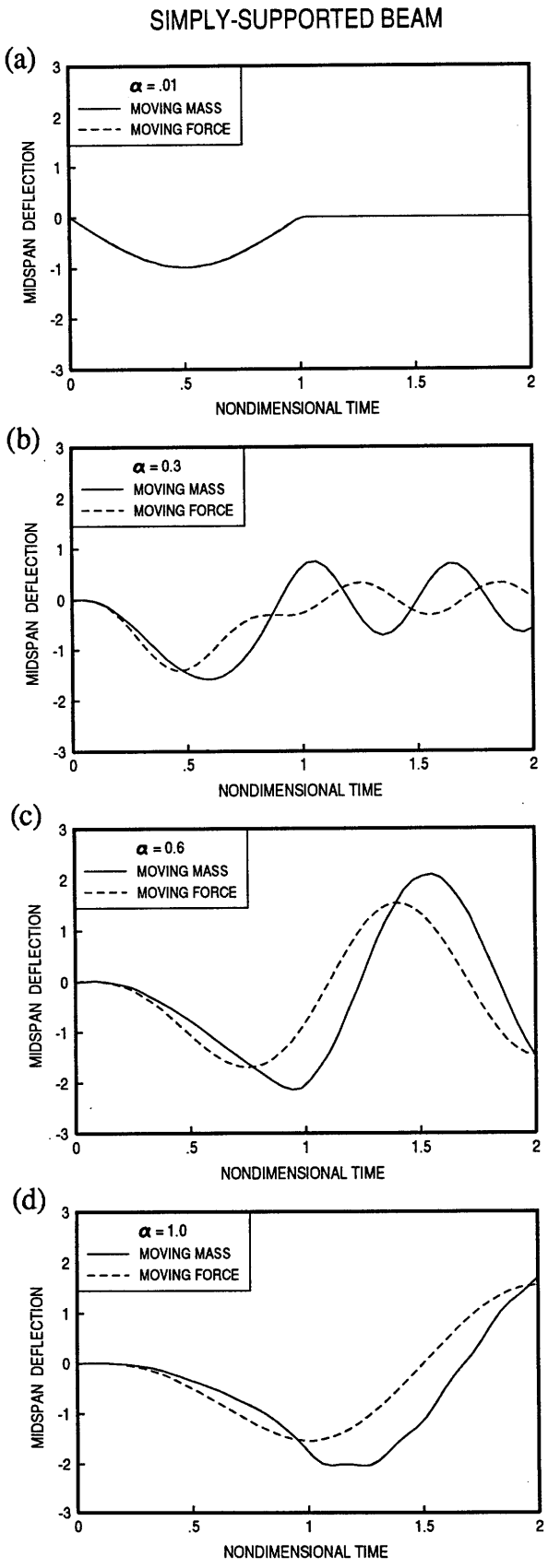

Figure 10. MM vs MF for different α, μm = 0.5.

the effective force of the moving mass and consequently increase the maximum deflection of the midspan displacement.

Figure 11

Figure 10 examined the difference between a moving mass and a moving force formulation for a μ_m of 0.5. For all the speeds except the static case of α = 0.01 there is a difference in the two formulations. In Figure 11, however, the speed parameter is kept constant, α = 0.3, but the mass ratio μ_m, is varied.

This study determines when it is permissible to treat the travelling load as a moving force rather than as a moving mass. For a mass ratio as small as 0.01, there is a difference between the two curves. A significant difference, however, is not seen until the ratio reaches 0.05. The curves diverge as τ approaches 1.

In Figures 11(a) through 11(d), the mass ratio is still fairly insignificant (less than or equal to 0.1). Because the inertial effects add damping as well as an additional stiffness for small values of μ_m, the deflection shown by the moving mass simulation is smaller than the deflection predicted by the moving force simulation. But, as can be seen in Figure 10(e) to 10(h), for larger values of μ_m the deflection predicted by the the moving mass formulation is larger than the deflection predicted by the moving force simulation.

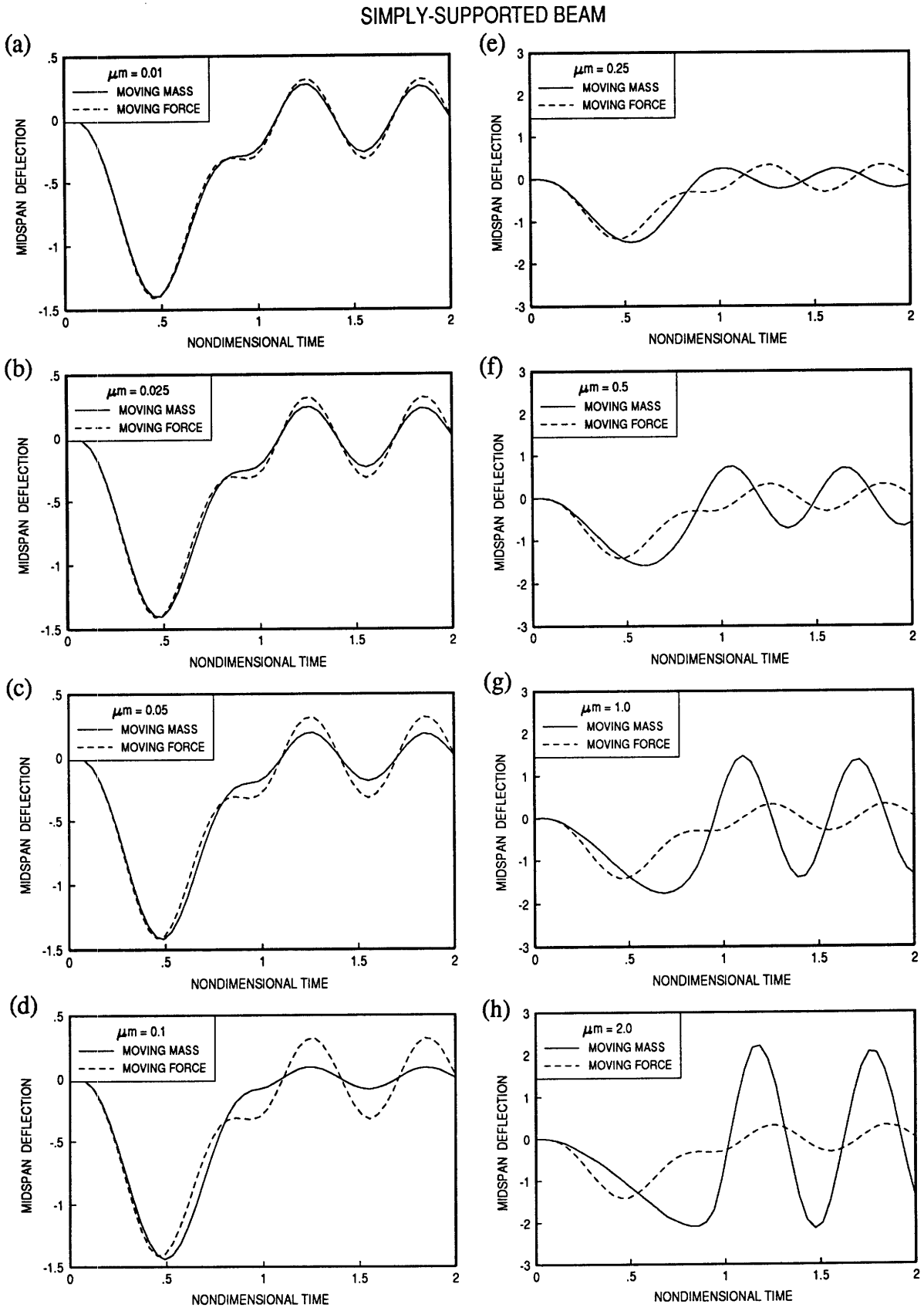

Figure 11. MM vs MF for different μm, α=0.3.

For small mass ratios, the moving force assumption could be treated as a conservative prediction. However, for an accurate solution, the inertial effects should be included in the derivation.

4.2.2 Results for a Free-Free Beam Results

Each study that follows, except for Figure 14, contains two figures, one for each beam tip. The two corresponding figures are discussed simultaneously. The plots are in terms of the nondimensioal deflections u/L, and the nondimensional time parameter $\tau = v_m t/L$.

Figures 12 and 13

Figures 12 and 13 compare the discrete (cubic) formulation and the continuous formulation for different speed parameters. In every simulation the formulations are identical. These curves successfully validate the discrete methodology for the free-free system.

Unlike Figure 6, the smallest speed parameter, $\alpha = 0.1$, displays the largest amount of high-frequency vibration. To understand this phenomenon it is important to remember that the free-free beam was given an initial vibration prior to the release of the moving mass. Therefore, in reality, Figures 12(a) and 13(a) display that for

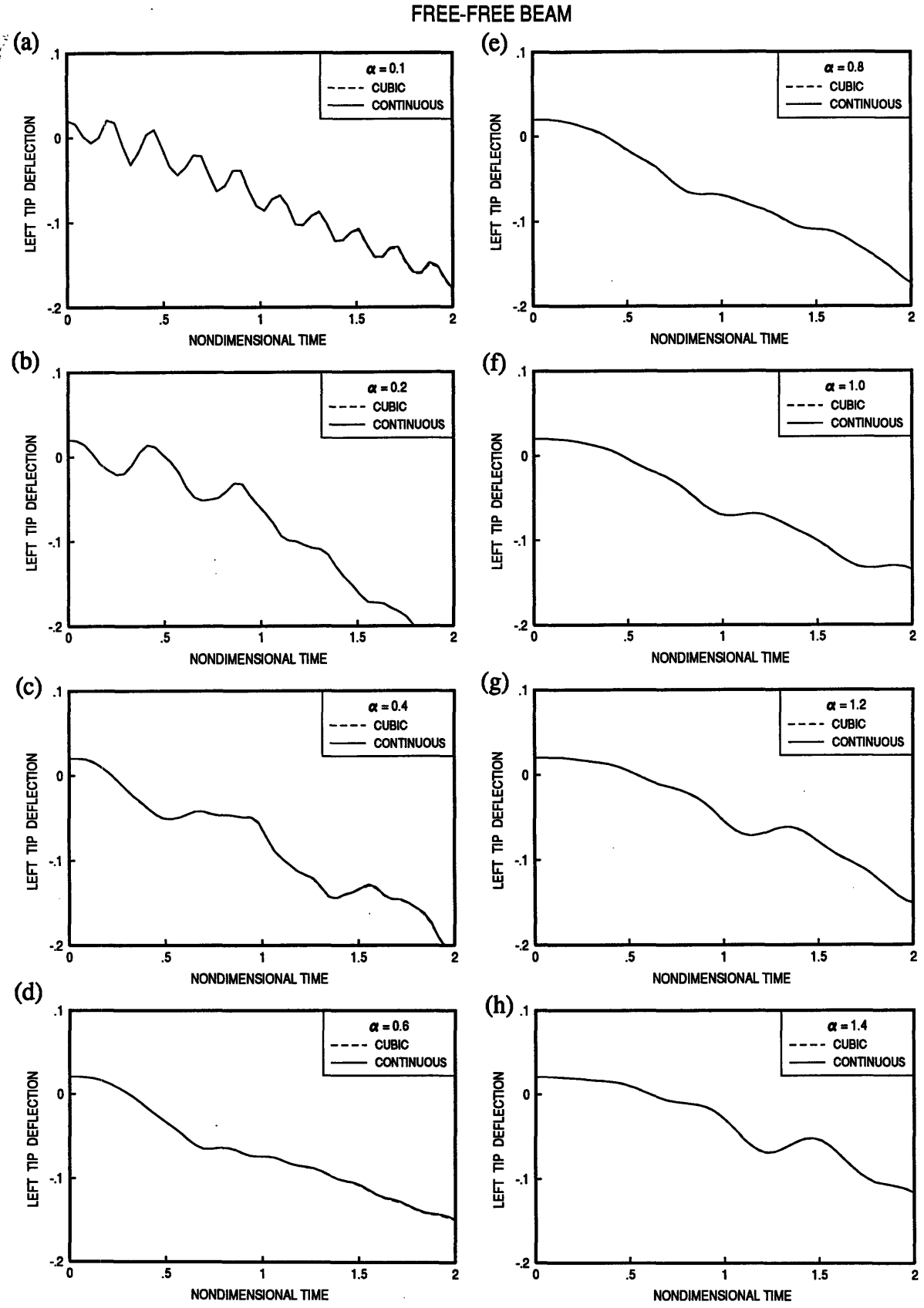

Figure 12. Disc. vs cont. for varying α, μm = 0.5, x = 0.

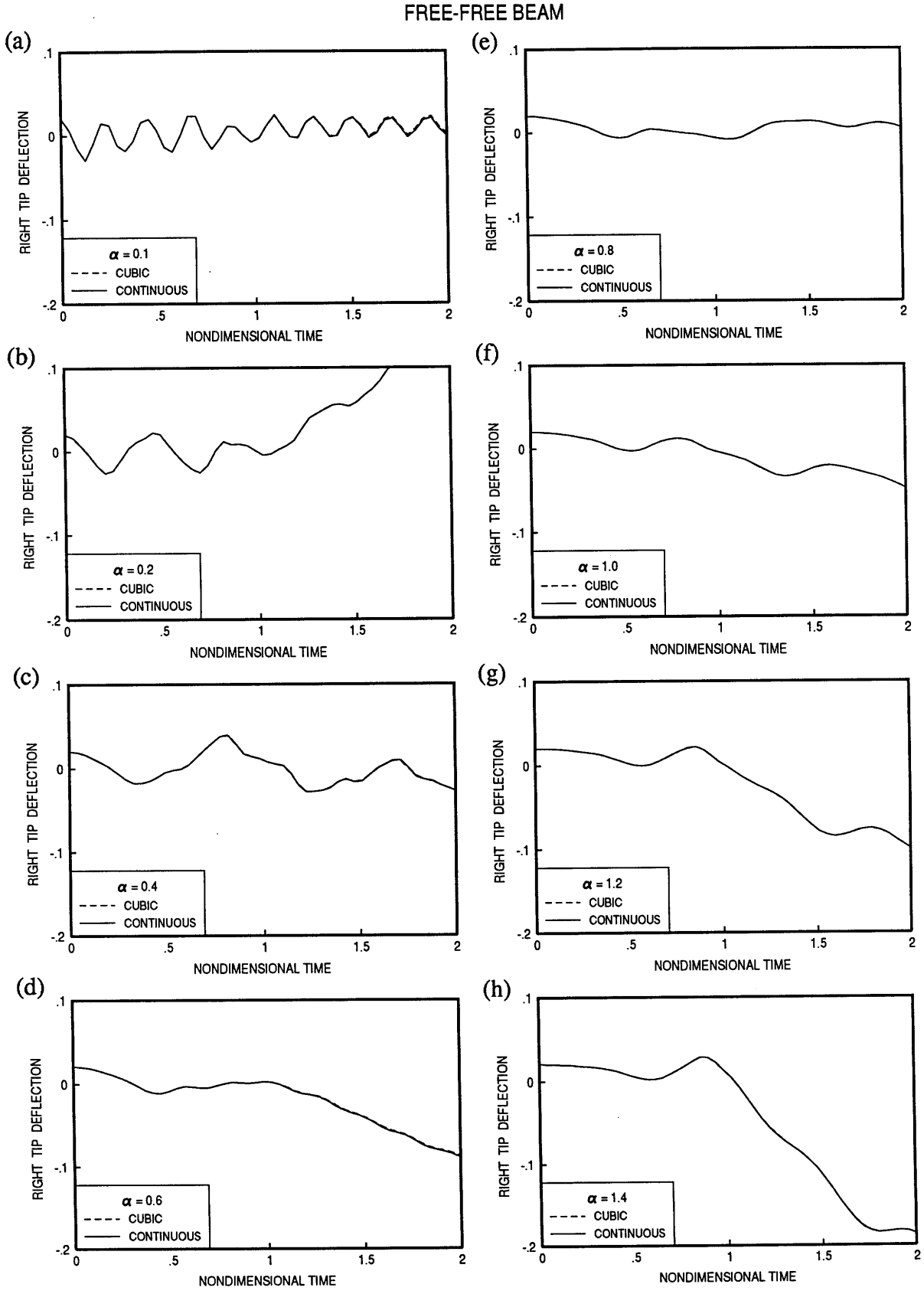

Figure 13. Disc. vs cont. for varying α, μm = 0.5, x = L

the smaller speed parameters, the moving mass does not affect the system dynamics. As the speed parameter increases, the beam's deflection is increased but the beam's initial vibration is damped out.

Figure 14

Figure 14 is the free-free system equivalent of Figure 9. The beam's profile for different time frames is displayed. Once again, Figure 14(a) represents the beam as the mass travels along its length and shows how the beam is vibrating due to the initial kick it received prior to the presence of the moving mass. The top curve, τ = 1.0, shows less vibration than the other intermediate curves. Figure 14(b) displays the free vibration of the beam after the mass has left. Since the beam is inertially free there is an absolute vertical motion of the entire beam. Figure 14(b) also displays an oscillatory motion of the beam.

Figures 15 and 16

Figures 15 and 16 compare the simulations with the moving mass to the simulations without the moving mass. The comparison uses a mass ratio of μ_m = 0.5 and different speed parameters. The simulations show a large discrepancy between the two formulations. Without the inertial effects, the beam is unaware that a mass is

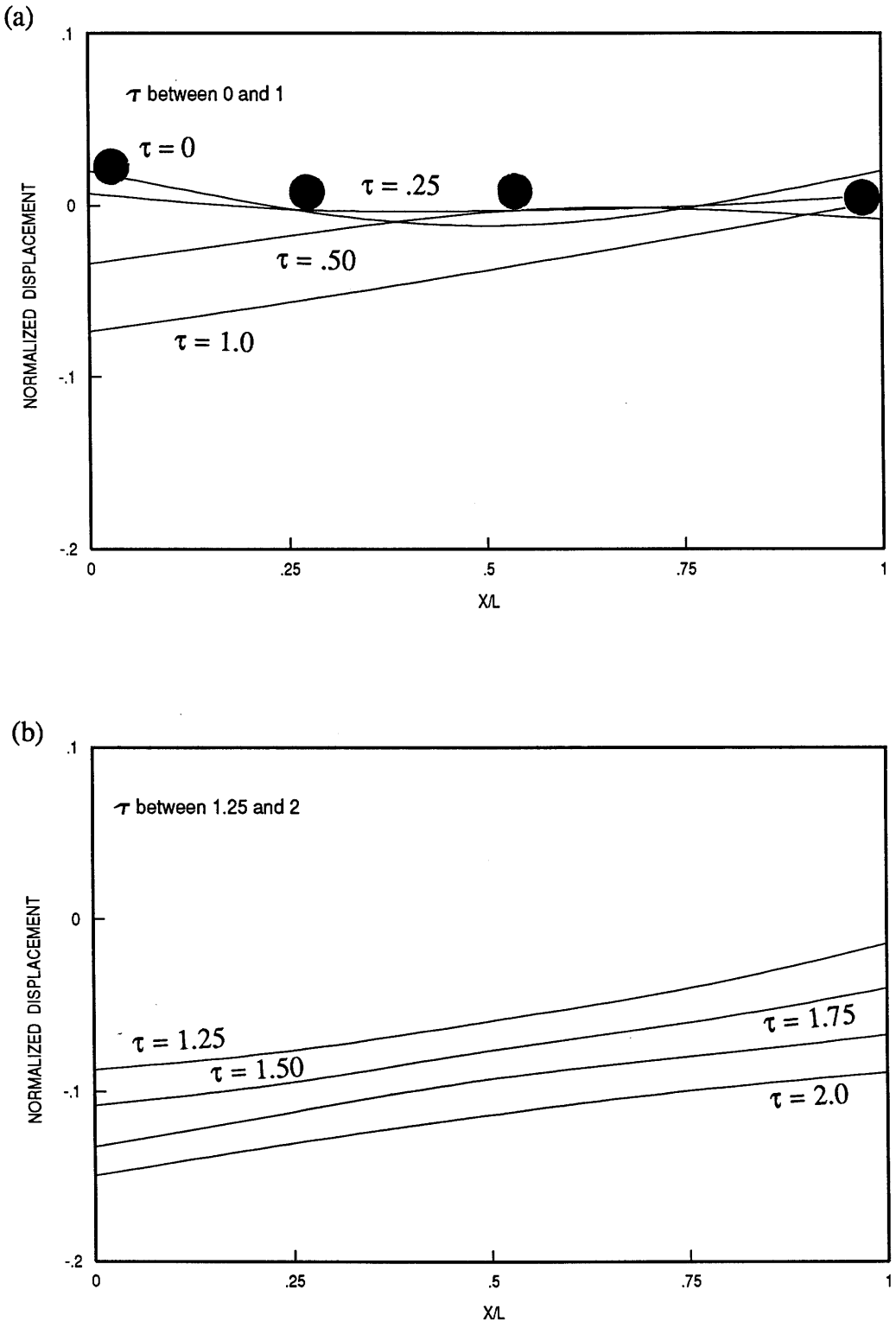

Figure 14. Snapshot of beam with α = 0.6, μm = 0.5.

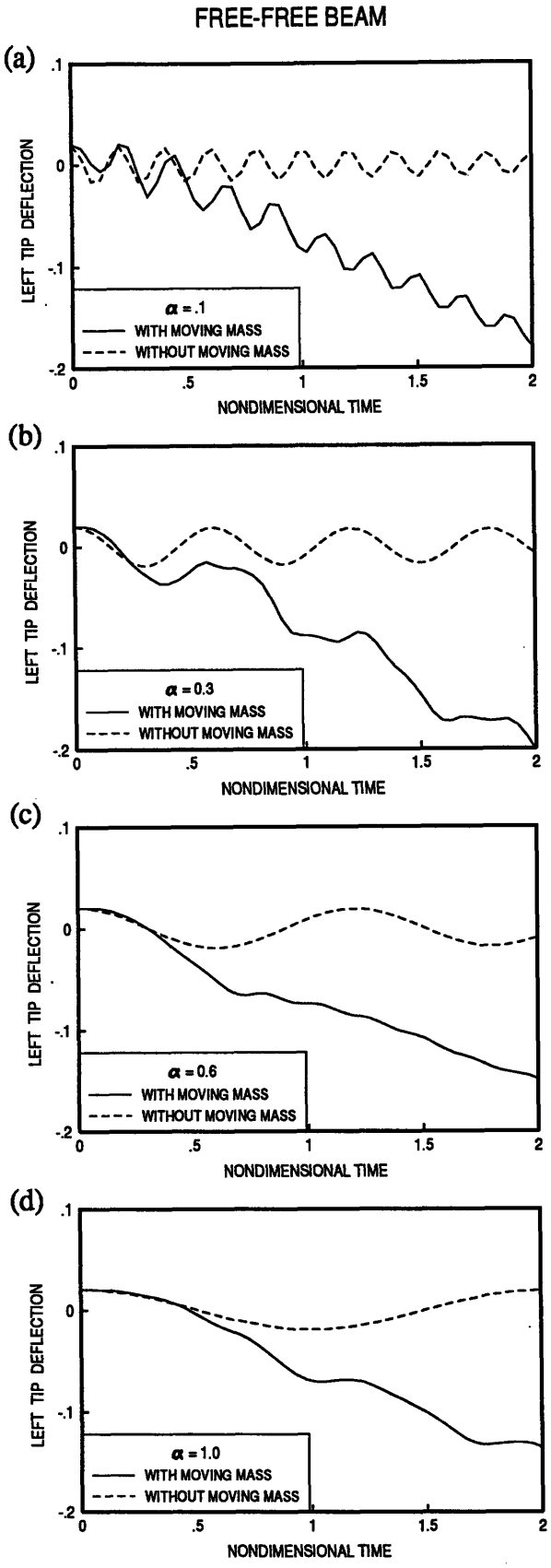

Figure 15. With and without moving mass for varying α, μm=0.5, x=0

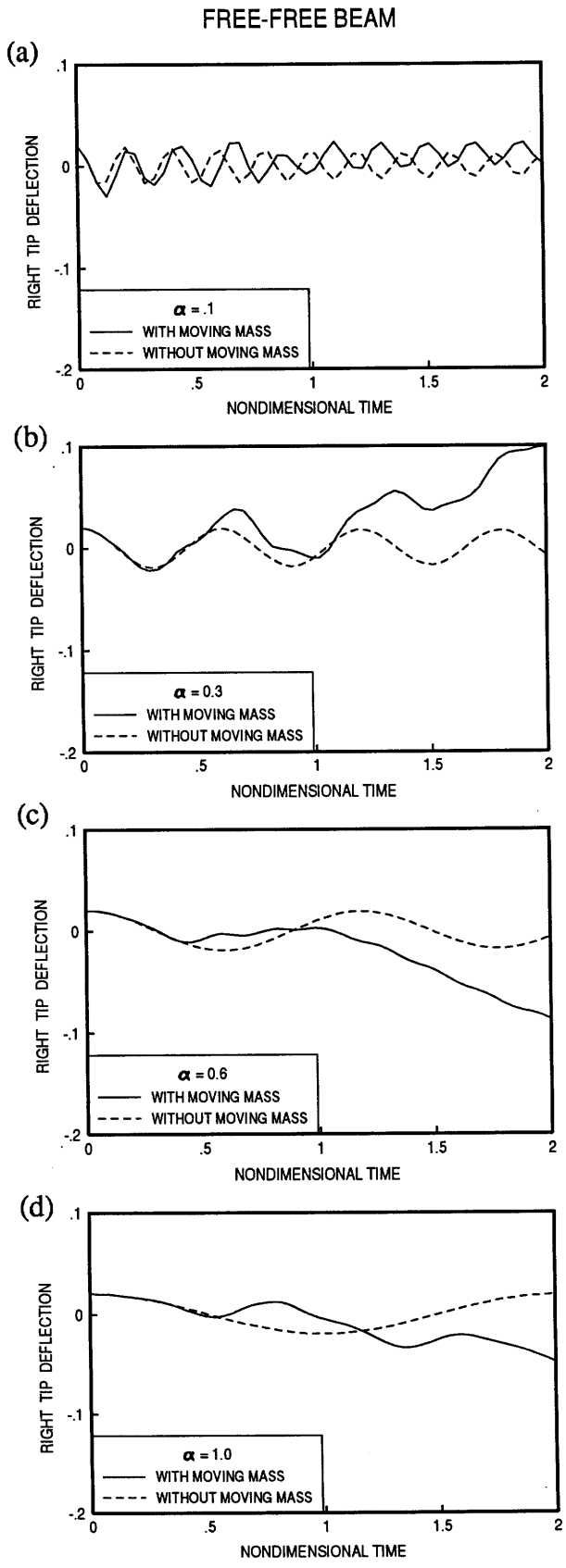

Figure 16. With and without moving mass for varying α, μm=0.5, x=L

travelling across its length and acts like it is in free vibration. As a result, there is no rigid body translation or rotation.

Figures 17 and 18

Figures 17 and 18 determine when it is permissible to ignore the inertial effects that cause the discrepancy in Figures 15 and 16. The two systems, with moving mass and without moving mass, are compared with a constant speed parameter, $\alpha = 0.3$, and varying mass ratios.

Similar to Figure 10, a small difference is detected even for a mass ratio as small as 0.01. It is not until $\mu_m = 0.05$, however, that the difference between the two formulations becomes significant. It is interesting to note that the difference between the two formulations is more dominant at the beam's left tip. The right tip deflections, predicted by the two deflections, are similar until a mass ratio is increased to 0.1.

Based on these simulations, it is not apparent that a moving mass assumption may be construed as a conservative approach for the free-free system. As concluded for Figure 10, to obtain accurate results, all inertial effects of the moving mass should be included.

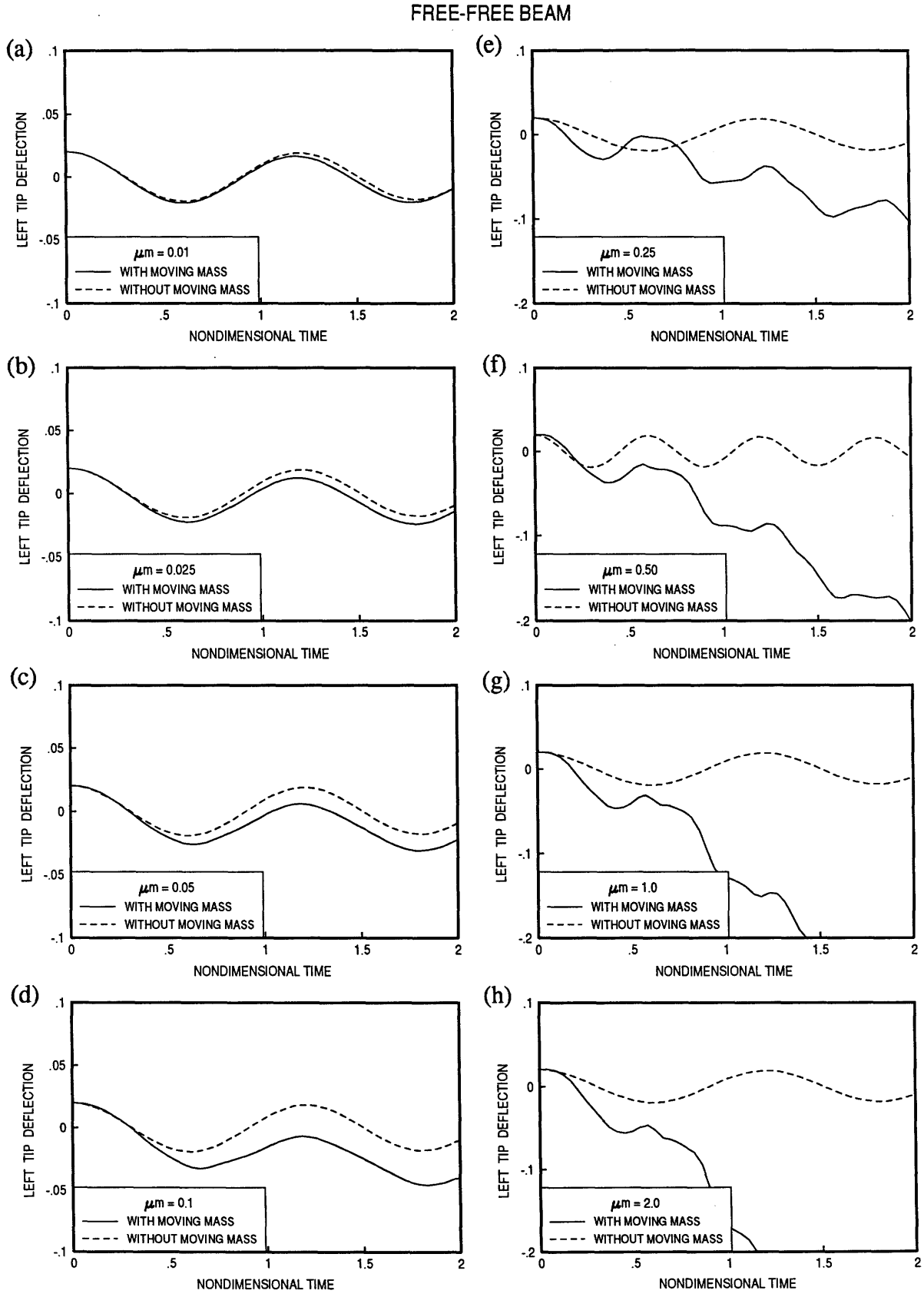

Figure 17. With and without MM for varying μm, α=0.3, x=0

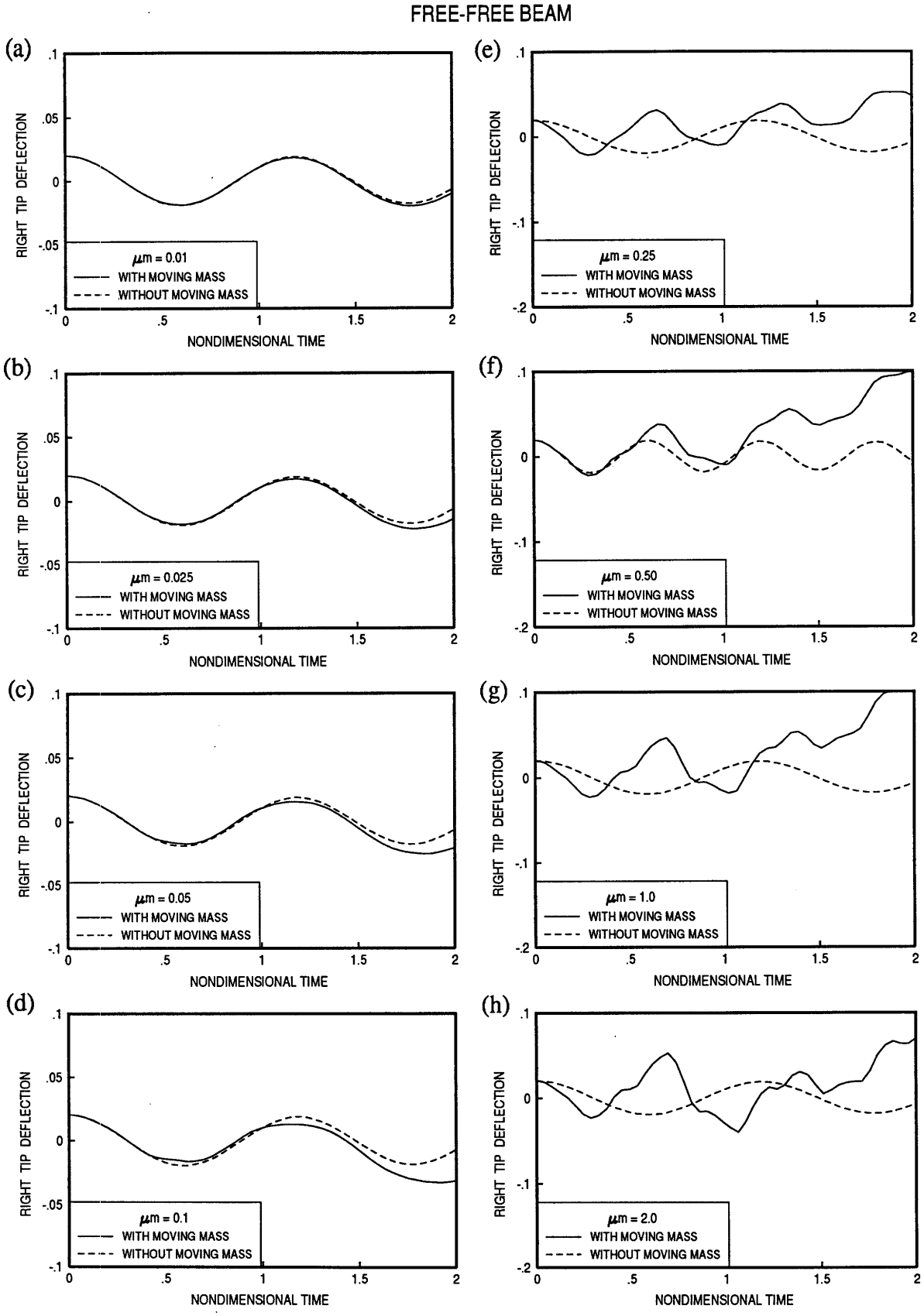

Figure 18. With and without MM for varying μm, α=0.3, x=L

Figures 19 and 20

Figures 18 and 19 focus on the formulation developed in Section 3.3, *Discrete Formulation for Free-Free Beam with Multipoint of Contact.* First, the curves are used to validate the multipoint-of-contact formulation. Second, the effect of the speed parameter on the multipoint-of-contact simulations is examined.

For each speed parameter, simulations are compared for different values of s, the contact spacing parameter defined in Eq. (4.9). The spacing between the two points of contact decreases as s decreases. In both Figures 19 and 20, as the value of s decreased, the curves approach the one-point-of-contact simulation, $s=0$. This trend is expected and consequently validates the multipoint-of-contact formulation derived in Section 3.3. As expected, for small-speed systems, the predicted deflections increase as the separation between the two points increases.

Figures 19 and 20 display another trend: as the speed parameter is increased, the separation between the two points of contact has little effect on the system dynamics. Also, the right tip sees more variation than the left tip, which can be contributed to the extra time that a part of the mass is present on the beam due to the additional point of contact. The right tip sees this effect more significantly because the mass travels left to right across the beam.

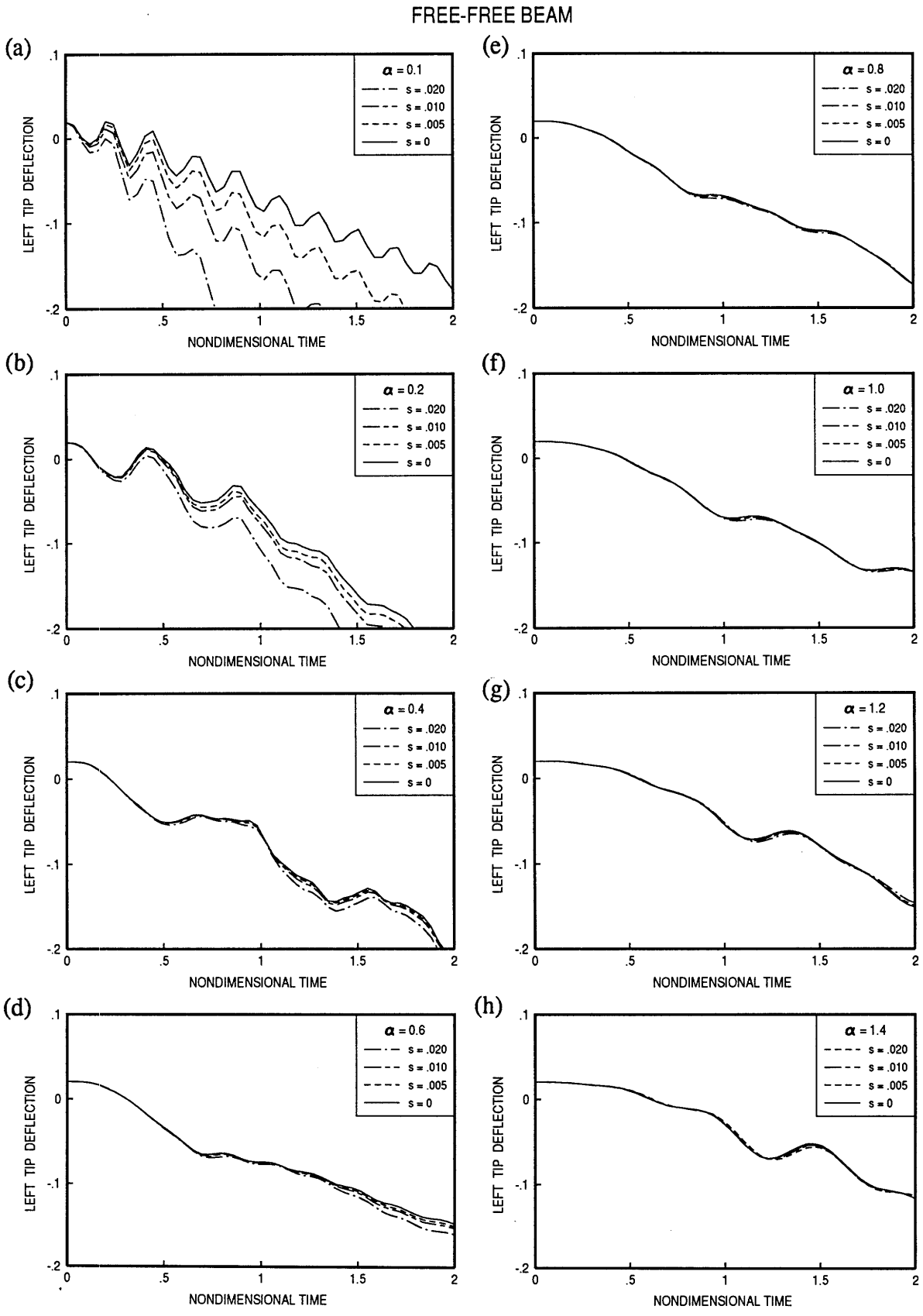

Figure 19. Different spacing for varying α, μm = 0.5, x = 0.

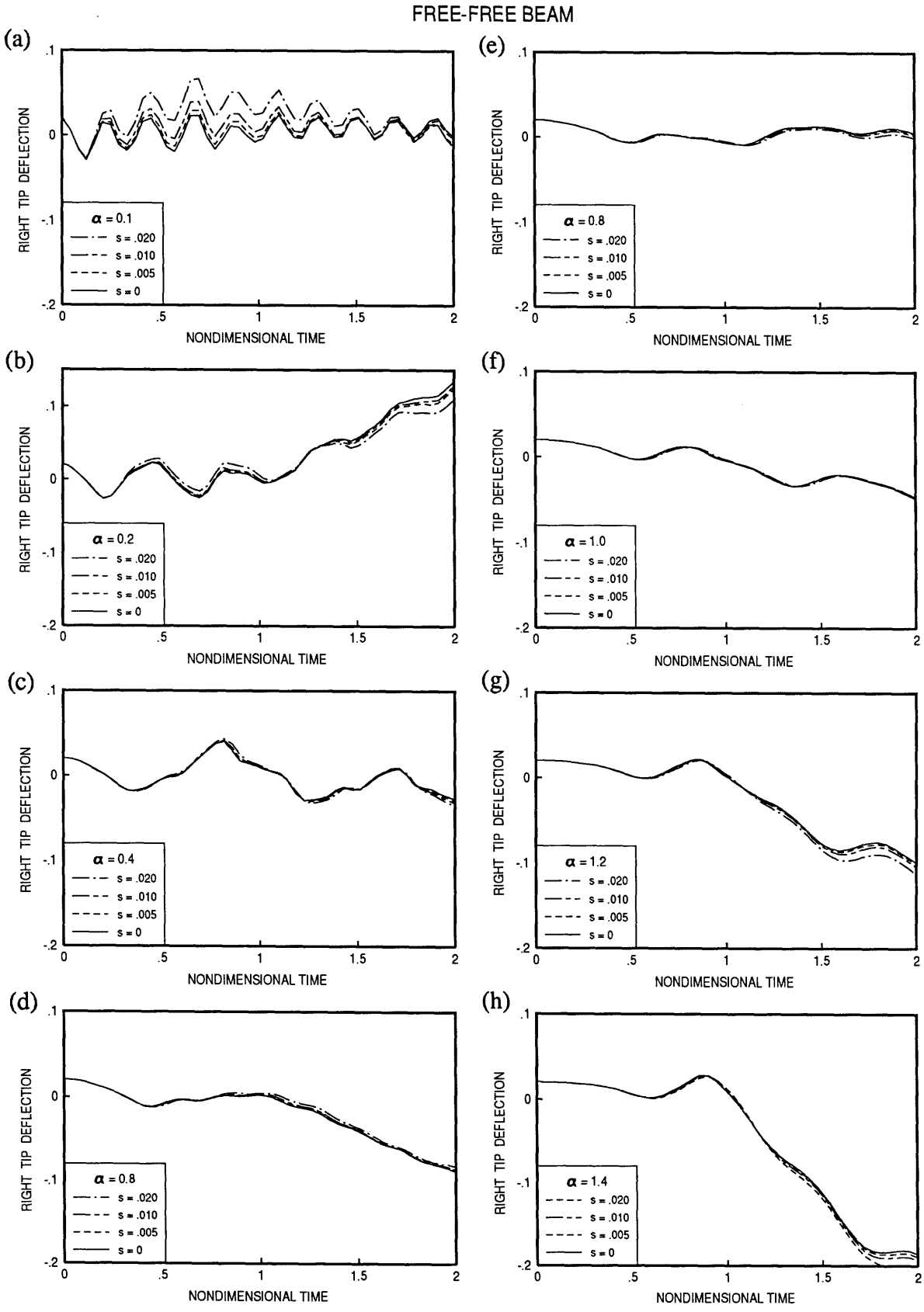

Figure 20. Different spacing for varying α, μm = 0.5, x = L.

CHAPTER 5
CONCLUSIONS

Chapter 5 discusses the important topics and conclusions presented in this thesis. The three different systems used to develop the methodology are examined, and conclusions reached for each system are discussed. Also presented in Chapter 5 is an overview of the different steps taken to develop the discrete formulation. Finally, Chapter 5 contains suggestions for future research.

5.1 SYSTEM MODELS

The primary goal of this research was to develop a methodology that may be used for modeling the inertially free Space Station-Mobile Transporter system using a discrete methodology. In order to validate the discrete formulation, a continuous formulation was developed. Three different systems were used

(1) Inertially fixed system (simply-supported beam).

(2) Inertially free system (free-free beam) with one point of contact.

(3) Inertially free system (free-free beam) with multipoint of contact.

Each system was progressively more accurate in creating a model that resembles the SS-MT system.

5.1.1 System (1): Inertially Fixed System (Simply-Supported Beam)

The inertially fixed system was modeled as a simply-supported beam and developed for methodology verification purposes. The inertially fixed model used in this analysis is the same model that would be used for a heavy load travelling over a bridge. Therefore, many papers are available that provide a simulation of this simply-supported system. The results could consequently be verified by mere comparison with previously published results.

The simplicity of the simply-supported modes enables easy formulation of the equations of motion. Not only are the equations easily formulated, but they can be fully expanded to display certain properties of the system (i.e., symmetry). Also, for a specific time, the mass, stiffness, damping, and force matrices can be determined by hand calculations, which provides a fast check for the computer code.

In addition to method verification, the effects of the nondimensional parameters representing the moving mass speed and the moving mass/flexible structure mass ratio were also examined. The dynamics of the simply-supported system can be easily interpreted by the results of the simulation; the situation is a bit

more involved for the free-free system. Thus, the simply-supported system helped to develop a firm understanding of the moving mass/flexible beam system and, once understood, the formulations can be extended for more advanced problems.

5.1.2 System (2): Inertially Free System (Free-Free Beam) with One Point of Contact

The SS-MT system is designed to orbit around the earth. Therefore, to eventually model that physical system, a free-free system would be needed. In this formulation a free-free beam is used to represent an inertially free system. When the mass was attached to the beam at only one point of contact, the method was validated by comparing continuous and discrete formulations. Similar to the simply-supported system, the effects of the nondimensional parameters, which alter the physical properties of the system, were examined.

The inertially free system with one point of contact successfully validates the discrete methodology that was developed. This system was also used to develop an understanding of how the nondimensional parameters affect the dynamics of the free-free system.

5.1.3 System (3): Inertially Free System (Free-Free Beam) with Two Points of Contact

The iteration to the inertially free one-point-of-contact system increased the complexity of the system but captured the train/track aspect of the SS-MT system. In the final formulation, the mass is attached at two points to the flexible structure.

A continuous formulation was not used to validate the discrete approach for this system. Instead, the discrete one-point-of-contact case was employed. A comparison was made between the two-point-of-contact and the one-point-of-contact simulations for different contact point spacing. As the spacing between the two points approached zero, the two-point-of-contact simulation approached the one-point-of-contact simulation. Because the multipoint-of-contact case approaches a simulation that has already been proved, this provides credence to the discrete methodology for the multipoint-of-contact system.

5.2 CONCLUSIONS

Using the three models described above, the discrete methodology was developed and used to simulate the dynamics of a mass moving over a flexible inertially free and inertially fixed system. The method was successfully validated for each system. An

extensive parametric study was then performed and provides substantial insight in understanding this class of moving-mass problems.

Six steps were taken to develop the discrete methodology:

(1) Develop the discrete equation for the flexible structure.

(2) Develop the discrete equation for the moving mass.

(3) Using compatibility and finite-element shape functions, combine the two discrete equations into a discrete system equation of motion.

(4) Place the system equation into a nondimensional form.

(5) Perform a modal reduction on the entire system.

(6) Place the nondimensional discrete system modal equation into a state space formulation for easy computational evaluation.

In Chapter 3, each of these steps was discussed in great detail for the three stages of the model. The thrust of the research focuses on performing steps (2) and (3) with great accuracy and efficiency. The continuous formulations that were developed for method verification were derived in an identical manner.

The analysis presented in this thesis develops a discrete methodology that will form the basis for formulating the SS-MT simulation. The simplified system examined here, an inertially free

(or fixed) beam with a mass travelling along its length, is also solved using a continuous formulation for methodology validation.

The method presented here is specifically designed with the SS-MT system in mind. This analysis formulated the dynamics of the Flexible Structure/Moving Mass system into a discrete form that is conducive to efficient computational analysis. The discrete formulation, which is in terms of nondimensional parameters that describe the necessary physical properties of the system, was placed in a form suitable for numerical integration. Modal reduction was used for computational feasibility.

5.3 SUGGESTED FUTURE RESEARCH

Using the methodology presented here, a simulation of the Space Station-Mobile Transporter can be developed. Since the dynamics of the system may be cast in a discrete representation that would be suitable for modal reduction, the approach can be employed in the case of large dynamical systems: SS-MT-Space Shuttle. Because these systems will interact, the presented approach can be used to develop a simulation for dynamic interaction studies.

For example, one possible scenario could be to examine the stability of the entire system when the mobile transporter is travelling along the space station while the shuttle is activating its

attitude control system. The interaction between the Space Shuttle's dynamics, the attitude control system, and the SS-MT dynamics is just an example of the potential use of the approach developed in this thesis.

REFERENCES

[1] Messac, A. and D. Herman, "Discrete Dynamics Modelling of a Rigid Body Moving on a Flexible Structure," AAS/AIAA Astrodynamics Conference, Paper # AAS 91-399, Durango, Colorado, August 1991.

[2] Messac, A. and D. Herman, "Dynamics Modeling of Multibody Flexible Systems with Travelling Multi Point Joints," 42nd Congress of the International Astronautical Federation, Paper # IAF 91-292, Montreal, Canada, October 1991.

[3] Nelson, H. D. and R. A. Conover, "Dynamic Stability of a Beam Carrying Moving Masses," *Journal of Applied Mechanics,* Transactions of the ASME, December 1971, pp. 1003-1006.

[4] Duffy, D. G., "The Response of an Infinite Railroad Track to a Moving, Vibrating Mass," *Journal of Applied Mechanics,* Transactions of the ASME, Vol. 57, March 1990, pp. 66-73.

[5] Shimogo, T., and M. Kurihara, "Vibration of an Elastic Beam Subjected to Discrete Moving Loads," *Journal of Mechanical Design*, Vol. 100, July 1978, pp. 514-519.

[6] Stanisic, M. M. and J. C. Hardin, "On the Response of Beams to an Arbitrary Number of Concentrated Moving Masses," *Journal of the Franklin Institute*, Vol. 187, No. 2, February 1969, pp. 115-123.

[7] Taheri, M. R. and T. C. Ting, "Dynamic Response of Plate to Moving Loads: Structural Impedence Method," *Computers & Structures*, Vol. 33, No. 6, 1989, pp. 1379-1393.

[8] Duffek, W. and W. Kortum, "Dynamic Load Computation for Flexible Guideways Under Moving Vehicles Within a Multibody Approach," 5th International Conference on Structural Safety and Reliability, 1989, pp. 1295, 1302.

[9] Cifuentes, A. O., "Dynamic Response of a Beam Excited by a Moving Mass," *Finite Elements in Analysis and Design 5*, Elsevier Science Publisher B.V., Amsterdam - Printed in the Netherlands, 1989, pp. 237-246.

[10] Bodley, C., D. Devers, and C. Park, "A Digital Computer Program for the Dynamic Interaction Simulation of Controls and Structure (DISCOS), Vol. I," NASA Technical Paper 1219, 1978.

[11] Nanda, S., "ADAMS Completion and its Applications," Kingston, Ont., Queen's University, 1979.

[12] CADSI, "DADS Reference Manual," July 1989.

[13] MSC/NASTRAN, *Applications Manual*, Section 2.14.

[14] Bathe, K., "ADINA: A Finite-Element Program for Automatic Dynamic Incremental Nonlinear Analysis," Cambridge, Accoustics and Vibration Laboratory, Mechanical Engineering Department, Massachusetts Institute of Technology, 1977.

[15] Karnopp, D. C., D. L. Margolis, and R. C. Rosenberg, "System Dynamics - A Unified Approach, Second Edition," John Wiley & Sons, New York, 1990.

[16] Meirovitch, L., "Elements of Vibration Analysis," McGraw-Hill Book Company, New York, 1986.

[17] Blevins, R. D., "Formulas for Natural Frequency and Mode Shape," Robert F. Kreiger Publishing Company, Malabar, Florida, 1979.

[18] Strang, G., "Introduction to Applied Mathematics," Wellesley-Cambridge Press, Wellesley, Massachusetts, 1986.

[19] Hildebrand, F., "Advanced Calculus for Applications, Second Edition," Prentice Hall, Inc., Englewood Cliffs, New Jersey, 1976.

[20] Boyce, W. E. and R. C. Diprima, "Elementary Differential Equations and Boundary Value Problems," John Wiley & Sons, New York, 1977.

[21] Ince, E. L., "Ordinary Differential Equations," Longmans, Green, London, 1927, Dover, New York, 1956.

[22] Fletcher, C. A. J., "Computational Techniques for Fluid Dynamics, Volume I, Fundamental and General Techniques," Springer-Verlag, New York, 1988.

[23] The MathWorks, Inc., "PRO-MATLAB User's Guide," January 1989.

NOMENCLATURE

NOMENCLATURE FOR CHAPTERS 1 THROUGH 5

B: : Discrete second derivative operator

C : Damping matrix of the entire system

C_o : Constant damping matrix

C_{var} : Time-varying damping matrix

E : Identity matrix

EI : Bending stiffness of the beam

$(EI)_e$: Elemental bending stiffness

F : Force matrix of the entire system

F_{ext} : Sum of all continuous forces acting on beam

$\tilde{F}_{ext}$: Discrete external force vector

F_m : Continuous force acting on the moving mass

$\tilde{F}_m$: Discrete force acting on the moving mass

F_t : Total force acting on the beam

$\tilde{F}_t$: Total discrete force acting on the beam

f_{c1} : Force due to first point of contact between moving mass and the beam

f_{c2} : Force due to the second point of contact between moving mass and beam

f_{ext} : Continuous external force applied to beam

$f_{\eta ext}$: Modal external force applied to beam

f_{ye} : Equivalent impulse force

I_i : Nondimensional integral where $i = 1, 2, 3$ and 4

i : Location of first point of contact

i' : Location of second point of contact

K : Stiffness matrix of the entire system

$\tilde{K}$: Beam's stiffness matrix

$\tilde{\tilde{K}}$: Nondimensional stiffness matrix of beam

K_O : Constant stiffness matrix

K_{var} : Time-varying stiffness matrix

k : Global stiffness matrix with translational and rotational degrees of freedom

K_t : Finite-element stiffness matrix with only translational degrees of freedom

L : Length of beam

l_e : Length of each beam element

M : Mass matrix for the entire system

$\tilde{M}$: Mass matrix of the beam

$\tilde{\tilde{M}}$: Nondimensional mass matrix of the beam

M_O : Constant mass matrix

M_t : Lumped mass matrix with only translational degrees of freedom

M_{var} : Time-varying mass matrix

m : Finite-element mass matrix with translational and rotational degrees of freedom

m_e : Mass of each beam element

m_i : Mass contribution of each node

m_m : Mass of moving load

N : Number of modes used to approximate the deformation

n : Number of elements used to model the beam

q : Beam's discrete displacement field

$\bar{q}$: Nondimensional discrete displacement field

q_m : Discrete mass displacement field

q_{m1} : Discrete displacement field for first point of contact

q_{m2} : Discrete displacement field for second point of contact

s : Contact point spacing in percent of beam length

T_i : Trial function for cubic shape function where i = $1, 2, 3$,and 4

Tp : Fundamental period of the beam

$u(x,t)$: Continuous displacement field of beam with respect to an inertial reference frame

u_i : Finite-element trial functions $i = 1, 2, 3$, and 4

u_m : Displacement field of moving mass with respect to an inertial reference frame $u_m = u_m(x_m(t),t)$

u_s : Maximum static deflection of the simply-supported beam

V : Generic shape function

V_i : Discretization vector $i = 1, 2, 3$, and 4

$V'i$: Discretization vector for the second point of contact

V_η : Modal form of V

V_1 : Linear shape function

$V3$: Cubic shape function

$V'3$: Cubic shape function for the second point of contact

$V\xi$: Derivative of V with respect to ξ

$V\xi\xi$: Second derivative of V with respect to ξ

$V\eta\xi$: Modal form of $V\xi$

$V\eta\xi\xi$: Modal form of $V\xi\xi$

v_m : Relative velocity of the moving mass

x : State vector

x_i : Position of the i^{th} beam element

$x_m(t)$: Position along the beam of the moving load

Greek Letters

α : Speed parameter

α_f : Speed parameter for the free-free beam

α_s : Speed parameter for the simply-supported beam

β_i : Parameter used for the i^{th} mode shape of a free-free beam

$\delta(\ )$: Dirac delta function

Δ : Distance between the two points of contact

Δt_e : Time required for the mass totravel over one finite beam element

λ : Nondimensional stiffness parameter

Λ : Diagonal matrix of eigenvalues

Λ_r : Reduced diagonal matrix of eigenvalues

$\bar{\eta}$: Vector of nondimensional modal displacements

$\eta_i(t)$: Modal displacement of the i^{th} mode

$\bar{\eta}_i(t)$: Nondimensional modal displacement of the i^{th} mode

ϕ : Modal matrix

ϕ_r : Reduced modal matrix

$\phi_i(x)$: Mode shape of the i^{th} mode

ϕ' : $\frac{d\phi}{dx}$

ϕ'' : $\frac{d^2\phi}{dx^2}$

ϕ^{IV} : $\frac{d^4\phi}{dx^4}$

ρ : Mass per unit length of the beam

σ_i : Parameter used for the i^{th} mode shape of a free free beam

τ : Nondimensional time parameter

μ_g : Nondimensional gravitational load parameter

μ_{fi} : Nondimensional force parameter

$\mu_{\bar{f}}$: Nondimensional discrete force parameter

μ_m : Nondimensional mass parameter

Ω_i : Nondimensional frequency of the i^{th} mode

Ω_{if} : Nondimensional frequency of the i^{th} mode for the free-free beam

Ω_{is} : Nondimensional frequency of the i^{th} mode for the simply-supported beam

ω_i : Dimensional frequency of the i^{th} mode

ω_1 : Natural frequency of the beam

ζ : Damping Ratio $(\zeta = .01)$

NOMENCLATURE FOR APPENDICES

I_C : Total mass moment of inertial of the system

$\mathfrak{L}$: Lagrangian

M_t : Mass of the beam and the moving mass system

$p(x,t)$: Vector locating deformed position of beam with respect to the undeformed position

p_m : Vector locating deformed position of moving mass with respect to the undeformed position $p_m = p_m(x_m(x,t),t)$

$r(t)$: Vector representing the translation of the embedded body reference frame with respect to the inertial reference frame.

S_C : Total static imbalance of the system

T : Total kinetic energy

T_b : Kinetic energy of the beam

T_m : Kinetic energy of the moving mass

V_b : Potential energy of the beam

v_b : Absolute Velocity of the beam

v_c : Absolute Velocity of the moving mass

v_m : Velocity of moving mass with respect to the embedded reference frame

$w(x,t)$: Vector representing the total displacement of the beam with respect to the embedded reference frame

w_m : Vector representing the total displacement of the mass with respect to the embedded reference frame

$w_m = w_m(x_m(x,t),t)$

θ : Angle representing rigid rotation between the embedded body frame and the inertial reference frame

$\tilde{\omega}$: Skew angular velocity of the embedded frame with respect to the inertial reference frame

$$\tilde{\omega} = \begin{bmatrix} 0 & -\dot{\theta} & 0 \\ \dot{\theta} & 0 & 0 \\ 0 & 0 & 0 \end{bmatrix}$$

APPENDIX A
LAGRANGE FORMULATION
OF CONTINUOUS FREE-FREE BEAM

Appendix A formulates the continuous equation of motion for the free-free beam using a Lagrangian approach. The continuous formulation used to numerically simulate the motion of the free-free system presented in Section 3.1 developed the equations using a Newtonian approach.

A Lagrangian formulation uses an energy approach whereas a Newtonian formulation uses force balance. If the individual forces of the system are known, it is easy to develop the equations using Newton's Laws of Motion. However, if the forces are difficult to identify, it is much harder to correctly develop the equations using a Newtonian approach. A Lagrangian formulation, on the other hand, uses the energy of the system. It is more difficult to formulate the equations but, if no algebraic errors are made, the equations are guaranteed to be correct. For this reason, for complex problems a Lagrangian formulation is developed to check the results obtained by the Newtonian method.

Appendix A is organized in the same manner as the individual sections of Chapter 3. First, the equation of motion is derived. Next, the equation is made nondimensional and placed into a

nondimensional form. This equation is then transformed from an equation in terms of the beam's natural coordinates, to an equation in terms of the beam's modal coordinates. Finally, a state space formulation is developed for this derivation.

A.1 MATHEMATICAL MODEL

For this formulation a different model is used for the free-free system (See Figure A-1). A reference frame is embedded at the beam's endpoints. With respect to this reference frame, the beam is simply supported at both ends. The reference frame is considered to undergo rigid body translation and rotation with respect to an inertial reference frame.

In Chapter 3, the beam was able to move in any direction with respect to the inertial reference frame. There is no "body frame" embedded in the flexible structure. In that analysis the two rigid body motions fall naturally from the modal analysis and are not considered separately. That formulation is easier and more exact for numerical computations; however, the derivation developed here provides a good check for the equations because it is more thorough and less error prone.

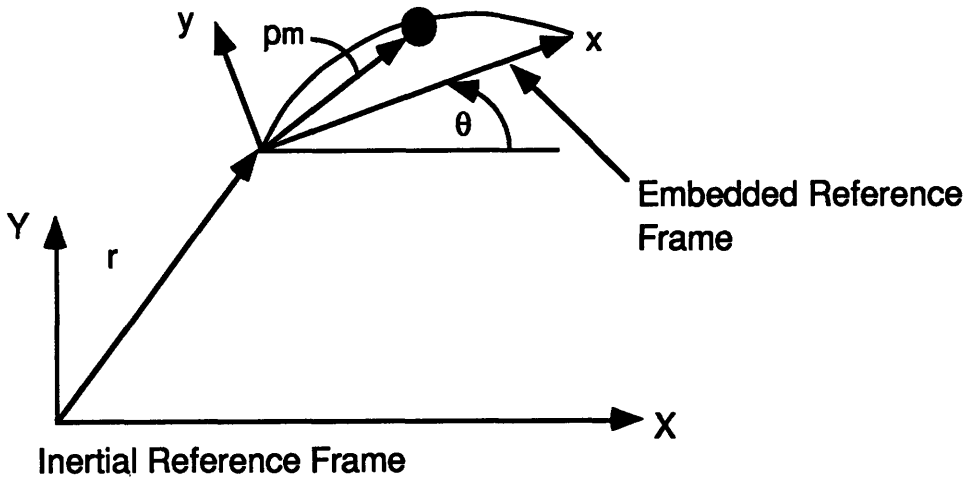

Figure A-1. Model used for Lagrangian Formulation.

A.2 EQUATIONS OF MOTION

The governing equations of motion are derived using basic energy principles. The kinetic and potential energy of the entire system is developed. These expressions are substituted into relations developed using Hamilton's principle. The resulting equations are known as Lagrange's equation.

To formulate the equations, the Lagrangian of the system, $\mathcal{L}$, is used. The Lagrangian is the difference between the system's kinetic and potential energies. Calculus of variations is used to determine a function such that the integral of the Lagrangian takes on a minimum value (Ref. [19]). The resulting formulation is known as Hamilton's principle and is represented in symbolic form as

$$\delta \int_{t_1}^{t_2} \mathcal{L}\, dt = 0 \tag{A.1}$$

Energy of the System

In order to obtain the system's Lagrangian, both the kinetic and potential energy of the system must be determined. The system's kinetic energy is the sum of the beam's kinetic energy and the moving mass' kinetic energy:

$$T = T_b + T_m \tag{A.2}$$

In determining the beam's kinetic energy, the flexible beam is considered to consist of an infinite number of beam elements. The moving mass is viewed as a rigid body.

$$T_b = \frac{1}{2} \int_0^L \rho\, \mathrm{v}_b^T\, \mathrm{v}_b\, dx \tag{A.3}$$

$$T_m = \frac{1}{2}\, m_m\, \mathrm{v}_c^T\, \mathrm{v}_c \tag{A.4}$$

In order to combine Eqs. (A.3) and (A.4) into a common kinetic energy expression, the velocity of the moving mass is rewritten using

the special property of the dirac delta function shown in Eq. (3.14). The velocity of the moving mass is expressed as

$$v_c(x_m, t) = \int_0^L v_b(x, t)\, \delta(x - x_m)\, dx \tag{A.5}$$

Note, as discussed previously, this expression's validity is due to the fact that at x_m the moving mass is firmly attached to the beam, ensuring equivalent velocities. Using the above relation, the total system's kinetic energy is reformulated as

$$T = \frac{1}{2} \int_0^L \left(\rho\, v_b^T v_b + m_m\, v_b^T v_b\, \delta(x - x_m) \right) dx \tag{A.6}$$

where the dependence on the independent values are omitted for brevity.

Because the beam's position vector is expressed in a reference frame that is moving with respect to the inertial reference frame, the inertial derivative contains two variables. The first variable reflects how the beam's position changes in time with respect to the embedded reference frame. The second value determines how the motion of this embedded frame changes with time with respect to the inertial frame. The expression for v_b is

$$v_b = \frac{\partial(r+p)}{\partial t} + \tilde{\omega}(r+p) \tag{A.7}$$

where the two vectors r and p are defined as

r: Vector locating the origin of the embedded reference frame with respect to the inertial reference frame. $r = [r_x \; r_y \; rz]^T$

p: Vector locating the beam's deformed position with respect to the undeformed position. It is expressed with respect to the embedded reference frame. $p = [x \; w \; 0]^T$

There are other vectors necessary to form the kinetic and potential energy expressions. They are:

θ: Angle representing the rigid rotation of the embedded reference frame about the inertial reference frame.

p_m: Vector locating the moving mass' deformed position with respect to the undeformed position. It is expressed with respect to the embedded reference frame. $pm = [x_m \; w_m \; 0]^T$

Using these vectors and Eq. (A.7) the velocity expressions in the x and y directions for the beam are:

$$(v_b)_x = \dot{r}_x - \dot{\theta} w \tag{A.8}$$

$$(v_b)_y = \dot{r}_y + \dot{w} + \dot{\theta} x \tag{A.9}$$

Since the reference frame embedded in the moving mass is moving, the velocity of the moving mass takes on a different form. It is expressed as

$$(v_c)_x = \dot{r}_x - \dot{\theta} w_m + v_m \tag{A.10}$$

$$(v_c)_y = \dot{r}_y + \dot{w}_m + v_m \frac{\partial w_m}{\partial x_m} + \dot{\theta} x_m \tag{A.11}$$

where v_m is the speed of the mass relative to the beam. Eqs. (A.10) and (A.11) represent the moving mass velocity that would be obtained using Eq. (A.5).

Next, the system's potential energy is defined. The system being examined is in a gravity-free environment. Thus, the only potential energy of the system is the strain energy due to the beam's deformation:

$$V_b = \int_0^L EI \left(\frac{\partial^2 w}{\partial x^2} \right)^2 dx \tag{A.12}$$

where EI is the effective bending stiffness of the beam. Note that the beam's material properties are assumed to be homogeneous. The potential and kinetic energies are used to form the Lagrangian, which is used in Hamilton's Principle.

Hamilton's Principle

Once the system's potential and kinetic energy are known, it is trivial (but tedious) to apply Hamilton's principle. First, the Lagrangian of the system is formed. Substituting Eqs. (A.6) and (A.12) into the Lagrangian expression yields Eq. (A.13):

$$\mathcal{L} = \int_0^L \frac{1}{2} \left(\rho \, \mathrm{v}_b^T \mathrm{v}_b + m_m \, \mathrm{v}_b^T \mathrm{v}_b \, \delta(x - x_m) - EI \left(\frac{\partial^2 w}{\partial x^2} \right)^2 \right) dx \tag{A. 13}$$

Equation (A.13) is substituted into Eq. (A.1). The variation of $\mathcal{L}$ is taken with respect to each of its dependent variables. In this system, $\mathcal{L}$ is a function of eight variables:

$$\mathcal{L} = \mathcal{L}\left(\dot{r}_x, \, r_y, \, \dot{r}_y, \, \dot{\theta}, \, \dot{w}, \, w_{,xx}, \, \dot{w}_m, \, w_{m,x_m} \right) \tag{A.14}$$

where $\dot{(\,)}$ and $(\,)_{,}$ represent derivatives with respect to time and spatial position, respectively. The r and w vectors have been previously defined. The other variables are:

It is necessary to take the first variation of $\mathcal{L}$ with respect to each of the variables shown in Eq. (A.14. In symbolic terms Eq. (A.1) becomes

$$\int_{t_1}^{t_2} \left[\left[\frac{\partial T}{\partial \dot{r}_x}\right] \delta \dot{r}_x + \left[\frac{\partial T}{\partial r_y}\right] \delta r_y + \left[\frac{\partial T}{\partial \dot{r}_y}\right] \delta \dot{r}_y + \left[\frac{\partial T}{\partial \dot{\theta}}\right] \delta \dot{\theta} + \left[\frac{\partial T}{\partial \dot{w}}\right] \delta \dot{w} \right] dt +$$

$$\int_{t_1}^{t_2} \left[\left[\frac{\partial T}{\partial \dot{w}_m}\right] \delta \dot{w}_m + \left[\frac{\partial T}{\partial w_{m,x_m}}\right] \delta w_{m,x_m} + \left[\frac{\partial V_b}{\partial w_{,xx}}\right] \delta w_{,xx} \right] dt = 0 \tag{A.15}$$

where the actual expressions for the kinetic and potential energy, Eqs. (A.6) and (A.12), have been omitted for clarity. It is desirable to have Eq. (A.14) in a form where the only variations are of the actual variables, not their respective derivatives. This form is:

$$\int_{t_1}^{t_2} \left[(\ldots)\, \delta r_x + (\ldots)\, \delta r_y + (\ldots)\, \delta w + (\ldots)\, \delta \theta \right] dt = 0 \tag{A.16}$$

To obtain the form outlined in Eq. (A.16), each term in Eq. (A.14) is integrated by parts. This type of integration separates two

functions. One function becomes a differential and the other is integrated upon. The form of this type of integration is:

$$\int u\, dv = uv - \int v\, du \tag{A.17}$$

The function chosen to be u takes on a differential form in the new integral. The function chosen to be dv is in its integrated form, v, for the new integral. The term in front of the new integral is evaluated at the endpoints of the integral.

This type of integration is performed on the terms in Eq. (A.15). The variation is chosen to be the dv function and the corresponding differential is the u function. The terms that are evaluated at the endpoints of the integral are the beam's boundary conditions. After the integration by parts, the equation is in the "strong form" (Ref. [18]).

The first term of Eq. (A.15) is used as an example

$$\int_{t_1}^{t_2} \left[\left[\frac{\partial T}{\partial \dot{r}_x} \right] \delta \dot{r}_x \right] dt = \left[\left[\frac{\partial T}{\partial \dot{r}_x} \right] \delta r_x \right]_{t_1}^{t_2} - \int_{t_1}^{t_2} \frac{\partial}{\partial t} \left[\frac{\partial T}{\partial \dot{r}_x} \right] \delta r_x \, dt \tag{A.18}$$

Once the terms are in the appropriate form, the additive property of integration is used to rewrite the integral, resulting in:

$$\int_{t_1}^{t_2} (\,)\,\delta r_x + \int_{t_1}^{t_2} (\,)\,\delta r_y + \int_{t_1}^{t_2} (\,)\,\delta\theta + \int_{t_1}^{t_2} (\,)\,\delta w = 0 \qquad \text{(A.19)}$$

These four integrals are separated to obtain four equations of motion.

Final Equations of Motion

For Eq. (A.19) to be true, each integral must vanish independently. To have each integral vanish for any arbitrary time period, the actual integrands of each integral must respectively go to zero. This leads to four equations.

The four equations are obtained by following three steps. First, the actual kinetic and potential energies outlined in Eqs. (A.6), (A.7), (A.8), (A.9), (A.11), and (A.12) are used in Eq. (A.15). The resulting expression is integrated (by parts) to obtain the form shown in Eq. (A.16). The additive property of this integration is used to separate the result into the four equations of motion, shown in Eqs. (A.20)-(A.23):

$$(m_m + \rho L)\,\ddot{r}_x = 0 \qquad \text{(A.20)}$$

$$(m_m + \rho L)\,\ddot{r}_y + \left(\frac{\rho L^2}{2} + m_m x_m\right)\ddot{\theta} + 2\, m_m v_m \dot{\theta} + \left(m_m \dot{w} + m_m v_m^2 \frac{\partial w}{\partial x} + 2\, m_m v_m \frac{\partial^2 w}{\partial t\, \partial x}\right)_{@\, x_m} + \int_0^L \rho\, \dot{w}\, dx = 0 \tag{A.21}$$

$$\left(\frac{\rho L^2}{2} + m_m x_m\right)\ddot{r}_y + \left(\frac{\rho L^3}{3} + m_m x_m^2\right)\ddot{\theta} + 2\, m_m v_m x_m \dot{\theta} + \left(m_m x_m \dot{w} + m_m x_m v_m^2 \frac{\partial w}{\partial x} + 2\, m_m x_m v_m \frac{\partial^2 w}{\partial t\, \partial x}\right)_{@\, x_m} + \int_0^L \rho\, x\, \dot{w}\, dx = 0 \tag{A.22}$$

$$\rho L\, \ddot{r}_y + \left(\rho L^2 + m_m x_m\right)\ddot{\theta} + 2\, m_m v_m \dot{\theta} + \left(m_m \dot{w} + m_m v_m^2 \frac{\partial^2 w}{\partial x^2} + 2\, m_m v_m \frac{\partial^2 w}{\partial t\, \partial x}\right)_{@\, x_m} + \rho\, \dot{w} + EI \frac{\partial^4 w}{\partial x^4} = 0 \tag{A.23}$$

Equations (A.20) and (A.21) represent Newton's second law in the horizontal and vertical direction, respectively. Equation (A.22) states that the sum of the moments around the origin of the embedded reference frame is zero. Equation (A.23) is the partial differential equation describing $w(t)$, the lateral vibration of the beam. These equations could have been written directly using Newton's Law of motion (see Section 3.1); however, it is important to account for all of the forces. The energy approach might be more time-consuming than if Newton's Law were immediately applied, but if done carefully it assures that all forces acting on the system have been represented correctly.

Equations (A.21) through (A.23) are next placed into the beam's modal coordinates. In this form it will be easier to compare the terms obtained in this derivation and the ones obtained during Section 3.1. Section 3.1 was derived for any boundary condition. This analysis is specific to the free-free beam.

Modal Solution

The beam's total deflection must be determined. The total deflection is the vector sum of the rigid body motions and the flexible motions of the beam. The horizontal motion of the system, Eq. (A.20), is decoupled from the other three motions, thereby not playing a role in the total deflection. The other three equations are completely coupled.

A linear superposition of modes is used to solve the three coupled equations, Eqs. (A.21), (A.22), and (A.23). As in Chapter 3, Galerkin's method is used to reduce the error of the approximation. However, unlike the lone partial differential equation shown in Eq. (3.10), there are two ordinary differential equations and one partial differential equation. A modal substitution for the beam's vibration is used in all three equations, but Galerkin's method is only applied to the partial differential equation.

The substitution shown in Eq. (3.11) is used for the beam's lateral vibration, $w(x,t)$. The modes chosen must reflect the beam's lateral vibration only and not the total displacement as was modeled in Chapter 3. After the modes are chosen, the three equations are transformed into modal coordinates and Galerkin's method is used where applicable.

Modes Used

The modes used are those of a simply-supported beam. This may seem incorrect since the beam itself is considered to be inertially free. However, this derivation was formulated so that the beam is simply supported with respect to the embedded reference frame and the embedded frame undergoes the rigid body motion with respect to the inertial frame. Therefore, the choice of simply-supported modes for the vibration of the beam is justified. The modes for the simply-supported beam are shown again for convenience.

$$\phi_i(x) = \sin \frac{i \pi x}{L} \tag{A.24}$$

These modes are nondimensional and orthogonal; however, it is noted once again that they are not orthonormal. Using these modes, Eqs. (A.21), (A.22), and (A.23) become

$$\left(m_m + \rho L\right)\ddot{r}_y + \left(\frac{\rho L^2}{2} + m_m x_m\right)\ddot{\theta} + 2\, m_m \mathrm{v}_m \dot{\theta} + \rho \sum_{i=1}^{N} \ddot{\eta}_i \int_0^L \phi_i\, dx +$$

$$+ m_m \sum_{i=1}^{N} \left(\phi_i \ddot{\eta}_i + 2\, \mathrm{v}_m \phi_i' \dot{\eta}_i + \mathrm{v}_m^2 \phi_i'' \eta_i\right)_{@\, x_m} = 0 \qquad \text{(A.25)}$$

$$\left(\frac{\rho L^2}{2} + m_m x_m\right)\ddot{r}_y + \left(\frac{\rho L^3}{3} + m_m x_m^2\right)\ddot{\theta} + 2\, m_m \mathrm{v}_m x_m \dot{\theta}$$

$$+ \rho \sum_{i=1}^{N} \ddot{\eta}_i \int_0^L x\, \phi_i\, dx$$

$$+ m_m \sum_{i=1}^{N} \left(x_m \phi_i \ddot{\eta}_i + 2\, x_m \mathrm{v}_m \phi_i' \dot{\eta}_i + x_m \mathrm{v}_m^2 \phi_i'' \eta_i\right)_{@\, x_m} = 0 \qquad \text{(A.26)}$$

$$\int_0^L \phi_j \left(EI \sum_{i=1}^{N} \phi_i^{IV} \eta_i + \rho \ddot{r}_y + \rho x \ddot{\theta} + \rho \sum_{i=1}^{N} \phi_i \ddot{\eta}_i\right) dx$$

$$+ m_m \phi_j \left(\ddot{r}_y + x_m \ddot{\theta} + 2\, \mathrm{v}_m \dot{\theta}\right)$$

$$+ m_m \left[\phi_j \sum_{i=1}^{N} \left(\phi_i \ddot{\eta}_i + 2\, \mathrm{v}_m \phi_i' \dot{\eta}_i + \mathrm{v}_m^2 \phi_i'' \phi_i\right)\right]_{@\, x_m} = 0 \qquad \text{(A.27)}$$

Equations (A.25), (A.26), and (A.27) represent the motion of the inertially free flexible beam with a mass moving along its length. The equations are in terms of the modal coordinates but are still in dimensional form. Therefore, the next step is to make them nondimensional.

Some nondimensional integrals are needed to place the equations into a nondimensional form. Two of the nondimensional integrals were already defined in Eqs. (3.15) and (3.16). They are rewritten below for convenience.

$$I_1(i,j) = \frac{1}{L}\int_0^L \phi_i \, \phi_j \, dx \tag{A.28}$$

$$I_2(i,j) = L^3 \int_0^L \phi_i^{IV} \, \phi_j \, dx \tag{A.29}$$

The two other integrals needed are actually just special cases of Eqs. (A.28) and (A.29) that incorporate the rigid body modes. Since these motions are not accounted for in the mode shapes, as in Chapter 3, the integrals must be defined separately. They are

$$I_3(i) = \frac{1}{L}\int_0^L \phi_i \; dx \tag{A.30}$$

$$I_4(i) = \frac{1}{L^2}\int_0^L x \, \phi_i \; dx \tag{A.31}$$

Equation (A.29) represents the rigid body translation and Eq. (A.31) is the rigid body rotation (i.e., $\phi j = 1$ and $\phi j = x$, respectively). The values of the $I1$ and I_2, for the simply-supported mode shapes, were

found in Eqs. (3.45) and (3.47). These values, together with I_3 and I_4, are

$$I_1(i,i) = \frac{1}{2} \tag{A.32}$$

$$I_2(i,i) = \frac{(i\,\pi)^4}{2} \tag{A.33}$$

$$I_3\ (i) = \frac{1 - \cos i\,\pi}{i\,\pi} \tag{A.34}$$

$$I_4\ (i) = -\frac{\cos i\,\pi}{i\,\pi} \tag{A.35}$$

For convenience the following variables are defined

$$M_t = \rho L + m_m \tag{A.36}$$

$$S_c = \frac{\rho L^2}{2} + m_m\, x_m \tag{A.37}$$

$$I_c = \frac{\rho L^3}{3} + m_m\, x_m^2 \tag{A.38}$$

where M_t is the mass of the beam and the moving mass, S_C is the total static imbalance, and I_C is the entire mass moment of inertia. Using the above identities and the four nondimensional integrals, the three equations of motion are rewritten in a further condensed form:

$$M_t \ddot{r}_y + S_c \ddot{\theta} + 2\, m_m \mathrm{v}_m \dot{\theta} + \rho L \sum_{i=1}^{N} I_3(i)\, \ddot{\eta}_i + m_m \sum_{i=1}^{N} \left(\phi_i \ddot{\eta}_i + 2\, \mathrm{v}_m \phi_i' \dot{\eta}_i + \mathrm{v}_m^2 \phi_i'' \eta_i\right)_{@\, x_m} = 0 \tag{A.39}$$

$$S_c \ddot{r}_y + I_c \ddot{\theta} + 2\, m_m x_m \mathrm{v}_m \dot{\theta} + \rho L^2 \sum_{i=1}^{N} I_4(i)\, \ddot{\eta}_i + m_m x_m \sum_{i=1}^{N} \left(\phi_i \ddot{\eta}_i + 2\, \mathrm{v}_m \phi_i' \dot{\eta}_i + \mathrm{v}_m^2 \phi_i'' \eta_i\right)_{@\, x_m} = 0 \tag{A.40}$$

$$\left(\rho L\, I_3(j) + m_m \phi_{j@\, x_m}\right) \ddot{r}_y + \left(\rho L^2\, I_4(j) + m_m x_m \phi_{j@\, x_m}\right) \ddot{\theta} + 2\, m_m \mathrm{v}_m \phi_j \dot{\theta} + \rho L \sum_{i=1}^{N} I_1(i,j)\, \ddot{\eta}_j + \frac{EI}{L^3} \sum_{i=1}^{N} I_2(i,j)\, \eta_j + m_m \left[\phi_j \sum_{i=1}^{N} \left(\phi_i \ddot{\eta}_i + 2\, \mathrm{v}_m \phi_i' \dot{\eta}_i + \mathrm{v}_m^2 \phi_i'' \eta_i\right)\right]_{@\, x_m} = 0 \tag{A.41}$$

It is important to note that the equations, as they stand, are valid for any mode shape used. The mode shapes should satisfy both the geometric and force boundary conditions.

This analysis uses modes shapes for a simply-supported beam, i.e., sine modes. With respect to the embedded frame, the beam is simply-supported; therefore, the modes do satisfy the geometric boundary conditions. They do not, however, satisfy the force

boundary conditions for the actual free-floating beam. Using the simply-supported modes, there is a shear force at the ends of the beam. For a free-floating beam there are no moments or shears at the endpoints. The natural frequencies of the above modal system, with the rigid motions constrained, resemble the natural frequencies of a free-free beam, but the shapes of the sine modes do not accurately model the motion of the actual beam. It is better to use the free-free mode shapes of the beam as in Chapter 3, which satisfy all boundary conditions at the ends.

For these reasons, the above derivation is not used to numerically determine the beam's total deflection due to the motion of the moving mass. Even though this derivation is not used to compute the actual results, it is presented as a check to the derivation of Chapter 3.

A.3 NONDIMENSIONAL EQUATIONS OF MOTION

Equations (A.39), (A.40), and (A.41) are placed into a standard nondimensional form using the procedure outlined in Chapter 3. The same nondimensional parameters that were defined in Eqs. (3.21)-(3.24) appear. This derivation is specific to the inertially free system; therefore, there is no external force applied to the beam. Since the mode shapes used are sine waves, the respective

derivatives are easy to evaluate and have also been included. The final three nondimensional equations are:

$$(1+\mu_m)\,\ddot{\bar{r}}_y + \left(\frac{1}{2}+\mu_m\tau\right)\ddot{\theta} + 2\,\mu_m\,\dot{\theta} + \sum_{i=1}^{N} I_3(i)\,\ddot{\bar{\eta}}_i + \mu_m\left(\sum_{i=1}^{N} \sin i\pi\tau\,\ddot{\bar{\eta}}_i + 2\,i\pi\cos i\pi\tau\,\dot{\bar{\eta}}_i - (i\pi)^2 \sin i\pi\tau\,\bar{\eta}_i\right) = 0 \tag{A.42}$$

$$\left(\frac{1}{2}+\mu_m\tau\right)\ddot{\bar{r}}_y + \left(\frac{1}{3}+\mu_m\tau^2\right)\ddot{\theta} + 2\,\mu_m\,\tau\,\dot{\theta} + \sum_{i=1}^{N} I_4(i)\,\ddot{\bar{\eta}}_i + \mu_m\,\tau\left(\sum_{i=1}^{N} \sin i\pi\tau\,\ddot{\bar{\eta}}_i + 2\,i\pi\cos i\pi\tau\,\dot{\bar{\eta}}_i - (i\pi)^2 \sin i\pi\tau\,\bar{\eta}_i\right) = 0 \tag{A.43}$$

$$\left(I_3(j)+\mu_m \sin j\pi\tau\right)\ddot{\bar{r}}_y + \left(I_4(j)+\mu_m\tau\sin j\pi\tau\right)\ddot{\theta} + 2\,\mu_m \sin j\pi t\,\dot{\theta} + \sum_{i=1}^{N} I_1(i,j)\,\ddot{\bar{\eta}}_j + \lambda\sum_{i=1}^{N} I_2(i,j)\,\bar{\eta}_j + \quad \text{for } j=1,..,N$$

$$\mu_m \sin j\pi\tau\left(\sum_{i=1}^{N} \sin i\pi\tau\,\ddot{\bar{\eta}}_i + 2\,i\pi\cos i\pi\tau\,\dot{\bar{\eta}}_i - (i\pi)^2 \sin i\pi\tau\,\bar{\eta}_i\right) = 0 \tag{A.44}$$

These three equations are the nondimensional counterparts of Eqs. (A.39), (A.40), and (A.41) and correspond to the expanded version of Eq. (3.27) Equations (A.42) and (A.43) correspond to the rigid body translation and rotation, respectively, and Eq. (A.44) corresponds to the flexible modes. Equation (A.44) along with $r_y = 0$,

$\theta = 0$ corresponds to the simply-supported beam case developed in Chapter 3.

Though these equations will not be used for numerical analysis, they are still placed into a state space form because it is easier to see the similarities and differences between the derivation presented here and the one reviewed in Chapter 3.

A.4 STATE SPACE REPRESENTATON

The three equations above, Eqs. (A.42), (A.43), and (A.44), are a coupled set of N first-order equations. The three equations are combined into one matrix equation that is dependent on the system states. In a state-determined system, all information needed about the system is summarized in a finite set of variables. First, the state variables are placed into a state vector. Using this vector, a matrix representation of the system is obtained.

State Vector

The following two vectors are defined.

$$x1 = \left\{ \begin{array}{cccc} \bar{r}_y & \theta & \bar{\eta}_1 & \cdots & \bar{\eta}_N \end{array} \right\}^T \tag{A.45}$$

$$x2 = \left\{ \begin{array}{cccc} \dot{\bar{r}}_y & \dot{\theta} & \dot{\bar{\eta}}_1 & \cdots & \dot{\bar{\eta}}_N \end{array} \right\}^T \tag{A.46}$$

The state vector x, is a combination of $x1$ and $x2$

$$x = \begin{Bmatrix} x1 \\ x2 \end{Bmatrix} \tag{A.47}$$

As stated previously, this state vector contains all the relevant information about the system.

Matrix Representation

Using the state vector of Eq. (A.47), the mass, damping, and stiffness matrices are derived. As indicated earlier, there is no external force applied to the beam; therefore, there is no external force matrix. The mass matrix is the only symmetric matrix. All the matrices are time varying.

For easy comparison to the earlier analysis, each matrix is divided into four different matrices. Three of the matrices have contributions from the rigid body modes. The fourth matrix contains contributions from the flexible modes only. These last matrices are identical to the matrices shown in Eqs. (3.47), (3.48), and (3.49).

The mass matrix is:

$$M = \begin{bmatrix} M1 & M2 \\ M2^T & M4 \end{bmatrix} \quad 2+N \times 2+N \tag{A.48}$$

where the three matrices are defined as

$$M1 = \begin{bmatrix} 1 + \mu_m & \frac{1}{2} + \mu_m \tau \\ \frac{1}{2} + \mu_m \tau & \frac{1}{3} + \mu_m \tau^2 \end{bmatrix} \quad 2 \times 2 \tag{A.49}$$

$$M2 = \begin{bmatrix} I_3(1) & \cdots & I_3(N) \\ + \mu_m \sin \pi\tau & & + \mu_m \sin N\pi\tau \\ I_4(1) & \cdots & I_4(N) \\ + \mu_m \tau \sin \pi\tau & & + \mu_m t\tau \sin N\pi\tau \end{bmatrix} \quad 2 \times N \tag{A.50}$$

$$M4 = \begin{bmatrix} I_1(1,1) + & & I_1(N,1) + \\ \mu_m \sin\pi\tau \sin\pi\tau & & \mu_m \sin\pi\tau \sin N\pi\tau \\ & \ddots & \\ sym & & I_1(N,N) + \\ & & \mu_m \sin N\pi\tau \sin N\pi\tau \end{bmatrix} \quad N \times N \tag{A.51}$$

Similarly, the damping and stiffness matrices are

$$C = \begin{bmatrix} C1 & C2 \\ C3 & C4 \end{bmatrix} \quad and \quad K = \begin{bmatrix} K1 & K2 \\ K3 & K4 \end{bmatrix} \tag{A.52}$$

where

$$C1 = \begin{bmatrix} 0 & 2\,\mu_m \\ 0 & 2\,\mu_m\,\tau \end{bmatrix} \quad 2 \times 2 \tag{A.53}$$

$$C2 = \begin{bmatrix} 2\,\mu_m \pi \sin \pi\tau & \cdots & 2\,\mu_m\, N\pi \sin N\pi\tau \\ 2\,\mu_m \tau\, \pi \sin \pi\tau & \cdots & 2\,\mu_m\, \tau\, N\pi \sin N\pi\tau \end{bmatrix} \quad N \times 2 \tag{A.54}$$

$$C3 = \begin{bmatrix} 0 & 2\,\mu_m \sin \pi\tau \\ \vdots & \vdots \\ 0 & 2\,\mu_m \sin N\pi\tau \end{bmatrix} \quad 2 \times N \tag{A.55}$$

$$C4 = \begin{bmatrix} 2\mu_m \pi sin\pi\tau cos\pi\tau + 2\zeta \times \frac{\sqrt{\lambda I_1(1,1)\, I_2(1,1)}}{2} & & 2\mu_m N\pi sin\pi\tau cosN\pi\tau \\ & \ddots & \\ 2\mu_m \pi sinN\pi\tau\, cos\pi\tau & & 2\mu_m N\pi sinN\tau cosN\pi\tau + 2\zeta \times \frac{\sqrt{\lambda I_1(N,N)\, I_2(N,N)}}{2} \end{bmatrix} N \times N \tag{A.56}$$

where modal damping has been added to the fourth damping matrix.

The stiffness matrices are

$$K1 = \begin{bmatrix} 0 & 0 \\ 0 & 0 \end{bmatrix} \; 2 \times 2 \tag{A.57}$$

$$K2 = \begin{bmatrix} -\mu_m(\pi)^2 sin\pi\tau & \cdots & -\mu_m(N\pi)^2 sinN\pi\tau \\ -\mu_m\tau(\pi)^2 sin\pi\tau & \cdots & -m_m\tau(N\pi)^2 sinN\pi\tau \end{bmatrix} N \times 2 \tag{A.58}$$

$$K3 = \begin{bmatrix} 0 & 0 \\ \vdots & \vdots \\ 0 & 0 \end{bmatrix} \; 2 \times N \tag{A.59}$$

$$K4 = \begin{bmatrix} \lambda I_2(1,1) - \mu_m \pi^2 sin\pi\tau \, sin\pi\tau & & \lambda I_2(N,1) - \mu_m (N\pi)^2 sin\pi\tau \, sinN\pi\tau \\ & \ddots & \\ \lambda I_2(1,N) - \mu_m \pi^2 sinN\pi\tau \, sin\pi\tau & & \lambda I_2(N,N) - \mu_m (N\pi)^2 sinN\pi\tau \, sinN\pi\tau \end{bmatrix}_{N \times 2} \quad \text{(A.60)}$$

These matrices form the mass, stiffness, and damping matrices that may be used to simulate the motion of the moving mass system. The values of I_1, I_2, I_3, and I_4 for the simply-supported case are given by Eqs. (A.32)-(A.35). In order to obtain the total deflection, the rigid body motions must be added to the beam's flexible deformation. This analysis functioned well as a check for the Newtonian method and for that reason has been included here. This formulation was not used for any numerical evaluation.

APPENDIX B

RUNGE KUTTA INTEGRATION SCHEME

• The most important and significant problems in engineering are formulated in mathematical terms as a function that satisfies an equation containing the derivatives of the unknown function (Ref. [20]). Such an equation is termed an ordinary differential equation. The theory of differential equations dates back to the seventeenth century with the beginnings of calculus (Ref. [21]). Solutions for different types of differential equations were derived by such great mathematicians as Newton, the Bernoulli brothers, and Euler. The French mathematicians, Lagrange and Laplace, also made great contributions toward the solutions of ordinary differential equations (Ref. [20]).

However, there are still a number of ordinary differential equations for which no analytical solution has been found. Instead, numerical integration is used to solve for the function satisfying the ordinary differential equation.

Before computers were invented, numerical integration was hand-calculated. The most well known numerical integration scheme is Euler's method, which can be derived by forming a Taylor Series expansion of the ordinary differential equation. For example, consider:

$$\dot{x} = F(x,t) \tag{B.1}$$

This ordinary differential equation is the type that must be solved to simulate the motion of the flexible-beam/moving-mass system.

A Taylor series expansion of Eq. (B.1) leads to

$$x_{k+1} = x_k + F_k \Delta t + H.O.T \tag{B.2}$$

where the subscript indicates the time level:

x_k: x at time t

x_{k+1}: x at time $t + \Delta t$

F_k: Function evaluated at x_k and t

Equation (B.2) is rearranged to obtain the forward Euler method of numerical integration.

$$F_k = \frac{x_{k+1} - x_k}{\Delta t} \tag{B.3}$$

Because only first-order terms are retained, this method is termed first-order accurate. The title "N^{th}-order accurate" implies that the accuracy is proportional to the n^{th} order of the time step, Δt^n.

Using hand calculations, Eq. (B.3) can be iterated. Because it is

first-order accurate, however, many iterations are needed to converge the method to the correct answer. Therefore, throughout the ages, more advanced numerical integration schemes have been developed. These new methods are more complicated and tend to have a higher order of accuracy.

It would not be practical to employ these more advanced methods by hand; but, using a computer they can be implemented very easily. As computing power increased, more and more numerical integration schemes were developed. Three of these methods are discussed: the step-by-step, the predictor corrector, and the alternating direction implicit methods.

The step-by-step method examines the function at intermediate time steps. These intermediate values are weighted and combined to obtain the appropriate answer. The accuracy of the step-by-step method increases as the number of intermediate steps used increases. Methods of this type are known as explicit schemes because they use the value at a previous time frame to determine the value at the current time.

Conversely, an implicit scheme uses the value at the current time to predict the value at a future time. The combination of an implicit and an explicit scheme is used to form a predictor-corrector method. An implicit scheme is used to predict the future value and

then an explicit scheme is used to correct this predicted value (Ref. [22]).

The alternating-direction implicit schemes are variations on the finite-element method. Unlike the first two methods, this scheme works best on a mesh of elements rather than on a string of nodal points. This type of numerical integration is only practical for two-dimensional (or three) problems. For half of the time step, a sweep is made in one direction, i.e., x; for the second half of the time step, a sweep is made in the other direction, i.e., y (Ref. [22]).

As well as the three categories discussed here, there are dozens of numerical integration schemes. These three were chosen to provide an overview of the different integration methods available. However, to simulate the motion of the flexible-beam/moving-mass system, a step-by-step integration scheme, a Runge Kutta integration scheme, was chosen.

Four intermediate steps were used so the scheme would be fourth-order accurate. The fourth-order Runge Kutta integration scheme for the type of ordinary differential equation shown in Eq. (B.1) is (Ref. [19]):

$$x_{k+1} \cong x_k + \frac{1}{6}(b_1 + 2b_2 + 2b_3 + b_4) \tag{B.4}$$

where

$$b_1 = \Delta t\, F_k(x_k,\, t_k) \tag{B.5}$$

$$b_2 = \Delta t\, F_k\left(x_k + \frac{1}{2} b_1\,,\, t_k + \frac{1}{2}\Delta t\right) \tag{B.6}$$

$$b_3 = \Delta t\, F_k\left(x_k + \frac{1}{2} b_2\,,\, t_k + \frac{1}{2}\Delta t\right) \tag{B.7}$$

$$b_4 = \Delta t\, F_k\left(x_k + \; b_2\,,\, t_k + \Delta t\right) \tag{B.8}$$

This integration scheme was also used to numerically integrate the nondimensional integrals for the free-free mode shapes. The values were then used to formulate the constant mass, damping, and stiffness matrices, the values of which are shown in Appendix C.

For numerical stability, the time step used in the integrations was smaller than one tenth of the shortest period for each system. If there are many modes retained, the shortest period can become very small. For computational efficiency only the first three flexible modes were retained for each system.

APPENDIX C
NUMERICAL VALUES

For clarity, the spatial derivatives of the shape functions, linear and cubic, used in the discrete formulation were kept in their symbolic form. The constant mass, damping, and stiffness matrices were also left in an unexpanded form because the nondimensional integrals needed to form these matrices were only obtained as numerical values as a result of a numerical integration scheme. This appendix presents the numerical values of these matrices and develops the appropriate derivatives of the shape functions with respect to the weighting function ξ.

C.1 NUMERICAL VALUES FOR THE CONSTANT MATRICES

The mode shapes used to model the free-free beam consisted of trigonometric and hyperbolic trigonometric functions. Due to the complexity of these mode shapes, the values of the nondimensional integrals needed to form the constant mass, damping, and stiffness matrices were determined by using the Runge Kutta integration scheme outlined in Appendix B.

As a refresher, the mode shapes used to model the free-free beam are rewritten:

$$\phi_1 = 1 \tag{C.1}$$

$$\phi_2 = \bar{x} - 1/2 \tag{C.2}$$

$$\phi_i = \cos \beta_i \bar{x} + \cosh \beta_i \bar{x} - \sigma_i \left(\sin \beta_i \bar{x} + \sinh \beta_i \bar{x}\right) \quad 3 \le i \le N \tag{C.3}$$

where, as before

$$\bar{x} = \frac{x}{L} \tag{C.4}$$

The numerical values of the parameters β_i and σ_i are shown in Table C-1 for the first three flexible modes (Ref. [17]).

Table C-1. Numerical Values of Parameters used for Free-Free Mode Shapes.

Mode Number	β_ι	σ_ι
1	4.730004074	0.98250221
2	7.85320462	1.00077731
3	10.99560783	0.99996645

The mode shapes defined by the parameters in Table C-1 were substituted into equations defining the nondimensional integrals, Eqs. (3.15) and (3.16). The numerical integration scheme was then used to determine the value of these integrals.

The integrals are needed to form the constant matrices that define the dynamics of the flexible structure. The symbolic form of the matrices were given by Eqs. (3.33), (3.37), and (3.38). They are rewritten here for convenience

$$[M_o]_{i,i} = I_1(i,i) \tag{C.5}$$

$$[C_o]_{i,i} = 2\,\zeta\,\sqrt{\lambda\, I_1(i,i)\, I_2(i,i)} \tag{C.6}$$

$$[K_o]_{i,i} = \lambda I_2(i,i) \tag{C.7}$$

The numerical values for the constant mass, damping, and stiffness matrices are shown for the first five modes. These modes correspond to rigid body translation, rigid body rotation, and the first three flexible modes, respectively. The matrices are:

$$[M_o] = \begin{bmatrix} 1 & & & & \\ & 1/12 & & & \\ & & 1 & & \\ & & & 1 & \\ & & & & 1 \end{bmatrix} \tag{C.8}$$

$$[C_o] = 2\,\zeta\,\sqrt{\lambda}\begin{bmatrix} 0 & & & & \\ & 0 & & & \\ & & 22.373 & & \\ & & & 61.672 & \\ & & & & 120.903 \end{bmatrix} \tag{C.9}$$

$$[K_o] = \lambda \begin{bmatrix} 0 & & & & \\ & 0 & & & \\ & & 500.56 & & \\ & & & 3804.53 & \\ & & & & 14{,}617.63 \end{bmatrix} \tag{C.10}$$

The time-varying components, due to the dynamics of the moving mass, are added to these matrices. The resulting matrices are used to simulate the motion of the entire system.

C.2 THE SPATIAL DERIVATIVES OF THE SHAPE FUNCTIONS

In the discrete formulation detailed in Section 3.2, the spatial derivatives of the shape functions were kept in their symbolic form. In this appendix, the required derivatives are obtained. Both shape functions, linear and cubic, are examined. The spatial derivatives are with respect to the weighting function ξ, which was defined by Eq. (3.85). Both the first and second spatial derivatives are evaluated.

Linear Shape Function

The linear shape function was defined by Eq. (3.87) and is rewritten here for convenience:

$$V_1 = (1 - \xi)\, V_i + \xi\, V_{i+1} \tag{C.11}$$

where V_i and V_{i+1} are constant vectors that select the appropriate nodal values.

The first spatial derivative, with respect to ξ, of V_1 is

$$V_{1_\xi} = V_{i+1} - V_i \tag{C.12}$$

Because V_1 is linear with respect to the weighting function, the second spatial derivative is zero. In the formulation, an impulse force was used to artificially add the effects of the missing derivative. To obtain a non-zero second derivative, a cubic shape function was formed.

Cubic Shape Function

The cubic shape function was defined in Eq. (3.92) and is rewritten here for convenience:

$$\begin{aligned} V_3 = {} & \left(1 - 3\,\xi^2 + 2\xi^3\right) V_i + \left(\xi - 2\,\xi^2 + \xi^3\right)\frac{1}{n} V_{i+1} \\ & + \left(3\,\xi^2 - 2\,\xi^3\right) V_{i+2} + \left(\xi^2 + \xi^3\right)\frac{1}{n} V_{i+3} \end{aligned} \tag{C.13}$$

where the V_{i+2} and the V_{i+3} vectors are constant vectors that serve a similar purpose to V_i and V_{i+1}.

The first and second spatial derivatives of Eq. (C.13) are

$$V_{3_\xi} = \left(-6\,\xi + 6\xi^2\right) V_i + \left(1 - 4\,\xi + 3\,\xi^2\right)\frac{1}{n} V_{i+1} + \left(6\,\xi - 6\,\xi^2\right) V_{i+2} + \left(2\,\xi + 3\,\xi^2\right)\frac{1}{n} V_{i+3} \tag{C.14}$$

$$V_{3_{\xi\xi}} = \left(-6 + 12\,\xi\right) V_i + \left(-4 + 6\,\xi\right)\frac{1}{n} V_{i+1} + \left(6 - 12\,\xi\right) V_{i+2} + \left(2 + 6\,\xi\right)\frac{1}{n} V_{i+3} \tag{C.15}$$

As shown by Eq. (C.15), the second derivative of V_3 is not only continuous but linear with respect to ξ.

APPENDIX D
DESCRIPTION OF COMPUTER CODE

Appendix D presents a general description of the computer code written to simulate the motion of the flexible-beam/moving-mass system. Five different systems were simulated: continuous-fixed, continuous-free, discrete-fixed, discrete-free, and discrete-multipoint-of-contact. Each simulation follows the same general format: the general procedure used in creating the simulations is explained, the differences between the systems examined are discussed, and as an example, a listing of the code written to simulate the discrete free system is presented.

The code was written using PRO-MATLAB (Ref. [23]), which is a product of The MathWorks, Inc. MATLAB is a high-performance interactive software package. It is designed for scientific and engineering numeric computation. In MATLAB, the problem solutions are expressed almost exactly as they are written mathematically. The simplicity of programming in PRO-MATLAB is having a matrix defined as a basic data element that does not require dimensioning (Ref. [23]). The simulations were performed on a UNIX-based SUN SPARCstation 2.

The purpose of the code was to numerically integrate the dynamic equations describing the motion of the flexible-

beam/moving-mass system. The parameters needed to describe the physical properties of the system are λ, μ_m, and μ_g, all of which were described in detail in Chapter 3. The values of these parameters used in the simulations were listed in Chapter 4.

A flowchart for the program is shown in Figure D-1. The required inputs are: the initial state vector x_O, the initial time t_O, the final time tf, and the nondimensional parameters. The desired output is the time history of the beam's displacement.

The constant components of the mass, damping, stiffness, and force matrices are determined. Because these are independent of time, they can be calculated outside of the numerical integration loop. After these constant matrices are known, a subroutine that performs the fourth-order Runge Kutta integration scheme is called, which, in turn, calls a dynamic subroutine to set up the matrix equation describing the system's dynamics.

The dynamic subroutine first formulates the time-varying components of the matrices. These components are then added to the constant matrices that were developed earlier. The total mass, damping, stiffness, and force matrices are combined into the form shown in Eq. (3.32).

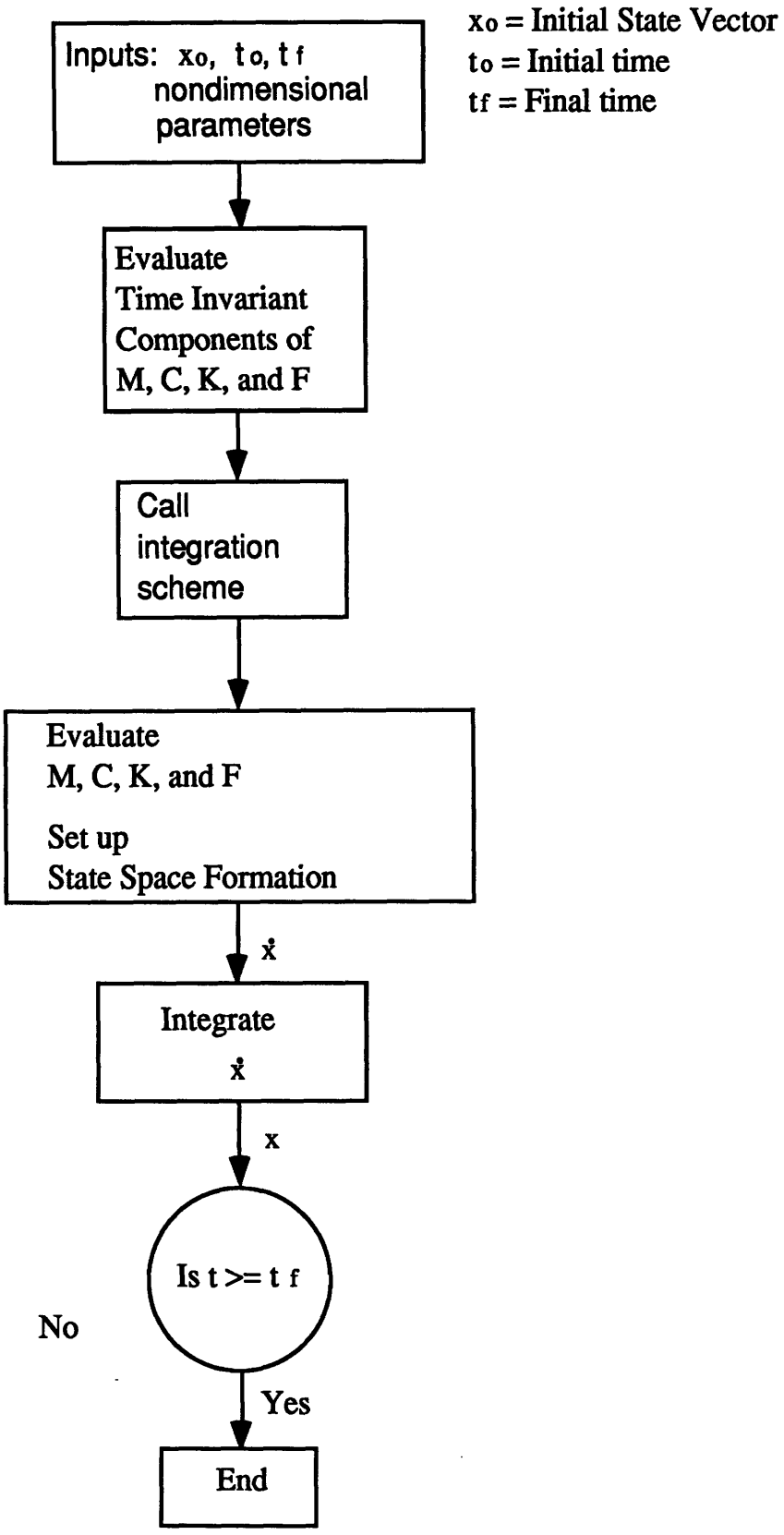

Figure D-1. Flow chart for numerical simulations.

The output of this dynamic subroutine is the derivative of the state vector $\dot{x}$. This vector is sent back to the Runge Kutta integration routine for numerical integration. This process, Runge Kutta-dynamic-Runge Kutta, is repeated until the entire time history of the state vector x is known. Since a fourth-order Runge Kutta integration scheme is used, the dynamic subroutine is called four times for each time step.

The state vector contains the time history of the modal displacements and velocities. The modal displacements are transformed to the natural coordinates of the beam using Eq. (3.11). The final result is the time history of the beam's displacement.

The procedure outlined by the flowchart shown in Figure D-1 represents the general format of the code. The following paragraphs discuss the variations used to formulate each system.

D.1 CONTINUOUS FORMULATIONS

The two continuous formulations differ only by the mode shapes used to describe the beam's deformation. This difference effects the constant mass, damping, and stiffness matrices as these matrices are functions of the nondimensional integrals and the nondimensional frequencies, which themselves are a function of the mode shapes.

For the simply-supported beam, the frequencies and the nondimensional integrals are determined analytically. In the code, they appear in their symbolic form. For the free-free beam, the nondimensional frequencies are inputed by hand according to the values dictated in Table C-1. The nondimenisonal integrals are evaluated using a Runge Kutta integration scheme.

Once these matrices are developed, the two continuous formulations are almost identical and both follow the general procedure described above.

D.2 DISCRETE FORMULATIONS

The discrete formulations are a little more involved. First, the finite element mass and stiffness matrices are determined. Using these matrices, the mode shapes and the nondimensional frequencies of the system are determined. If the beam is free-free, the matrices are not altered before the eigenvalue decomposition. For the simply-supported beam, the boundary conditions at the endpoints must be implemented before the eigenvalue decomposition can take place.

These mode shapes and frequencies are next truncated to contain only the number of modes used in the simulation. These

truncated values are used to form the constant discrete stiffness and damping matrices.

To formulate the time-varying components, it is necessary to develop the shaping functions, which are evaluated at every time step. A different subroutine was written for the both the linear and the cubic shape functions. Unlike the linear shaping function, the cubic shaping function is also altered if there is more than one point of contact.

The shape functions are used to formulate the time-varying components of the matrices. Once the matrices are known, the same procedure outlined above is followed.

D.3 LISTING OF CODES

A listing of the code used to solve the discrete free single point of contact system is presented. The cubic shape function is used to model the displacements

```
function [q,t] = mload(n,m,us,ug,um)
%
% This function will simulate the motion
% of the beam due to the moving load.
%
%  The inputs to the system are
%     n = number of finite elements
%     m = number of modes retatined
%      us = nondimensional stiffness parameter
%      ug = nondimensional load parameter
%     um = nondimensional mass ratio
%
% It will first set up all the system
% properties.
%
% Then it will use this property to
% create all the variables that are
% not dependent on time.
%
% It will next  call integrate which will
% numerically integrate the state vector
%
% In order to do this the initial state
% vector must be set up
%
```

```
% After the numerical integration of
% the state vector, the modes will be transformed
% to the physical non-dimensional deflection
% at the midspan of the beam.
%
% Set up the variables that are not dependent on time
%
% Compute the eigenvalues, discrete m and k matrices
%
[phi,w,k,mt] = pinnedf3(n);
%
% Normalize the eigevector wrt to m
%
phin = normeig(phi,mt,n);
%
% Reduce to the number of modes retained
%
[phir,wr] = reduce3(phin,w,n,m);
%
% Caluculate constant compontents of K and C
%
[c,kr] = stiffdamp(wr,m,us);
%
% Now set up variables needed for integrate
%
```

```
% Time
%
t0 = 0.0;
tf = 0.010;
delt = .001;
%
% Inital state vector
%
[lam,sig] = coef(1);
q0 = qint(lam,sig,n);
x0 = xint(phir,q0);
j=1+m;
 while j < 2*m + 1
  x0(j,1) = 0.0;
 j=j+1;
 end
%
%
% Call integrate
%
[tt,x] = integrate(t0,tf,delt,x0,n,m,um,ug,phir,c,kr);
%
%
% Next do a transformation back to
% physical coordinates
```

```
%
% Call trans
%
x=x';
qq  =  trans(phir,x,m);
skip = 10;
i=1;
m=1;
[n,j] = size(tt);
while i < j+1
 q(:,m) = qq(:,i);
 t(m) = tt(i);
 i=i+skip;
 m=m+1;
end
```

```
function [x,y,kk,mm] = pinned3f(n)
%
% This function will calculate
% the mass and stiffness matrices
% for the free free beam.
%
% It will also calculate the eigenvalues and eignevectors
% of the pinned - pinned
%
% The program is broken up into two parts
%
% Part one sets up the global mass matrix
%  and the global stiffness matrix
%
% Part two sets up the eigenvalue problem and solves
% for the natural frequencies of the beam.  The boundary
% conditions (if there are any) would also taken care of in this part.
%
% INPUTS
%
% n represents the number of elements to be used
%
% OUTPUTS
%
% y represents the matrix of eigenvvalues that represent
```

```
% the frequencies of the beam
%
% x represents the matrix of eigenvectors that will
% will be used as the shape functions during modal
% analysis
%
% But First .....
%
% Certain variables are declared
%
% LENGTH OF BEAM
l=1.0;
%
% DENSITY OF BEAM
p=1;
%
% MODULUS OF ELASTICITY
e=1;
%
% WIDTH OF BEAM
w=1;
%
% DEPTH OF BEAM
d=1;
%
```

```
% AREA MOMENT OF INERTIA OF BEAM
im= 1;
%
%
% The length of one element is
le = l/n;
%
%
% PART ONE
%
k11 = [12    6*le
      6*le 4*le^2];
k12 = [-12   6*le
      -6*le 2*le^2];
k21 = [-12   -6*le
      6*le  2*le^2];
k22 = [12    -6*le
      -6*le 4*le^2];
%
m11 = [156    22*le
      22*le 4*le^2];
m12 = [54   -13*le
      13*le -3*le^2];
m21 = [54   13*le
      -13*le  -3*le^2];
```

```
m22 = [156    -22*le
      -22*le 4*le^2];
%
% Assemble the global stiffness matrix and mass matrix
%
k(1:2,1:2)=k11;
k(2*n+1:2*n+2,2*n+1:2*n+2)=k22;
k(2*n+1:2*n+2,2*n-1:2*n)=k21;
k(1:2,3:4)=k12;
%
m(1:2,1:2)=m11;
m(2*n+1:2*n+2,2*n+1:2*n+2)=m22;
m(2*n+1:2*n+2,2*n-1:2*n)=m21;
m(1:2,3:4)=m12;
%
i=2;
while i <= ((2*n)/2)
  k(2*i-1:2*i,2*i-3:2*i-2)=k21;
  k(2*i-1:2*i,2*i-1:2*i)=k11+k22;
  k(2*i-1:2*i,2*i+1:2*i+2)=k12;
%
  m(2*i-1:2*i,2*i-3:2*i-2)=m21;
  m(2*i-1:2*i,2*i-1:2*i)=m11+m22;
  m(2*i-1:2*i,2*i+1:2*i+2)=m12;
i=i+1;
```

```
end
%
kk=e*im*k/le^3;
mm = (m*le)/420;
%
% PART TWO
%
%
%
% Next do an eigenvalue decomposition
%
[xx,y] = eig(kk,mm);
y = diag(y);
%
% Next diagonalize the eigenvector matrix
%
p1o = xx(:,2*n+1);
p2o = xx(:,2*n+2);
%
alpha = 1/sqrt(p1o'*mm*p1o);
p1n = alpha*p1o;
%
p2n = p2o - (p2o'*mm*p1n)*p1n;
%
x = [xx(:,1:2*n) p1n p2n];
```

```
function phin = normeig(phi,mt,n)
%
% This function will normalize the
% eigenvector matrix so
% phi'*mt*phi = I
%
%
i = 1;
while i < 2*n+3
   alpha = sqrt(phi(:,i).'*mt*phi(:,i));
   phin(:,i) = phi(:,i)./alpha;
 i=i+1;
 end
```

```
function [phir,yr] = reduce3(phi,y,n,m)
%
% This function will reduce the
% matrix of eigenvectors to the
% number of modes that are
% actually wanted in the simulation
% versus the number of degrees of
% freedom in the model
%
% The inputs are
%  phi = the normalized matrix of eigenvectors
%  y = the eigenvalues
%  n = number of elements used
%  m = number of modes wanted
%
% The output is
%  phir = the normalizes and reduced eigenvector matrix
%  yr = the reduced eigenvalue matrix
%
diff = 2*n-m+3;
phir=phi(:,diff:2*n+2);
yr=y(diff:2*n+2);
```

```
function [c,kr] = stiffdamp(yr,m,us)
%
% This function will return
% the stiffness and damping
% matrices to be used in the
% state vector.
%
% Its inputs are
%  yr = the reduced eigenvalue
%       matrix
%   m = the number of reduced
%       modes
%   us = nondimensional stiffness parameter
%
j=1;
chi = 0.01;
while j < m + 1
 c(j,j) = 2*chi*sqrt(yr(j)*us);
 kr(j,j) = yr(j)*us;
 j=j+1;
end
```

```
function [tout,xout] =
integrate(t0,tf,delt,x0,n,m,um,ug,phir,c,kr)
%
% This function will numerically integrate
% the state vector to simulate the motion
% of the model
%
% The inputs are
%  t0 = inital time
%  tf = final time
%  x0 = inital state vector
%  delt = delta t
%  All the rest are
%    model parameters which have
%    previosly been defined
%
%  The output is
%    tout = the column vector containing all the times used
%    xout = the final state vector
%
% First initialize and set the tolerance
%
flag=(tf-t0)/delt;
flag2 = 2*m;
xout = zeros(flag,flag2);
```

```
tout = zeros(1,flag);
%
%
 xout(1,1:flag2) = x0';
 tout(1) = t0;
%
xk = x0;
t = t0;
%
tol = .1e-06;
%
% Next set up the loop
%
count=2;
%
while t < tf
   xd1 = eqn3(t,xk,n,m,um,ug,phir,c,kr);
  b1 = delt*xd1;
%
   tt = t + delt*0.5;
   xt =  xk + 0.5*b1;
    xd2 = eqn3(tt,xt,n,m,um,ug,phir,c,kr);
  b2 = delt*xd2;
%
  xt = xk + 0.5*b2;
```

```
   xd3 = eqn3(tt,xt,n,m,um,ug,phir,c,kr);
  b3 = delt*xd3;
%
   tt = t + delt;
   xt = xk + b3;
    xd4 = eqn3(tt,xt,n,m,um,ug,phir,c,kr);
  b4 = delt*xd4;
%
  x = xk + (1/6)*(b1 + 2*b2 + 2*b3 + b4);
%
% Set up output vectors
%
  t = t+delt;
   xout(count,1:flag2) = x';
   tout(count) = t;
%
  count = count +1;
%
% Get ready for next iteration
%
   xk = x;
%
end
```

```
function  xd  =  eqn3(t,x,n,m,um,ug,phir,c,kr)
%
% This function is called by
% integrate
%
% It sets up the state vector and its derivatives
%
% The inputs are
%   t = time
%    x = state vector at time t
%     The rest of parameters have been defined previously.
%
% First set up the load matrices
% which are dependent on time
%
if t >=1.0
 um = 0.0;
 ug = 0.0;
end
%
% Call loadf3
%
[v,vd,vdd] = loadf3(t,n);
[d,e] = size(v);
 if d == 1
```

```
  v=v';
 end
[g,h] = size(vd);
 if g ==1
   vd=vd';
end
%
% Call loadn3
%
[vn,vdn,vddn] = loadn3(v,vd,vdd,phir,t);
%
%
% Next set up the mass, stiffness, damping and force matrices
%
%
%
   ma = mass(m,um,vn,t);
   da = damp(c,um,vn,vdn);
   ka = stiff(kr,um,vn,vddn);
%  fa  = force(n,ug,t,phir);
%
% Set up the state vector
%
%
% Without r and theta, Simply Supported Case
```

```
%
%
%mn = ma(3:2+m,3:2+m);
%dn = da(3:2+m,3:2+m);
%kn = ka(3:2+m,3:2+m);
%fn = fa(3:2+m,1);
%
%
%xd(3:2+m,:) = x(5+m:2*(2+m),:);
%xd(5+m:2*(2+m),:) = inv(mn)*(fn - kn*x(3:2+m,:) - dn*xd(3:2+m,:));
%
%
% With r and theta, Free-Free Case
%
xd(1:m,:) = x(1+m:2*m,:);
%
% With Forcing term
%
%xd(1+m:2*m,:) = inv(ma)*(fa - ka*x(1:m,:) - da*xd(1:m,:));
%
%Without Forcing term
%
xd(1+m:2*m,:) = inv(ma)*(- ka*x(1:m,:) - da*xd(1:m,:));
```

```
function  [v,vd,vdd]  =  loadf3(t,n)
%
% This function will return the vectors
% v, vd, vdd, which weights the effect of the moving
% load on the neigboring nodes.  It is a
% function of time since the load is moving
%
%
% The inputs are
%     t  is time
%       n   is number of elements used
%          for the modeling
%
% The outputs are
%       v cubic weighting function
%      vd first derivative of v
%     vdd second derivative of v
%
%
% Evaluate i, and alpha
% All of which are a function of
% time
%
  i = fix(t*n) + 1;
  alpha = (t*n - i + 1);
```

```
%
% Set up a dummy array of zeros
%
  v1 = zeros(1,2*n+2);
  v2 = zeros(1,2*n+2);
  v3 = zeros(1,2*n+2);
  v4 = zeros(1,2*n+2);
%
% Determine v for n less than the
% number of elements
%
 if i < n+1
  v1(1,2*i-1) = 1;
  v2(1,2*i) = 1;
  v3(1,2*i+1) = 1;
  v4(1,2*i+2) = 1;
 end
%
% Correct last value of
% v2 when appriopriate
%
 if i == n+1
  v1(1,2*i-1) = 1;
  v2(1,2*i) = 1;
 end
```

```
%
va = (1-3*alpha^2 + 2*alpha^3)*v1 + (alpha - 2*alpha^2 +
alpha^3)*(1/n)*v2;
vb = (3*alpha^2 - 2*alpha^3)*v3 + (-alpha^2 + alpha^3)*(1/n)*v4;
%
v = va + vb;
%
vc = (-6*alpha + 6*alpha^2)*v1 + (1-4*alpha+3*alpha^2)*(1/n)*v2;
ve = (6*alpha - 6*alpha^2)*v3 + (-2*alpha + 3*alpha^2)*(1/n)*v4;
%
vd = (vc + ve)*n;
%
vcc = (-6 + 12*alpha)*v1 + (-4+6*alpha)*(1/n)*v2;
vccc = (6 - 12*alpha)*v3 + (-2 + 6*alpha)*(1/n)*v4;
%
vdd = (vcc + vccc)*(n^2);
%
v = v';
vd = vd';
vdd = vdd';
```

```
function [vn,vdn,vddn] = loadn(v,vd,vdd,phir,t)
%
% This function will calculate
% vn = phir'*v
% vdn = phir'*vd
% vddn = phir'*vdd
%
% phir has already been reduced to the appropriate
% amount of modes desired.
%
vn = phir'*v;
vdn = vd'*phir;
vddn = vdd'*phir;
```

```
function  ma  =  mass(m,um,vn,t)
%
% This function will calculate the mass matrix
%
%
% The inputs are
%
%    m = number of modes used
%    um = non dimensional mass parameter
%   vn = load vector
%    t = non dimensional time
%
%
%
%
 ma = eye(m,m) + um*vn*vn';
```

```
function  da  =  damp(c,um,vn,vdn)
%
% This function will calculate the
% damping matrix
%
%  The inputs are
%    c = diagonal structual damping matrix
%    um = non dimensional mass parameter
%   vn = load vector
%    vdn = derivative of load vector
%
da = c + 2*um*vn*vdn;
```

```
function ka = stiff(kr,um,vn,vddn);
%
% This function will calculate the stiffess
% matrix
%
% Its inputs are
%   kr = constant component of k
%   um = mass ratio
%   load vectors vn and vddn
%
fy = um*vn*vddn;
ka = kr + fy;
```

```
function  x  =  trans(phir,xx,m)
%
% This function will transform the
% modal displacements into natural
% displacements
%
x = phir*xx(1:m,:);
```